NTNU

Norwegian University of
Science and Technology

Adaptive Observer for Bottomhole Pressure During Drilling

Øyvind Nistad Stamnes

Master of Science in Engineering Cybernetics
Submission date: December 2007
Supervisor: Ole Morten Aamo, ITK

Norwegian University of Science and Technology
Department of Engineering Cybernetics

Problem Description

Estimation of the annular pressure at critical locations in the well is crucial for high-precision pressure control. Certain parameters which are important in order to determine the pressure profile of the well (in particular the friction factor, bulk modulus and density in the annulus), are encumbered with high uncertainty and are besides, continuously, but slowly changing. The objective of the thesis is to design an adaptive observer for estimation of the bottomhole pressure and certain important parameters/slowly varying variables, during drilling.

Topics that should be addressed are:

1) Literature review of existing estimation schemes for drilling

2) Design an adaptive observer that estimates the bottomhole pressure and adapts to uncertain parameters during common drilling scenarios.

3) Analyze performance of the parameter estimation. Determine which parameters are reasonable to estimate.

4) Analyze the adaptive observer with respect to the following cases: pipe connection, drill string movements, changes in choke valve opening and mud pump flow.

5) Analyze performance/robustness with respect to unmodeled dynamics.

Assignment given: 23. August 2007
Supervisor: Ole Morten Aamo, ITK

Preface

This master thesis was written during the fall of 2007 as a compulsory part of the Master of Technology program at the Norwegian University of Science and Technology, Department of Engineering Cybernetics. The work on pressure estimation during drilling has been time consuming and hard but truly awarding and it has motivated me to pursue a Ph.D. within automation of drilling operations.

A special thanks goes out to Professor Ole Morten Aamo here at NTNU and to Dr. Glenn-Ole Kaasa at StatoilHydro Porsgrunn for their guidance. I would also like to thank post-doc Jing Zhou for her help and guidance with the Lyapunov proofs, Dr. Gerhard Nygaard for answers to drilling related questions and help with the WeMod simulator and my fellow students Jørn , Marte, Øyvind and Thomas for their advice. Finally I would like to thank my girlfriend Amarpreet for her support and patience during this last semester.

Øyvind Nistad Stamnes
Trondheim, December 2007

Abstract

To satisfy the increasing petroleum consumption on a world wide basis there is a need to find new resources. As mature fields are drained, reservoir pressure falls, which again leads to tight pressure margins. To reduce down time due to hole stability problems (e.g. kicks) there is a demand for accurate control of the pressure profile in the well. As the pressure profile is not known and depends on unknown factors such as friction loss there is a need to estimate the pressure.

In this thesis an observer that adapts to unknown factors, such as friction and density changes, and estimates the bottomhole pressure is presented. Furthermore, a parameter estimator for the bulk modulus in the annulus is developed as an extension to the observer to facilitate for future control design. Both designs are based on a third order model and provide rigid proofs of stability and convergence of the estimated pressure and parameters. The pressure estimate from the observer is shown to converge to the true pressure under reasonable conditions. For parameter estimates to converge to their true values conditions on excitation are presented.

The observer and parameter estimator are tested in simulations and also on log data from a well drilled at the Grane field in the North Sea. Simulation results show that the observer performs very well during typical drilling procedures affecting choke valve opening, pump flows and drill string movements. The observer shows promising behavior when tested on log data from the Grane field.

Contents

List of Figures

List of Tables

Abbreviations

BOP	Blow Out Preventer
PE	Persistent Excitation
PI	Proportional Integral
LTI	Linear Time Invariant
LTV	Linear Time Varying
MIMO	Multiple Input Multiple Output
MPD	Managed Pressure Drilling
MPT	Mud Pulse Telemetry
MTOE	Million Tons of Oil Equivalent
NMPC	Nonlinear Model Predictive Control
NTNU	Norwegian University of Science and Technology
ODE	Ordinary Differential Equation
PDE	Partial Differential Equation

Chapter 1

Background

1.1 Motivation and Introduction to Drilling

To meet the increasing demand for oil and gas on a world wide basis, see figure 1.1, there is a need to find new reserves and to extract these. The remaining resources are harder to extract as the easier resources have already been developed (Hydro 2007). Challenges related to drilling complex wells with narrow pressure margins, e.g., drilling into depleted reservoirs, demand accurate pressure control. At the same time more wells need to be drilled as the remaining reservoirs are smaller. Therefore there is a demand for drilling technologies that provide precise pressure control, while still being cost and time efficient (Hydro 2007).

As an introduction to drilling consider the drill rig set-up illustrated in figure 1.2. The figure illustrates a jacket platform performing offshore drilling. At the top of the derrick the drill string is attached to the topdrive which is a motor that turns the drill string. The drill string can move up and down inside the derrick as the topdrive is attached to a hook that can be lowered or raised. As the drilling progresses the top of the drill string sinks towards the drill floor. After approximately $27m$ a new stand of drill pipe is connected to the top and drilling resumes. This procedure is referred to as a pipe connection. For a typical rate of penetration of $15\frac{m}{hr}$ a pipe connection is performed roughly every two hours.

During drilling, down hole cuttings need to be transported out of the bore hole. This is done by using a mud circulation system. On board the rig, tanks filled with drilling mud feed the main mud pump which pumps the drilling fluid through the topdrive and into the drill string. The mud then flows down through the bit and up through the annulus carrying the cuttings along before the flow exits through a choke. After exiting the fluid is recycled and returned to the mud tanks. The example illustrated in figure 1.2 has a rotating control device which seals off the annulus from the outside while a choke controls the flow of mud out from the annulus. Conventional drilling techniques do not

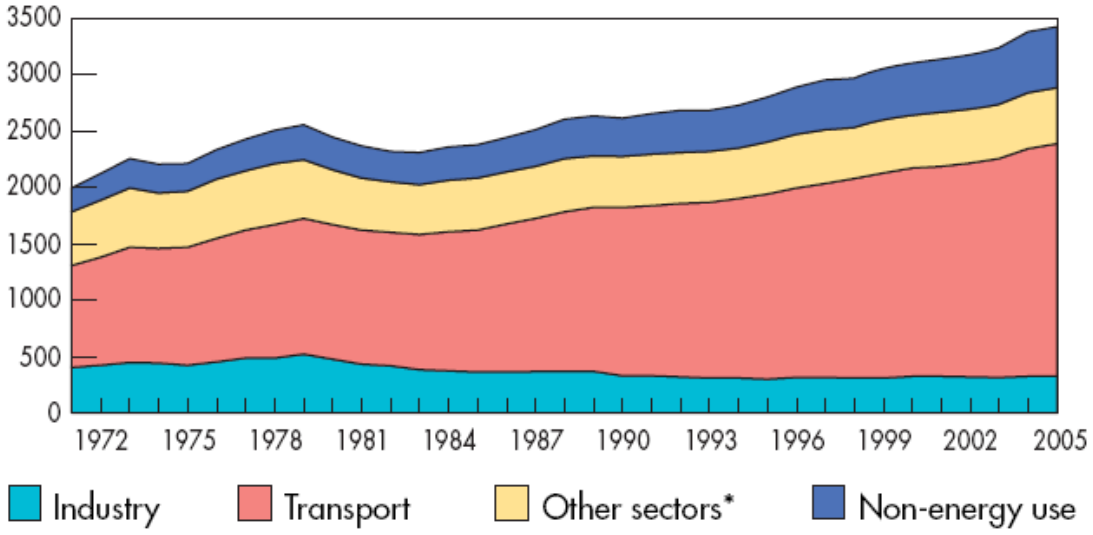

Figure 1.1: Total final consumption of oil worldwide, by sector. (*Key World Energy Statistics* 2007)

have a sealed off annulus. This is cheaper and less complex but does not allow for the pressure control rendered possible by the seal and choke.

The main reason for pressure control is to prevent uncontrolled reservoir influx which in the worst case scenario can lead to a surface blowout with large financial losses, environmental damages and possible loss of lives. Controlling the pressure is also important to prevent the bore hole from collapsing or fracturing and to reduce skin damage. Skin damage is caused by drill mud entering and clogging porous sections in the reservoir which lowers production at a later stage.

The pressure in the annulus is mainly affected by the hydrostatic weight and the pressure due to friction losses (Brill & Mukherjee 1999). In addition, if the annulus is closed off, the pressure at the top of the annulus will significantly affect the pressure in the well.

There are several operational procedures that affect the pressure in the annulus. Pipe connection affects the pressure as the main pump must be disconnected to attach a new section of drill pipe, this leads to zero flow and loss of pressure due to friction. Moving the drill string all the way out/in of the well (tripping) increases/decreases the volume in the annulus. Tripping out pipe can lead to reduced fluid column height which will lead to a reduced pressure in the annulus. On the other hand tripping in can create a surge in the pressure. Similarly effects can be experienced due to heave when drilling from a floater.

Drilling into depleted sections of the reservoir can lead to a partial or complete loss of mud which is both critical to hole stability and directly linked to financial losses

through the cost of mud. On the other hand drilling into high pressure zones will increase the pressure which can bring with it kicks (reservoir fluid influx) which if not handled correctly can lead to the above mentioned blowout scenario.

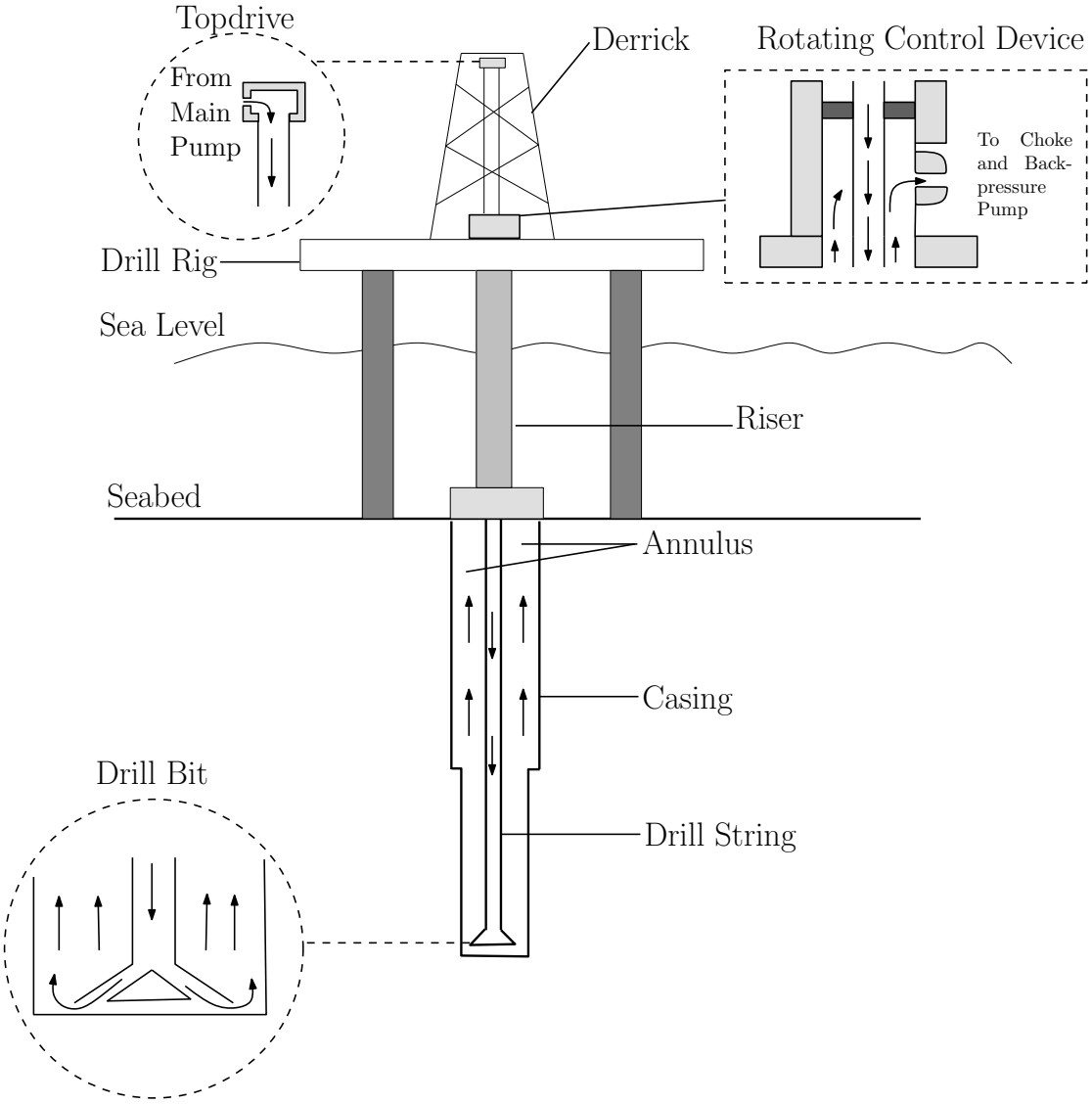

Figure 1.2: Example of Drilling System

1.2 Pressure Control

As described in the previous section there is a demand for accurate control of the annulus pressure. As a response to these demands a fairly new (for offshore drilling) technology for pressure control has emerged (Hannegan 2006). It is named Managed Pressure Drilling (MPD) and is defined by the IADC Underbalanced Operations Committee as: *"Managed Pressure Drilling is an adaptive drilling process used to precisely control the annular pressure profile throughout the well bore. The objectives are to ascertain the down hole pressure environment limits and to manage the annular hydraulic pressure profile accordingly"* (Hannegan, Todd, Pritchard & Jonasson 2004).

An important part of MPD is to determine the annular pressure profile. The pressure profile can be hard to obtain as it is a complex function of geometry, fluid velocity, friction, density, etc. Therefore the bottom hole pressure (BHP) is often used as the variable to control (Nygaard & Nævdal 2006), (Nygaard, Johannessen, Gravdal & Iversen 2007), (Nygaard, Vefring, Fjelde, Nævdal, Lorentzen & Mylvaganam 2004). The bottomhole pressure (BHP) can be measured but the measurement is usually based on mud-pulse telemetry. It is therefore hampered with slow sampling and no signal when the circulation is low, e.g., during pipe connection procedures. Wired drill pipe is an emerging technology that will make the BHP more accessible in future, but at the moment it is not fully developed (Fischer 2003), (Hydro 2007). As mentioned there are several factors such as pressure drop due to friction, pressure variations due to movement of the drill string and reservoir influx affecting the BHP. Friction and influx are cumbered with high degree of uncertainty as there is no direct way of measuring them. Because of this the BHP has to be estimated and uncertainties should be taken into account when doing so.

1.3 Pressure Estimation in Wells

This section gives a brief overview of existing estimation/observer designs for MPD found in the literature. The (possibly) multiphase flow dynamics of a well can be described accurately by a set of partial differential equations (PDE's), see e.g. (Lage 2000), (Nygaard 2006). The models found in (Lage 2000) and (Nygaard 2006) are based on mass balance equations and a simplified momentum balance known as the drift-flux formulation. These models can be discretized and implemented (for simulation) as a large set of ordinary differential equations (ODEs). Such flow simulators can be used to predict the pressure gradient in the well if all parameters are known and inputs (such as pump flows and choke flows) are measured and fed into the simulator. This is basically an open-loop estimation scheme as the estimation error is not used to adjust the future estimate. In (Fossil & Sangesland 2004) a new MPD concept which uses a modified version of OLGA 2000 to provide an estimate of the pressure profile in the annulus is presented. OLGA 2000 is a powerful multiphase flow simulator developed for the

petroleum industry (*SPT Group* 2007). The behavior of complex estimation schemes like these in conjunction with a control system is hard to analyze in a rigid manner. Verification by simulation or trials seem to be the preferred method to guarantee proper functionality.

The complexity is increased by the fact that many of the parameters in such models are uncertain/unknown and possibly slowly changing, which implies that they would need to be tuned as operating conditions change. This tuning can be done by an experienced operator or by using automatic tuning methods such as parameter estimation algorithms. In (Gravdal, Lorentzen, Fjelde & Vefring 2005) an unscented Kalman filter was used to update the friction estimate in both the drill string and the annulus. The scheme uses a measurement of the BHP to update the parameters every 30 seconds. Although no formal proofs are shown the estimation scheme shows promising behavior with better estimates of the BHP than without the unscented Kalman filter, and fairly accurate estimation of the friction factors.

Attempts at using low order models for control and estimation of the BHP can be found in (Nygaard, Imsland & Johannessen 2007) and (Nygaard, Johannessen, Gravdal & Iversen 2007). In (Nygaard, Imsland & Johannessen 2007) nonlinear model predictive control (NMPC) was used together with an unscented Kalman filter to control the BHP. A third order nonlinear model was used as the basis for the control and estimation design. The Kalman filter was used to estimate the states, and the friction and choke coefficients. The estimated parameters showed unwanted and unexplained spikes and oscillations during and after a pipe connection procedure. The BHP was kept fairly stable. In (Nygaard, Johannessen, Gravdal & Iversen 2007) it is shown that pressure variations in the BHP during surge and swab can be suppressed by controlling the choke and main pump. The control is based on a fourth order model and assumes that all parameters and the BHP is known, hence there is no estimation scheme involved.

1.4 Scope and Emphasis

The main goal for this thesis is to develop an adaptive observer, based on a low order model, that:

1. Estimates the bottomhole pressure during common drilling scenarios.
2. Adapts to key unknown parameters to give robustness to the estimate.
3. Provides rigid proofs and conditions for stability and convergence.
4. Facilitates for future control design.

The performance and robustness of the observer should be verified and analyzed through simulations. Due to time constraints the following assumptions will be made in the observer design:

- Only fluid phase
- No reservoir influx

Depending on the drilling conditions the first assumption can be justified if the amount of gas in the drilling mud is low. The second assumption should be removed as part of future work.

1.5 Thesis Outline

The thesis is divided into four main parts.

1. In Chapter 2 the low order model used as a basis for the observer design is derived. Inputs, disturbances and measurements are described.
2. In Chapter 3 observers based on a linearized version of the nonlinear model derived in Chapter 2 are presented. Important limitations in design based on the linearized model are pointed out. The chapter thus serves as an introduction to Chapter 4.
3. The main result of this thesis is presented in Chapter 4 where an adaptive observer based on the nonlinear model presented in Chapter 2 is derived.
4. In Chapter 5 simulations are presented to illustrate the performance of the observer derived in Chapter 4. In Chapter 6 conclusions are drawn, main contributions are highlighted and future work commented.

Chapter 2

Modeling

To facilitate the design of an observer a dynamic model for the system will be derived in this chapter. As stated in Section 1.4 only fluid phase flow will be considered. The third order model consists of nonlinear ODE's with a nonlinear measurement equation for the pressure at the bit. The model is originally developed in the internal document (Kaasa 2007), therefore the derivation will be shown here. A similar model for two phase flow in a well can be found in (Nygaard & Nævdal 2006).

For modeling purposes we divide the well into two separate compartments. Figure 2.1 shows the two control volumes considered, one control volume for the drill string and one for the annulus. The volumes are connected through the drill bit. There is a mud pump that pumps drilling mud into the drill string. Under normal conditions the mud flows from the pump through the drill string, the drill bit, and then up through the annulus and out through the choke. After the choke the mud is recycled and returned to the mud reservoir. The purpose of the drilling mud circulation is to clean out cuttings and to help maintain a correct pressure profile in the well bore. The pressure in the well bore at constant flow consist of three main components. The largest component is the hydrostatic weight of the mud, the second largest is the choke pressure and finally there is a pressure component due to friction (Brill & Mukherjee 1999). Equation (2.1) shows these main components for the steady state pressure at the bit ($p_{bit_{ss}}$), a more detailed derivation will follow later in this chapter.

$$p_{bit_{ss}} = \rho_a g h_{bit} + p_c + F_a |q_a| q_a \tag{2.1}$$

ρ_a is the density of the mud in the annulus, g is gravity, h_{bit} is the depth, p_c is the choke pressure, F_a is the friction factor and q_a is the volume flow in the annulus. From the equation we can see that changing the density ρ_a, choke pressure p_c or flow q_a will effect $p_{bit_{ss}}$. Changing ρ_a takes time as it is necessary to circulate out old mud before changes become effective. Changing p_c gives a much faster response as it can be controlled by using the choke opening. When the choke is fully closed p_c can be

increased by using the back-pressure pump. q_a can be changed by changing the flow through the mud pump.

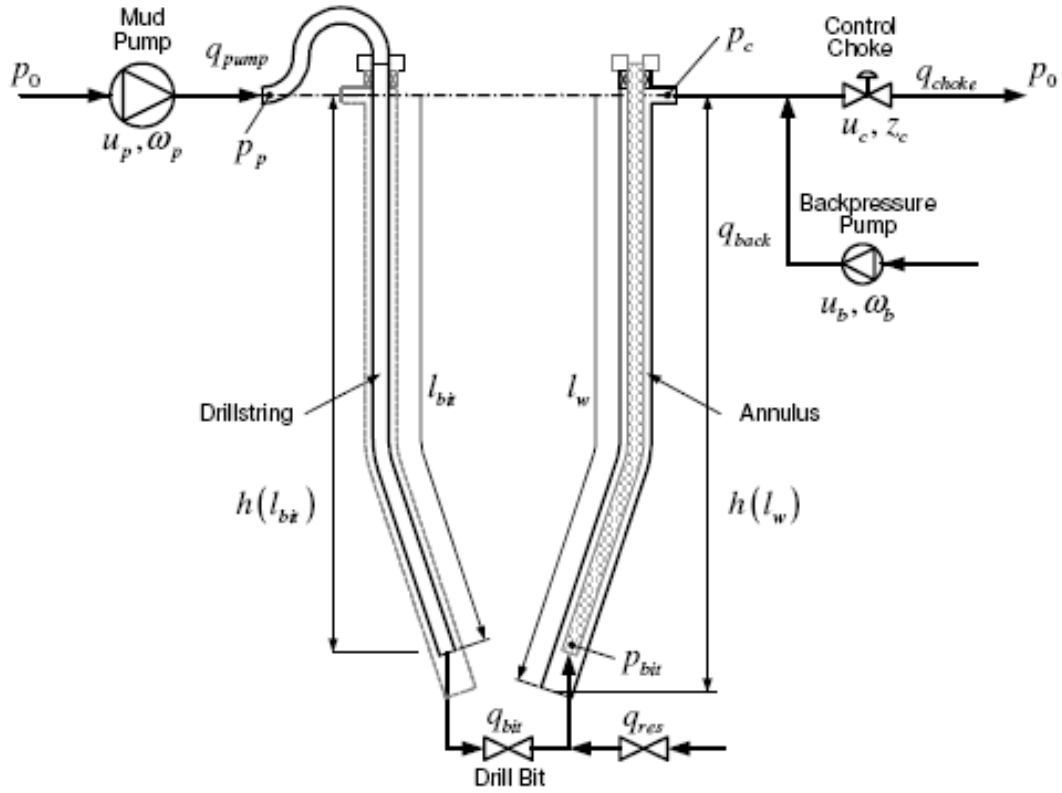

Figure 2.1: Division of system into two control volumes

2.1 Pressure dynamics

The model for the system in Figure 2.1 will be developed using mass and momentum balance relations. First, using the mass balance, expressions for the pressure dynamics will be found. The method used can be found in (Merrit 1967). Consider the control volume shown in Figure 2.2 with mass

$$m = \bar{\rho} V,$$

where $\bar{\rho}$ is the average density in the volume V defined by

$$\bar{\rho} = \frac{1}{V} \int_0^L \rho(x) A(x) \mathrm{d}x, \tag{2.2}$$

where L is the length of the volume in the x-direction and $A(x)$ is the cross-sectional area. For a circular pipe, $A(x) = \frac{\pi}{4} d_i(x)^2$ where $d_i(x)$ is the inner diameter. Conservation

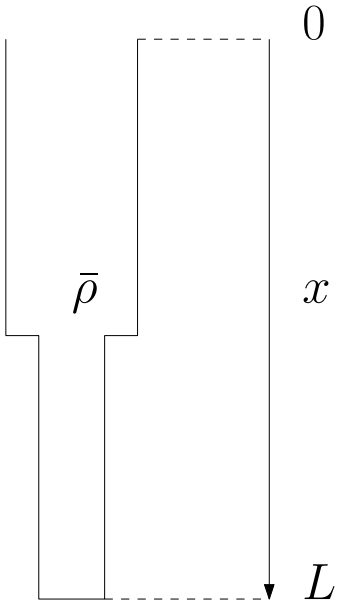

Figure 2.2: General Control Volume

of mass (m) gives

$$\begin{aligned} \sum m_{in} - \sum m_{out} &= \dot{m} \\ &= \frac{\mathrm{d}(\bar{\rho} V)}{\mathrm{d}t} \\ &= V \frac{\mathrm{d}\bar{\rho}}{\mathrm{d}t} + \bar{\rho} \frac{\mathrm{d}V}{\mathrm{d}t}. \end{aligned} \tag{2.3}$$

As we want to find an expression for the dynamics of the pressure we make the customary assumption (Egeland & Gravdahl 2002)

$$\frac{\mathrm{d}\rho}{\rho} = \frac{\mathrm{d}p}{\beta}, \tag{2.4}$$

where the assumption 1 has been made.

Assumption 1. Isothermal conditions in the fluid.

The bulk modulus β is given as (Merrit 1967)

$$\beta = -V_0 \left. \frac{\partial p}{\partial V} \right|_{T_0}. \tag{2.5}$$

Substituting (2.4) into (2.3) and using $\rho = \bar{\rho}$ and $p = \bar{p}$, where $\bar{p}$ is the average pressure in the control volume gives

$$\sum m_{in} - \sum m_{out} = V\frac{\bar{\rho}}{\beta}\frac{\mathrm{d}\bar{p}}{\mathrm{d}t} + \bar{\rho}\frac{\mathrm{d}V}{\mathrm{d}t} \tag{2.6}$$

$$\Rightarrow \frac{V}{\beta}\dot{\bar{p}} + \dot{V} = \frac{1}{\bar{\rho}}(\sum m_{in} - \sum m_{out}). \tag{2.7}$$

We further assume that:

Assumption 2. $\sum m_{in} = \sum q_{in}\bar{\rho}$ and $\sum m_{out} = \sum q_{out}\bar{\rho}$

This gives

$$\frac{V}{\beta}\dot{\bar{p}} + \dot{V} = \sum q_{in} - \sum q_{out}. \tag{2.8}$$

Making the assumption:

Assumption 3. The change w.r.t. time in average pressure is the same as the change in pressure anywhere in the control volume, $\dot{\bar{p}} = \dot{p}$.

Using assumption 3 and (2.8) gives

$$\frac{V}{\beta}\dot{p} + \dot{V} = \sum q_{in} - \sum q_{out}, \tag{2.9}$$

which describes the pressure dynamics anywhere in the control volume. Applying (2.9) to the control volume in the drill string, see Figure 2.1, we have one flow in from the main pump (q_{pump}) and one flow out through the bit (q_{bit}). The pressure dynamics for the pump pressure (p_p) is therefore given by

$$\frac{V_d}{\beta_d}\dot{p}_p = q_{pump} - q_{bit} - \dot{V}_d, \tag{2.10}$$

where V_d is the drill string volume and β_d is the bulk modulus of the drilling mud. As the drill string volume is constant between each pipe connection $\dot{V}_d = 0$ and (2.10) reduces to

$$\frac{V_d}{\beta_d}\dot{p}_p = q_{pump} - q_{bit}. \tag{2.11}$$

The same procedure for the control volume in the annulus gives the choke pressure dynamics, see Figure 2.1,

$$\frac{V_a}{\beta_a}\dot{p}_c = q_{bit} + q_{back} - q_{choke} + q_{res} - \dot{V}_a, \tag{2.12}$$

where $V_a(t)$ is time varying as the volume is dependent on drill string movements and drilling progress. q_{back} is the flow from the back pressure pump, q_{choke} is the flow through the choke and q_{res} is reservoir influx. The flow through the choke can be modeled by the classic orifice equation (Manring 2005)

$$q_{choke} = K_c z_c \sqrt{\frac{2}{\bar{\rho}_a}(p_c - p_0)}, \tag{2.13}$$

where the flow constant $K_c = A_c C_d$, with A_c being the valve opening at fully open valve and C_d being the discharge coefficient of the choke valve. $z_c \in [0\ 1]$ is the normalized choke opening and p_0 is the pressure at vena contracta which will be approximated with the pressure further downstream of the choke. Note that the orifice equation is based on assumptions of steady, incompressible, high-Reynholds-number flow (Manring 2005). The assumptions of steady and incompressible flow are not valid for our system. For simplicity these assumptions will be neglected when using (2.13).

2.2 Flow dynamics

Equations (2.11) and (2.12) describe the dynamics of the pump and choke pressure. They both depend on q_{bit}. Using the momentum balance the q_{bit} dynamics will be derived. One important simplification will be used in this derivation:

Assumption 4. ρ is constant in the flow dynamics, compressible flow effects due to pressure variations will be neglected, this implies that the flow will be considered rigid (q is constant along the flow path).

Using results found in (White 1999, p. 224) the momentum balance for a differential volume is

$$\sum F = \rho \frac{\mathrm{d}V}{\mathrm{d}t} \mathrm{d}x \mathrm{d}y \mathrm{d}z, \tag{2.14}$$

where $\sum F$ is the sum of forces acting on the differential volume, ρ is the mass density in the differential volume, and V is the velocity vector. For one-dimensional flow in the x-direction with cross-sectional area $A(x)$, (2.14) reduces to

$$\sum F_x = \rho \frac{\mathrm{d}u}{\mathrm{d}t} A(x) \mathrm{d}x, \tag{2.15}$$

where u is the velocity in the x-direction, see Figure 2.3. The forces acting on the differential volume in the x-direction are

$$\sum F_x = F_{surf} + F_{grav}. \tag{2.16}$$

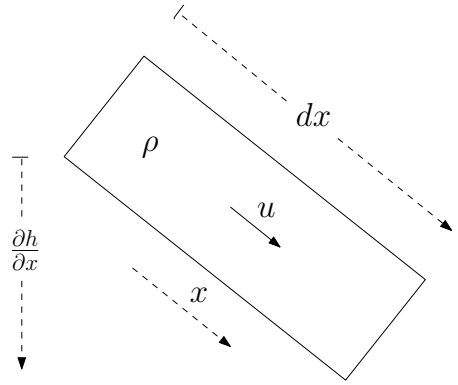

Figure 2.3: Differential Control Volume

F_{surf} is due to stresses on the sides of the control volume consisting of the hydrostatic pressure gradient plus the viscous stresses (friction). Hence $F_{surf} = -\frac{\partial p}{\partial x}A(x)\mathrm{d}x - \frac{\partial F_f}{\partial x}\mathrm{d}x$, where F_f is the friction force acting on the flow. F_{grav} is the gravity force in the x-direction and can be expressed as $F_{grav} = \rho g \frac{\partial h}{\partial x}A(x)\mathrm{d}x$, where $\frac{\partial h}{\partial x}$ is the depth gradient, see Figure 2.3. For a more detailed derivation of this result see (White 1999, ch. 4). Using (2.15), (2.16) and the above mentioned expressions we get

$$\rho\frac{\mathrm{d}u}{\mathrm{d}t}A(x)\mathrm{d}x = -\frac{\partial p}{\partial x}A(x)\mathrm{d}x - \frac{\partial F_f}{\partial x}\mathrm{d}x + \rho g\frac{\partial h}{\partial x}A(x)\mathrm{d}x \tag{2.17}$$

$$\Rightarrow \rho\frac{\mathrm{d}u}{\mathrm{d}t}\mathrm{d}x = -\partial p - \frac{1}{A(x)}\frac{\partial F_f}{\partial x}\mathrm{d}x + \rho g\,\partial h. \tag{2.18}$$

Inserting $q = A(x)u$, integrating (2.18) along the flow path (x-direction), using assumption 4 and replacing ρ with $\bar{\rho}$ defined in (2.2) gives

$$\begin{aligned}\int_0^l \frac{\bar{\rho}}{A(x)}\mathrm{d}x\frac{\mathrm{d}q}{\mathrm{d}t} &= -\int_{p(0)}^{p(l)}\partial p - \int_0^l \frac{1}{A(x)}\frac{\partial F_f}{\partial x}\mathrm{d}x + \int_{h(0)}^{h(l)}\bar{\rho}g\,\partial h \\ &= p(0) - p(l) - \int_0^l \frac{1}{A(x)}\frac{\partial F_f}{\partial x}\mathrm{d}x + \bar{\rho}g\left[h(l) - h(0)\right].\end{aligned} \tag{2.19}$$

Figure 2.1 explaines the notation. The pressure loss due to friction is given by the term $\int_0^l \frac{1}{A(x)}\frac{\partial F_f}{\partial x}\mathrm{d}x$. The expressions for the friction gradient, $\frac{\partial F_f}{\partial x}$, can be quite complex depending on amongst other the Reynolds number, density and geometry (White 1999, chp. 6). As the mud flow in the well is dynamic (volume flow changes, geometry changes, density changes) so will the friction gradient be. This complexity can be avoided by stating the pressure loss due to friction directly. Using formulations found in (Manring 2005), the loss can be divided into minor and major losses. Note that major and minor do not have anything to do with the size of the loss. Major losses are losses

that occur over straight sections of pipe while minor losses are losses due to bends in the flow path or obstructions such as valves. Figure 2.4 illustrates an example of how the system can be divided into major and minor loss sections. Section S_1 illustrates the main length of the drill string which would be a major loss. Section S_2 illustrates the bit (dynamics similar to a valve) which would be a minor loss. While S_3 and S_4 illustrate the annulus with a varying diameter, representing major losses.

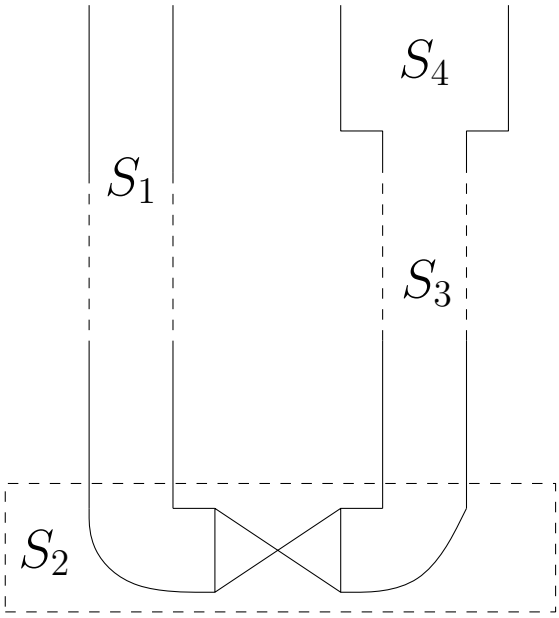

Figure 2.4: Sections of major and minor losses

A general expression for a major pressure loss is (where $u \geq 0$ has been assumed) (Manring 2005)

$$\Delta p_{maj} = f \frac{1}{2} \frac{l}{D} \rho u^2, \tag{2.20}$$

If the flow can flow both ways (no assumption on u) (2.20) can be written as

$$\Delta p_{maj} = f \frac{1}{2} \frac{l}{D} \rho |u| u, \tag{2.21}$$

where f is called the friction factor which is dependent on the Reynolds number, surface roughness and diameter. u is velocity, l is length and D diameter. The pressure loss from minor losses can be described in a similar manner as

$$\Delta p_{min} = K_l \frac{1}{2} \rho |u| u, \tag{2.22}$$

where K_l has to be determined experimentally and will according to dimensional analysis (Manring 2005) vary with the Reynolds number and the geometry. The total pressure loss due to friction in the drill string is thus simply the sum of all major and minor losses in the drill string. Using (2.21) and (2.22) this can be stated as

$$\Delta p_{fd} = \sum_i f_i \frac{1}{2} \rho_i \frac{l_i}{D_i} |u_i| u_i + \sum_i K_{l_i} \frac{1}{2} \rho_i |u_i| u_i. \tag{2.23}$$

Changing from velocity to volume flow using $u_i = \frac{q_i}{A_i}$ gives

$$\Delta p_{fd} = \sum_i f_i \frac{1}{2} \rho_i \frac{l_i}{A_i^2 D_i} |q_i| q_i + \sum_i K_{l_i} \frac{1}{2} \frac{\rho_i}{A_i^2} |q_i| q_i. \tag{2.24}$$

Using assumption 4 which implies $\rho_i = \rho = \bar{\rho} \ \forall \ i$, where $\bar{\rho}$ is the average density defined by (2.2), and $q_i = q \ \forall \ i$ gives

$$\Delta p_{fd} = \left[\sum_i f_i \frac{l_i}{A_i^2 D_i} + \sum_i \frac{K_{l_i}}{A_i^2} \right] \frac{1}{2} \bar{\rho} |q| q. \tag{2.25}$$

Defining

$$F_d = \left[\sum_i f_i \frac{l_i}{A_i^2 D_i} + \sum_i \frac{K_{l_i}}{A_i^2} \right] \frac{1}{2} \bar{\rho}, \tag{2.26}$$

gives

$$\Delta p_{fd} = F_d |q| q. \tag{2.27}$$

Similarly for the annulus we get

$$\Delta p_{fa} = \left[\sum_i f_i \frac{l_i}{A_i^2 D_i} + \sum_i \frac{K_{l_i}}{A_i^2} \right] \frac{1}{2} \bar{\rho} |q| q \tag{2.28}$$

$$= F_a |q| q. \tag{2.29}$$

Note that both F_d and F_a will change with operating conditions as the factors in (2.26) and (2.28) will vary. In the observer design later on this is an important reason for designing an observer that adapts to changes in friction.

Inserting (2.27) for the friction term in (2.19) the flow dynamics for the drill string (where the bit is considered a part of the drill string) are

$$\int_0^{L_{dN}} \frac{\bar{\rho}_d}{A_d(x)} \mathrm{d}x \frac{\mathrm{d}q_d}{\mathrm{d}t} = p_p - p_{bit} - F_d |q_d| q_d + \bar{\rho}_d g h_{bit}, \tag{2.30}$$

where L_{dN} is the total length of the drill string, q_d is the volume flow in the drill string, p_p is the pump pressure, p_{bit} is the pressure just after the bit and $h_{bit} = h(l_{bit})$. See Figure 2.1 for further description. Defining

$$M_d = \int_0^{L_{dN}} \frac{\bar{\rho}_d}{A_d(x)} \mathrm{d}x \tag{2.31}$$

$$= \bar{\rho}_d \int_0^{L_{dN}} \frac{1}{A_d(x)} \mathrm{d}x \tag{2.32}$$

simplifies (2.30) to

$$M_d \dot{q}_d = p_p - p_{bit} - F_d |q_d| q_d + \bar{\rho}_d g h_{bit}. \tag{2.33}$$

Deriving the dynamics for the volume flow in the annulus in a similar manner gives

$$M_a \dot{q}_a = p_{bit} - p_c - F_a |q_a| q_a - \bar{\rho}_a g h_{bit}, \tag{2.34}$$

where

$$M_a = \bar{\rho}_a \int_0^{l_w} \frac{1}{A_a(x)} \mathrm{d}x. \tag{2.35}$$

From Figure 2.1 and assumption 4 it can be seen that $q_{bit} = q_d$, where q_{bit} is the volume flow through the bit. It can also be seen that $q_a = q_{bit} + q_{res}$ where q_{res} is reservoir influx/out flux. Using these relations and adding (2.33) and (2.34) together gives

$$\begin{aligned} M_d \dot{q}_d + M_a \dot{q}_a &= p_p - p_{bit} - F_d |q_d| q_d + \bar{\rho}_d g h_{bit} + p_{bit} - p_c - F_a |q_a| q_a - \bar{\rho}_a g h_{bit} \\ &= p_p - p_c - F_d |q_d| q_d - F_a |q_a| q_a + (\bar{\rho}_d - \bar{\rho}_a) g h_{bit} \\ \Rightarrow M \dot{q}_{bit} &= p_p - p_c - F_d |q_{bit}| q_{bit} - F_a |q_{bit} + q_{res}| (q_{bit} + q_{res}) + (\bar{\rho}_d - \bar{\rho}_a) g h_{bit}, \end{aligned} \tag{2.36}$$

where $M = M_d + M_a$. Note that $\dot{q}_a = \dot{q}_{bit} + \dot{q}_{res} = \dot{q}_{bit}$ by the assumption:

Assumption 5. q_{res} is constant.

2.3 Model summary

A simplified model for control and observer design has been presented. The pressure dynamics are given by (2.11) and (2.12), while the volume flow dynamics are given by

(2.36). Summarizing the equations we have

$$\frac{V_d}{\beta_d}\dot{p}_p = q_{pump} - q_{bit} \tag{2.37}$$

$$\frac{V_a}{\beta_a}\dot{p}_c = q_{bit} + q_{back} - q_{choke} + q_{res} - \dot{V}_a \tag{2.38}$$

$$M\dot{q}_{bit} = p_p - p_c - F_d|q_{bit}|q_{bit} - F_a|q_{bit} + q_{res}|(q_{bit} + q_{res}) + (\bar{\rho}_d - \bar{\rho}_a)gh_{bit}. \tag{2.39}$$

As mentioned in the beginning of Chapter 2 the pressure profile in the well is of main concern. To limit the scope of this thesis only the pressure at the bit will be considered. Note that the bit is usually the place where the pressure margins are smallest. The pressure at the bit can be found from (2.33) giving

$$\begin{aligned} p_{bit} &= p_p - M_d\dot{q}_d - F_d|q_d|q_d + \bar{\rho}_d g h_{bit} \\ &= p_p - M_d\dot{q}_{bit} - F_d|q_{bit}|q_{bit} + \bar{\rho}_d g h_{bit}. \end{aligned} \tag{2.40}$$

It can also be found from (2.34) which gives

$$p_{bit} = p_c + M_a\dot{q}_a + F_a|q_a|q_a + \bar{\rho}_a g h_{bit}. \tag{2.41}$$

Inserting (2.39) for $\dot{q}_a$ and $q_a = q_{bit} + q_{res}$ gives

$$\begin{aligned} p_{bit} &= p_c + M_a\dot{q}_{bit} + F_a|q_{bit} + q_{res}|(q_{bit} + q_{res}) + \bar{\rho}_a g h_{bit} \\ &= \frac{M_a}{M}p_p + \frac{M_d}{M}p_c + (\frac{M_d}{M}F_a - \frac{M_a}{M}F_d)|q_{bit} + q_{res}|(q_{bit} + q_{res}) \\ &\quad + (\frac{M_d}{M}\bar{\rho}_a + \frac{M_a}{M}\bar{\rho}_d)g h_{bit}, \end{aligned} \tag{2.42}$$

where the steady state solution to (2.41) is (2.1) introduced in the beginning of this chapter. The derivation from (2.41) to (2.42) can be found in the appendix A.1.

2.3.1 Reservoir Influx/Out flux

The reservoir influx/out flux q_{res} can be both positive (reservoir fluids entering the well) or negative (mud loss). It is an unknown disturbance that enters in equations (2.38)–(2.42). The main complexity due to the reservoir flux is caused by the friction term in the annulus, $F_a|q_{bit} + q_{res}|(q_{bit} + q_{res})$. The friction term is very complex as it has both an absolute term and a multiplicative term involving an unknown disturbance. Therefore, to limit the scope of this thesis the reservoir influx will assumed to be zero.

Assumption 6. $q_{res} \equiv 0$

2.3.2 Constant Parameters and Time Varying Signals

The model presented in (2.37)– (2.42) has both constant parameters and time varying signals. $V_a(t)$ and $\dot{V}_a(t)$ are the volume and the change in volume of the annulus. They will change with drill string movement and drilling (which increases the volume). Drill string movements can be caused by surge or swab (moving the drill string down or up), heave (if drilling from a floater) or tripping (moving the drill string all the way out/in of/to the well). $h_{bit}(t)$ also varies with drill string movements and drilling. $M(t) = M_a(t) + M_d(t)$, further defined in (2.32) and (2.35), varies with the length of the well. To limit the scope of this thesis only $M = M(t) = constant$ will be considered here. Note that M only affects transient behavior, see equations (2.39) and (2.41). The density in the annulus ρ_a, the bulk modulus β_a and the friction factor $F = F_a + F_d$ all vary slowly due to the amount of cuttings and the length of the well. The following parameters are constant: V_d, β_d, $\bar{\rho}_d$, g.

2.3.3 Drill Bit Check Valve

To prevent flow from the annulus back into the drill string there is a check valve in the bit (Altermann, Bingham, Grayson, Linenberger, Mueller, Odelius & Taylor 2007). This implies that $q_{bit} \geq 0$. This physical constraint limits the validity of the model summarized in Section 2.3 as $\dot{q}_{bit}$ is not described by (2.39) for $q_{bit} = 0$. At $q_{bit} = 0$, $\dot{q}_{bit}$ can be described by

$$M\dot{q}_{bit} = \max\left\{0,\, p_p - p_c + (\bar{\rho}_d - \bar{\rho}_a)gh_{bit}\right\} \quad \text{for } q_{bit} = 0, \tag{2.43}$$

where assumption 6 has been used. This gives the complete model

$$M\dot{q}_{bit} = \begin{cases} p_p - p_c - (F_d + F_a)|q_{bit}|q_{bit} + (\bar{\rho}_d - \bar{\rho}_a)gh_{bit} & q_{bit} > 0 \\ \max\left\{0,\, p_p - p_c + (\bar{\rho}_d - \bar{\rho}_a)gh_{bit}\right\} & q_{bit} = 0 \end{cases}, \tag{2.44}$$

where the max function is defined as:

$$\max\{a, b\} = \begin{cases} a & a \geq b \\ b & a < b \end{cases}. \tag{2.45}$$

The added complexity in the q_{bit} dynamics will not only affect q_{bit} but more importantly it will affect p_{bit}, see equation (2.41), as $\dot{q}_{bit}$ enters the measurement equation. Furthermore it is not possible to use equation (2.40) for the pressure at the bit when the check valve is active as the pressure in the drill string does not affect p_{bit}. The complexity in (2.44) will directly affect the main results in this thesis derived in Chapter 4.

2.4 Measurements

2.4.1 Pressures

Standard measurements include measurement of top-side pressures, p_p and p_c. The down hole pressure p_{bit} is measured and transmitted to the surface through mud-pulse-telemetry (MPT). MPT requires a minimum flow velocity to function hence this measurement is not available at pipe connections. MPT also has low sampling rate (Kaasa 2007) and it is unreliable as the pressure sensor operates in a harsh environment. Due to these impediments the p_{bit} measurement will not be used for estimation.

2.4.2 Flows

For pump volume flows q_{pump} and q_{back} there might be flow meters, if not, one can estimate the volume flow by using the known pump speeds (ω_p), the number of pistons (N_p) and volume per stroke per piston (V_p) according to

$$\begin{aligned} q_{pump} &= N_p V_p 2\pi \omega_p \\ &= K_p \omega_p, \end{aligned} \tag{2.46}$$

where pump leakage has been neglected. The volume flow through the choke, q_{choke} is sometimes measured with a flow meter. If not it can be estimated using the relationship given in equation (2.13).

2.4.3 Geometry

Drill string geometry is well known as both length and drill pipe dimensions are measured/known. Annulus geometry is well known as bore hole diameter and casing geometry is well known. The depth of the bit h_{bit} is measured. Hence $h_{bit}(t)$, $V_a(t)$, $\dot{V}_a(t)$ and V_d are known signals. $h_{bit}(t)$, $V_a(t)$ and $\dot{V}_a(t)$ will be treated as known disturbances while V_d will be treated as a constant. To summarize, the measurement assumption is:

Assumption 7.

- p_p and p_c are measured
- p_{bit} is measured at low sampling rate and is unreliable
- q_{pump}, q_{back} and q_{choke} are measured
- $h_{bit}(t)$, $V_a(t)$ and $\dot{V}_a(t)$ are measured
- V_d is known

Chapter 3

Linear Observer Design

In this chapter an adaptive observer based on a linearized version of the model summarized in Section 2.3 will be derived. The observer will try to estimate the BHP (p_{bit}), and adapt to an unknown friction parameter in the annulus. Due to the serious limitations in using a linear model, the designs proposed in this chapter should be seen as an introduction to the main result of this thesis, presented in Chapter 4, not as a design that should be used. Before the adaptive observer is derived, the state space model defined in (2.37) – (2.39) and the measurement equation (2.42) will be linearized and a multiple input multiple output (MIMO) linear observer will be designed. Only the case where $q_{bit} > 0$ will be considered. The goals for this chapter are:

- Find a linear model that is suitable for linear observer design.
- Design a linear observer.
- Design an adaptive observer that adapts to an unknown friction parameter.

3.1 Linearization of State Space Model

The model defined by equations (2.37) – (2.39) and (2.42) is, using assumption 6 ($q_{res} = 0$)

$$\frac{V_d}{\beta_d}\dot{p}_p = q_{pump} - q_{bit} \tag{3.1}$$

$$\frac{V_a}{\beta_a}\dot{p}_c = q_{bit} + q_{back} - q_{choke} - \dot{V}_a \tag{3.2}$$

$$M\dot{q}_{bit} = p_p - p_c - (F_d + F_a)|q_{bit}|q_{bit} + (\bar{\rho}_d - \bar{\rho}_a)gh_{bit} \tag{3.3}$$

$$p_{bit} = \frac{M_a}{M}p_p + \frac{M_d}{M}p_c + (\frac{M_d}{M}F_a - \frac{M_a}{M}F_d)|q_{bit}|q_{bit} + (\frac{M_d}{M}\bar{\rho}_a + \frac{M_a}{M}\bar{\rho}_d)gh_{bit}. \tag{3.4}$$

Defining the state (x), input (u), and known time varying disturbance (v) vectors to be

$$x = \begin{bmatrix} p_p \\ p_c \\ q_{bit} \end{bmatrix} \quad u = \begin{bmatrix} q_{pump} \\ q_{back} - q_{choke} \end{bmatrix} \quad v = \begin{bmatrix} V_a \\ \dot{V}_a \\ h_{bit} \end{bmatrix}. \tag{3.5}$$

Inserting these definitions into (3.1) – (3.4) gives

$$\frac{V_d}{\beta_d}\dot{x}_1 = u_1 - x_3 \tag{3.6}$$

$$\frac{v_1}{\beta_a}\dot{x}_2 = x_3 + u_2 - v_2 \tag{3.7}$$

$$M\dot{x}_3 = x_1 - x_2 - (F_d + F_a)|x_3|x_3 + (\bar{\rho}_d - \bar{\rho}_a)g\,v_3 \tag{3.8}$$

$$p_{bit} = \frac{M_a}{M}x_1 + \frac{M_d}{M}x_2 + (\frac{M_d}{M}F_a - \frac{M_a}{M}F_d)|x_3|x_3 + (\frac{M_d}{M}\bar{\rho}_a + \frac{M_a}{M}\bar{\rho}_d)g\,v_3. \tag{3.9}$$

Defining

$$f_1(x,u) = \frac{\beta_d}{V_d}(u_1 - x_3) \tag{3.10}$$

$$f_2(x,u,v) = \frac{\beta_a}{v_1}(x_3 + u_2 - v_2) \tag{3.11}$$

$$f_3(x,v) = \frac{1}{M}(x_1 - x_2 - (F_d + F_a)|x_3|x_3 + (\bar{\rho}_d - \bar{\rho}_a)g\,v_3) \tag{3.12}$$

$$h(x,v) = \frac{M_a}{M}x_1 + \frac{M_d}{M}x_2 + (\frac{M_d}{M}F_a - \frac{M_a}{M}F_d)|x_3|x_3 + (\frac{M_d}{M}\bar{\rho}_a + \frac{M_a}{M}\bar{\rho}_d)g\,v_3, \tag{3.13}$$

results in a more compact formulation

$$\dot{x} = f(x,u,v) \tag{3.14}$$

$$p_{bit} = h(x,v), \tag{3.15}$$

where f is a vector consisting of f_1, f_2 and f_3.

The compact model stated in (3.14) and (3.15) can be linearized around a solution $(x^0(t), u^0(t))$ where $v(t)$ will be treated as a known time varying signal. Using the approach found in (Egeland & Gravdahl 2002) we get

$$\dot{x}^0(t) = f(x^0(t), u^0(t), v(t)). \tag{3.16}$$

Defining the perturbations in x, u and p_{bit} as

$$x(t) = x^0(t) + \Delta x(t) \tag{3.17}$$
$$u(t) = u^0(t) + \Delta u(t) \tag{3.18}$$
$$p_{bit}(t) = h(x^0(t), v(t)) + \Delta p_{bit} \tag{3.19}$$
$$= p^0(t) + \Delta p_{bit}, \tag{3.20}$$

and using a Taylor series expansion around $(x^0(t), u^0(t))$ gives

$$\dot{x} = f(x^0(t), u^0(t), v(t)) + \left.\frac{\partial f}{\partial x}\right|_{x^0(t)} \Delta x + \left.\frac{\partial f}{\partial u}\right|_{u^0(t)} \Delta u \tag{3.21}$$
$$p_{bit} = h(x^0(t), v(t)) + \left.\frac{\partial h}{\partial x}\right|_{x^0(t)} \Delta x. \tag{3.22}$$

Inserting (3.16) into (3.21) and comparing the result with the derivative w.r.t. time of (3.17) gives

$$\Delta\dot{x} = \left.\frac{\partial f}{\partial x}\right|_{(x^0(t),u^0(t))} \Delta x + \left.\frac{\partial f}{\partial u}\right|_{(x^0(t),u^0(t))} \Delta u. \tag{3.23}$$

Inserting (3.22) into (3.19) gives

$$\Delta p_{bit} = \left.\frac{\partial h}{\partial x}\right|_{x^0(t)} \Delta x. \tag{3.24}$$

Define the matrices A , B and C as

$$A(x^0(t), u^0(t), v(t)) = \left.\frac{\partial f}{\partial x}\right|_{(x^0(t),u^0(t))} \tag{3.25}$$
$$B(x^0(t), u^0(t), v(t)) = \left.\frac{\partial f}{\partial u}\right|_{(x^0(t),u^0(t))} \tag{3.26}$$
$$C(x^0(t)) = \left.\frac{\partial h}{\partial x}\right|_{x^0(t)}. \tag{3.27}$$

Using (3.10) – (3.12) and (3.13) A, B and C can be expressed as

$$A(x^0(t), v(t)) = \begin{bmatrix} 0 & 0 & -\frac{\beta_d}{V_d} \\ 0 & 0 & \frac{\beta_a}{v_1} \\ \frac{1}{M} & \frac{-1}{M} & \frac{-2(F_d+F_a)|x_3^0(t)|}{M} \end{bmatrix} \tag{3.28}$$

$$B(x^0(t), u^0(t), v(t)) = B(v(t)) = \begin{bmatrix} \frac{\beta_d}{v_d} & 0 \\ 0 & \frac{\beta_a}{v_1} \\ 0 & 0 \end{bmatrix} \tag{3.29}$$

$$C(x^0(t)) = \begin{bmatrix} \frac{M_a}{M} \\ \frac{M_d}{M} \\ 2\left(\frac{M_d}{M}F_a - \frac{M_a}{M}F_d\right)|x_3^0(t)| \end{bmatrix}^T, \tag{3.30}$$

where the relationship

$$\begin{aligned} \frac{\partial |x| x}{\partial x} &= \begin{cases} \frac{\partial x^2}{\partial x} & x \geq 0 \\ -\frac{\partial x^2}{\partial x} & x < 0 \end{cases} \\ &= \begin{cases} 2x & x \geq 0 \\ -2x & x < 0 \end{cases} \\ &= 2|x|, \end{aligned} \tag{3.31}$$

has been used.

A linearized model for the system described by (3.1) – (3.4) has been developed. The model is valid for small perturbations $(\Delta x, \Delta u)$ around the solution $(x^0(t), u^0(t))$. The equations defining the model are (3.17)–(3.19), (3.23) and (3.24), summarized compactly in Table 3.1. Note that the solution $(x^0(t), u^0(t))$ selected is usually chosen to be steady state solution thereby satisfying $\dot{x}_0 = f(x^0(t), u^0(t), v(t)) = 0$.

Table 3.1: Linearized model

Nonlinear system	$\dot{x} = f(x,u,v)$ $p_{bit} = h(x,v)$ $x = \begin{bmatrix} p_p & p_c & q_{bit} \end{bmatrix}^T$
Linearized system	$\Delta\dot{x} = A(x^0(t), v(t))\Delta x + B(v(t))\Delta u(t)$ $\Delta p_{bit} = C(x^0(t))\Delta x$
Perturbations	$x(t) = x^0(t) + \Delta x(t)$ $u(t) = u^0(t) + \Delta u(t)$ $p_{bit}(t) = h(x^0(t), v(t)) + \Delta p_{bit}$
Design Choices	Solution $(x^0(t), u^0(t))$ that satisfies, $\dot{x}_0 = f(x^0(t), u^0(t), v(t))$

3.2 Reduced Order Linear Observer

As stated in Section 2.4.1 the pressures p_c and p_p are both measured reliably, while the measurement of p_{bit} is encumbered with slow sampling, and during pipe connections, it is not available. In this section a reduced order observer will be designed for the linear time varying (LTV) system found in the previous section, see Table 3.1. We will assume that $(x^0(t), u^0(t))$ has been chosen and that M_d and M_a, see (3.28)-(3.30), are constant. The observer will estimate the unmeasured state Δx_3. Using the estimated Δx_3 and the measured states Δx_1 and Δx_2 an estimate of the output Δp_{bit} will be constructed. The system considered is

$$\Delta\dot{x} = A(t)\Delta x + B(t)\Delta u(t) \tag{3.32}$$
$$\Delta p_{bit} = C(t)\Delta x, \tag{3.33}$$

where Δx_1 and Δx_2 are measured and, see (3.28)–(3.30),

$$A(t) = \begin{bmatrix} 0 & 0 & a_{13} \\ 0 & 0 & a_{23}(t) \\ a_{31} & -a_{31} & a_{33}(t) \end{bmatrix} \tag{3.34}$$

$$B(t) = \begin{bmatrix} b_{11} & 0 \\ 0 & b_{22}(t) \\ 0 & 0 \end{bmatrix} \quad C(t) = \begin{bmatrix} c_1 \\ c_2 \\ c_3(t) \end{bmatrix}^T, \tag{3.35}$$

where $b_{22}(t)$, $a_{23}(t)$ are bounded since the volume in the annulus $v_1 \geq c > 0$. And $a_{33}(t)$, $c_3(t)$ are bounded by assuming $|x_3^0(t)|$ bounded.

3.2.1 Observer for Δx_3

For the observer design we will assume that Δx and Δu are bounded. Using an approach similar to one found in (Narendra & Annaswamy 1989) we divide the states (3.32) into measured and unmeasured states,

$$\left.\begin{aligned} \Delta\dot{x}_1 &= a_{13}\Delta x_3 + b_{11}\Delta u_1 \\ \Delta\dot{x}_2 &= a_{23}(t)\Delta x_3 + b_{22}(t)\Delta u_2 \end{aligned}\right\} \text{Measured} \tag{3.36}$$

$$\Delta\dot{x}_3 = a_{31}\Delta x_1 - a_{31}\Delta x_2 + a_{33}(t)\Delta x_3 \quad \text{Unmeasured.} \tag{3.37}$$

Note that (3.36) implies that the system is observable, since Δx_1 and Δx_2 are measured, hence it should be possible to design an observer for Δx_3. For a definition of observability for LTV systems see e.g. (Skelton, Iwasaki & Grigoriadis 1998). Define the observer to be

$$\Delta\widehat{x}_3 = \xi - l_1\Delta x_1 - l_2\Delta x_2 \tag{3.38}$$

$$\dot{\xi} = F\xi + g_1\Delta x_1 + g_2\Delta x_2 + h_1\Delta u_1 + h_2\Delta u_2. \tag{3.39}$$

The estimation error is defined as

$$e = \Delta x_3 - \Delta\widehat{x}_3. \tag{3.40}$$

Differentiating (3.40) w.r.t. time the dynamics of the estimation error are

$$\dot{e} = \Delta\dot{x}_3 - \Delta\dot{\widehat{x}}_3.$$

Differentiating (3.38) w.r.t. time and inserting for $\Delta\dot{\widehat{x}}_3$.

$$\dot{e} = \Delta\dot{x}_3 - \dot{\xi} + l_1\Delta\dot{x}_1 + l_2\Delta\dot{x}_2$$

Using (3.36),(3.37) and (3.39) with $\xi = \Delta\widehat{x}_3 + l_1\Delta x_1 + l_2\Delta x_2$ gives

$$\begin{aligned}\dot{e} &= a_{31}\Delta x_1 - a_{31}\Delta x_2 + a_{33}\Delta x_3 - F(\Delta\widehat{x}_3 + l_1\Delta x_1 + l_2\Delta x_2) - g_1\Delta x_1 \\ &\quad - g_2\Delta x_2 + l_1(a_{13}\Delta x_3 + b_{11}\Delta u_1) + l_2(a_{23}\Delta x_3 + b_{22}\Delta u_2) - h_1\Delta u_1 - h_2\Delta u_2 \\ &= (a_{33} + l_1a_{13} + l_2a_{23})\Delta x_3 - F\Delta\widehat{x}_3 + (a_{31} - Fl_1 - g_1)\Delta x_1 \\ &\quad + (-a_{31} - Fl_2 - g_2)\Delta x_2 + (-h_1 + l_1b_{11})\Delta u_1 + (-h_2 + l_2b_{22})\Delta u_2. \qquad (3.41)\end{aligned}$$

From (3.40) we have $\Delta\widehat{x}_3 = \Delta x_3 - e$, inserting this gives

$$\begin{aligned}\dot{e} &= (a_{33} + l_1a_{13} + l_2a_{23})\Delta x_3 - F(\Delta x_3 - e) + (a_{31} - Fl_1 - g_1)\Delta x_1 \\ &\quad + (-a_{31} - Fl_2 - g_2)\Delta x_2 + (-h_1 + l_1b_{11})\Delta u_1 + (-h_2 + l_2b_{22})\Delta u_2 \\ &= Fe + (a_{33} + l_1a_{13} + l_2a_{23} - F)\Delta x_3 + (a_{31} - Fl_1 - g_1)\Delta x_1 \\ &\quad + (-a_{31} - Fl_2 - g_2)\Delta x_2 + (-h_1 + l_1b_{11})\Delta u_1 + (-h_2 + l_2b_{22})\Delta u_2. \qquad (3.42)\end{aligned}$$

To zero out the terms multiplying Δx_3, Δx_2, Δx_1, Δu_1 and Δu_2 we choose

$$F(t) = a_{33}(t) + l_1a_{13} + l_2a_{23}(t) \qquad (3.43)$$
$$g_1(t) = a_{31} - F(t)l_1 \qquad (3.44)$$
$$g_2(t) = -a_{31} - F(t)l_2 \qquad (3.45)$$
$$h_1 = l_1b_{11} \qquad (3.46)$$
$$h_2(t) = l_2b_{22}(t), \qquad (3.47)$$

where the dependence on t has been included. This gives

$$\dot{e} = F(t)e \Rightarrow e(t) = e(0)\exp^{\int_0^t F(\tau)d\tau}, \qquad (3.48)$$

which implies that $e(t) = \Delta x_3 - \Delta\widehat{x}_3$ converges to zero exponentially if $\int_0^t F(\tau)d\tau < 0\ \forall\ t$. Conditions on the gains l_1 and l_2 such that $\int_0^t F(\tau)d\tau < 0\ \forall\ t$ will now be found. Using (3.43) we have

$$\int_0^t F(\tau)d\tau = \int_0^t a_{33}(\tau) + l_1a_{13} + l_2a_{23}(\tau)d\tau.$$

Since $a_{33}(t) = -\frac{2(F_d+F_a)|x_0^3(t)}{M} \leq 0\ \forall\ t$ we get

$$\begin{aligned}\int_0^t a_{33}(\tau) + l_1a_{13} + l_2a_{23}(\tau)d\tau &\leq \int_0^t l_1a_{13} + l_2a_{23}(\tau)d\tau \\ &< 0 \quad \text{for} \quad l_1a_{13} + l_2a_{23}(t) < 0\ \ \forall \quad t. \qquad (3.49)\end{aligned}$$

Using the fact that $a_{13} < 0$ and $a_{23}(t) > 0\ \forall\ t$ and therefore choosing $l_1 > 0$ and $l_2 < 0$ satisfies (3.49). To summarize, the estimate $\Delta\widehat{x}_3(t)$ defined by equations (3.38) and (3.39) converges exponentially to the true state $\Delta x_3(t)$ for any initial conditions provided the gains are chosen to satisfy (3.43) – (3.47) and (3.49). The convergence rate can be made arbitrarily fast by proper choice of l_1 and l_2.

3.2.2 Convergence of $\Delta\tilde{p}_{bit}$

The observer designed in the previous section exponentially tracks the unmeasured state, but what happens to the estimation error in Δp_{bit}? Constructing the estimate of Δp_{bit} as

$$\Delta\widehat{p}_{bit} = c_1\Delta x_1 + c_2\Delta x_2 + c_3(t)\Delta\widehat{x}_3, \tag{3.50}$$

gives the estimation error, see (3.33),

$$\begin{aligned}\Delta\tilde{p}_{bit} &= \Delta p_{bit} - \Delta\widehat{p}_{bit} &(3.51)\\ &= c_3(t)\Delta\tilde{x}_3. &(3.52)\end{aligned}$$

As $c_3(t)$ is bounded and $\tilde{x}_3$ converges exponentially to zero, $\Delta\tilde{p}_{bit}$ converges exponentially to zero and the convergence rate can be made arbitrarily fast by proper choice of l_1 and l_2.

3.2.3 Example, Observer

To illustrate some of the functionality of the designed observer a simulation was carried out. The observer was based on a linear model around the steady state solution to the nonlinear system (3.1) – (3.3) with

$$\begin{aligned}q_{pump} = -q_{choke} &= 1000\frac{l}{min} &(3.53)\\ q_{back} = \dot{V}_a &= 0 &(3.54)\\ h_{bit} &= 2000\,m, &(3.55)\end{aligned}$$

which gives

$$u_1^0 = u_2^0 = x_3^0 = 1000\frac{l}{min}. \tag{3.56}$$

Using (3.2) and the orifice equation (2.13) with $x_2 = p_c$ gives

$$\begin{aligned}0 &= x_3^0 + q_{back} - q_{choke}\\ &= x_3^0 - K_c z_c\sqrt{\frac{2}{\bar{\rho}_a}(x_2^0 - p_0)}\\ \Rightarrow x_2^0 &= \frac{\bar{\rho}_a}{2}\left(\frac{1}{K_c z_c^0}x_3^0\right)^2 + p_0) = 86.6 \quad z_c \neq 0. &(3.57)\end{aligned}$$

For x_1^0 we use (3.3) to find the last element x_1^0 to be

$$x_1^0(t) = x_2^0(t) + (F_d + F_a)|x_3^0(t)|x_3^0(t) - (\bar{\rho}_d - \bar{\rho}_a)gh_{bit} = 126. \tag{3.58}$$

Table 3.2: Parameter values for simulation of linear observer

Parameter	Value	Description
V_d	28.2743	Volume drill string (m^3)
β_d	14000	Bulk modulus drill string (bar)
V_a	96.1327	Volume annulus (m^3)
β_a	14000	Bulk modulus annulus (bar)
K_c	0.0046	Choke valve constant
z_c^0	0.04	Normalized choke valve opening
p_0	1	Pressure outside system (bar)
$\bar{\rho}_a$	0.0119	Density annulus ($10^{-5} \times \frac{kg}{m^3}$)
$\bar{\rho}_d$	0.0125	Density drill string ($10^{-5} \times \frac{kg}{m^3}$)
F_d	165000	Friction factor drill string
F_a	20800	Friction factor annulus
M_a	1.6009×10^3	($10^{-5} \times \frac{kg}{m^4}$)
M_d	5.7296×10^3	($10^{-5} \times \frac{kg}{m^4}$)

The parameters used are shown in Table 3.2.

In the simulation the nonlinear model (3.1) – (3.4) was considered the true system and the observer was used to estimate $x_3(t)$ and $p_{bit}(t)$ using equations (3.17), (3.19) and (3.50) in the following manner

$$\widehat{q}_{bit}(t) = x_3^0 + \Delta\widehat{x}_3(t) \tag{3.59}$$

$$\widehat{p}_{bit}(t) = h(x^0, v(t)) + \Delta\widehat{p}_{bit} \tag{3.60}$$

$$= h(x^0, v(t)) + c_1\Delta x_1 + c_2\Delta x_2 + c_3(t)\Delta\widehat{x}_3. \tag{3.61}$$

The gains in the observer were chosen to be $l_1 = 5 \times 10^{-3}$ and $l_2 = -5 \times 10^{-3}$. The initial condition $\xi(0) = 0$. The simulation consisted of three parts. After an initial period to allow the system to reach steady state the choke valve was opened at $t = 2\ min$ giving an increased flow $-u_2 = q_{choke}$ through the valve, see Figure 3.1(d). This results in a small perturbation away from (x^0, u^0). From figures 3.1(a) and 3.1(b) it can be seen that $\widehat{q}_{bit}$ follows q_{bit} with a very small deviation. As a consequence the estimated BHP $\widehat{p}_{bit}$ follows p_{bit} well, see Figure 3.1(c). Note that the gains l_1 and l_2 can be increased to give a smaller deviation but at the same time this will amplify noise. In the second part of the simulation ($t = 8\ min$), the choke valve is tightened back to its original setting which gives a similar response as before. The third part ($t = 14 min$) consist of a reduction of the main pump flow to $500\frac{l}{min}$, see Figure 3.1(d). Due to the reduction the steady state $q_{bit_{ss}} = 500\frac{l}{min} \neq x_3^0$ which uncovers a major weakness of the observer. It only gives a good estimate as long as the solution stays around x_3^0.

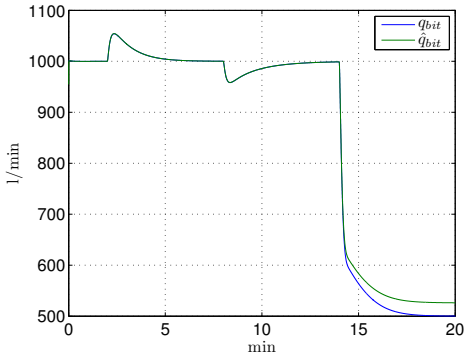

(a) q_{bit} and $\widehat{q}_{bit}$

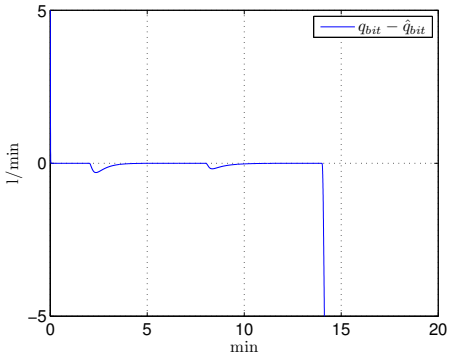

(b) $\tilde{q}_{bit} = q_{bit} - \widehat{q}_{bit}$

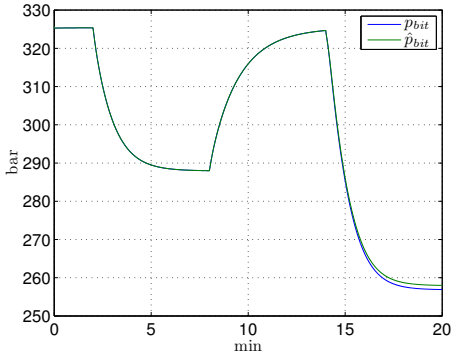

(c) p_{bit} and $\widehat{p}_{bit}$

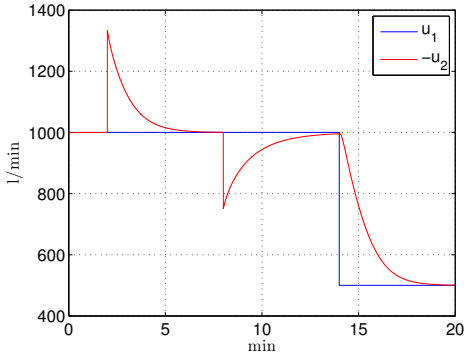

(d) Main pump flow u_1 and flow through choke $-u_2$

Figure 3.1: Simulation results linear observer

3.3 Adaptive Observer

As mentioned in Chapter 2 the friction parameter in the annulus F_a, see equation (2.28), is slowly changing and unknown. Therefore the observer should simultaneously estimate q_{bit} and F_a. In this section an adaptive observer based on the LTV model in Table 3.1 will be designed. The main purpose of this design is to serve as an introduction to the adaptive observer design in Chapter 4 and to highlight some of the short comings of an approach based on a linear model. Considering the same system as in the previous section

$$\Delta\dot{x} = A(t)\Delta x + B(t)\Delta u(t) \tag{3.62}$$
$$\Delta p_{bit} = C(t)\Delta x, \tag{3.63}$$

where Δx_1 and Δx_2 are measured and

$$A(t) = \begin{bmatrix} 0 & 0 & a_{13} \\ 0 & 0 & a_{23}(t) \\ a_{31} & -a_{31} & a_{33}(t) \end{bmatrix} \tag{3.64}$$

$$B(t) = \begin{bmatrix} b_{11} & 0 \\ 0 & b_{22}(t) \\ 0 & 0 \end{bmatrix} \quad C(t) = \begin{bmatrix} c_1 \\ c_2 \\ c_3(t) \end{bmatrix}^T, \tag{3.65}$$

with $a_{23}(t) = \frac{\beta_a}{v_1}$, $a_{33}(t) = \frac{-2(F_d+F_a)|x_3^0(t)|}{M}$ and $c_3(t) = 2(\frac{M_d}{M}F_a - \frac{M_a}{M}F_d)|x_3^0(t)|$, from the definition of A, B and C in (3.28)–(3.30). We will only consider the case where $x_3^0(t) = x_3^0$ is a positive constant. As a_{33} is dependent on F_a we will simply denote $\theta = a_{33}$ and estimate θ. An estimate of F_a can then be found as $\widehat{F}_a = \frac{-\widehat{\theta}M}{2x_3^0(t)} - F_d$, where $\widehat{\theta}$ is an estimate of θ. Using a similar approach as in Section 3.2.1, we divide the states (3.23) into measured and unmeasured states according to

$$\left.\begin{aligned} \Delta\dot{x}_1 &= a_{13}\Delta x_3 + b_{11}\Delta u_1 \\ \Delta\dot{x}_2 &= a_{23}(t)\Delta x_3 + b_{22}(t)\Delta u_2 \end{aligned}\right\} \text{Measured} \tag{3.66}$$

$$\Delta\dot{x}_3 = a_{31}\Delta x_1 - a_{31}\Delta x_2 + \theta\Delta x_3 \quad \text{Unmeasured.} \tag{3.67}$$

As in the previous section we will assume that Δx and Δu are bounded.

3.3.1 Error dynamics

Motivated by the approach found in (Tan, Kanellakopoulos & Jiang 1998), define the change of coordinates

$$\xi = \Delta x_3 + l_1\Delta x_1, \tag{3.68}$$

where l_1 is an injection gain. Note that it is possible to include feedback from Δx_2. This might give better noise attenuating but has been omitted for simplicity. Differentiating (3.68) w.r.t. time, the dynamics for ξ are

$$\begin{aligned}\dot{\xi} &= \Delta\dot{x}_3 + l_1\Delta\dot{x}_1 \\ &= a_{31}\Delta x_1 - a_{31}\Delta x_2 + \theta\Delta x_3 + l_1(a_{13}\Delta x_3 + b_{11}\Delta u_1) \\ &= a_{31}\Delta x_1 - a_{31}\Delta x_2 + (\theta + l_1 a_{13})\Delta x_3 + l_1 b_{11}\Delta u_1. \end{aligned} \tag{3.69}$$

Let the estimate of Δx_3 be denoted $\Delta\widehat{x}_3$ and the estimate of θ be denoted as $\widehat{\theta}$. An observer for Δx_3 is

$$\Delta\widehat{x}_3 = \widehat{\xi} - l_1\Delta x_1 \tag{3.70}$$

$$\dot{\widehat{\xi}} = a_{31}\Delta x_1 - a_{31}\Delta x_2 + (\widehat{\theta} + l_1 a_{13})\Delta\widehat{x}_3 + l_1 b_{11}\Delta u_1. \tag{3.71}$$

The estimation error is, using (3.68) and (3.70),

$$\Delta\tilde{x}_3 = \Delta x_3 - \Delta\widehat{x}_3 = \xi - \widehat{\xi} = \tilde{\xi}. \tag{3.72}$$

Using (3.69) and (3.71) the estimation error dynamics are can be found to be

$$\begin{aligned}\dot{\tilde{\xi}} &= \dot{\xi} - \dot{\widehat{\xi}} \\ &= (\theta + l_1 a_{13})\Delta x_3 - (\widehat{\theta} + l_1 a_{13})\Delta\widehat{x}_3 \\ &= \theta\Delta x_3 - \widehat{\theta}\Delta\widehat{x}_3 + l_1 a_{13}\Delta\tilde{x}_3 \end{aligned} \tag{3.73}$$

As $\theta\Delta x_3 - \widehat{\theta}\Delta\widehat{x}_3 = \theta\Delta x_3 - \theta\Delta\widehat{x}_3 + \theta\Delta\widehat{x}_3 - \widehat{\theta}\Delta\widehat{x}_3 = \theta\Delta\tilde{x}_3 + \tilde{\theta}\Delta\widehat{x}_3$ the error dynamics can be written as

$$\begin{aligned}\dot{\tilde{\xi}} &= \theta\Delta\tilde{x}_3 + \tilde{\theta}\Delta\widehat{x}_3 + l_1 a_{13}\Delta\tilde{x}_3 \\ &= (\theta + l_1 a_{13})\Delta\tilde{x}_3 + \tilde{\theta}\Delta\widehat{x}_3 \\ &= (\theta + l_1 a_{13})\tilde{\xi} + \tilde{\theta}\Delta\widehat{x}_3, \end{aligned} \tag{3.74}$$

where (3.72) has been used.

3.3.2 Lyapunov analysis

For the error system described by the ξ-dynamics in (3.74), and $\tilde{\theta}$ dynamics to be decided consider the Lyapunov function candidate

$$V(\tilde{\xi}, \tilde{\theta}) = \frac{1}{2}\tilde{\xi}^2 + \frac{1}{2\gamma}\tilde{\theta}^2 \tag{3.75}$$

Where $\gamma > 0$. Differentiating w.r.t. time and using (3.74) gives

$$\begin{aligned}\dot{V} &= \tilde{\xi}\dot{\tilde{\xi}} + \frac{1}{\gamma}\tilde{\theta}\dot{\tilde{\theta}} \\ &= \tilde{\xi}((\theta + l_1 a_{13})\tilde{\xi} + \tilde{\theta}\Delta\widehat{x}_3) + \frac{1}{\gamma}\tilde{\theta}\dot{\tilde{\theta}} \\ &= (\theta + l_1 a_{13})\tilde{\xi}^2 + \tilde{\theta}(\Delta\widehat{x}_3\tilde{\xi} + \frac{1}{\gamma}, \dot{\tilde{\theta}}) \end{aligned} \tag{3.76}$$

which suggest choosing the parameter estimation error dynamics as

$$\dot{\tilde{\theta}} = -\gamma\Delta\widehat{x}_3\tilde{\xi}. \tag{3.77}$$

This gives the adaptive law $\dot{\widehat{\theta}} = -\dot{\tilde{\theta}} = \gamma\Delta\widehat{x}_3\tilde{\xi}$ since θ is assumed slowly varying which gives $\dot{\theta} = 0$. Note that the adaptive law can not be used for implementation as $\tilde{\xi}$ is an unknown signal. This issue will be resolved in Section 3.3.3. Continuing with the Lyapunov analysis by inserting (3.77) into (3.77) we get

$$\dot{V} = (\theta + l_1 a_{13})\tilde{\xi}^2. \tag{3.78}$$

Noticing that $\tilde{\xi} = \tilde{\theta} = 0$ is an equilibrium for the system (3.74), (3.77) and that the system is locally Lipschitz in $(\tilde{\xi}, \tilde{\theta})$ uniformly in t if Δq_{bit} is bounded. See (Khalil 2002) for details on Lipschitz conditions. Choosing l_1 to satisfy $(\theta + l_1 a_{13}) \leq 0$, we can conclude, using LaSalle-Yoshizawa theorem, see appendix A.4, that all solutions to (3.74), (3.77) are globally uniformly bounded and satisfy

$$\lim_{t\to\infty}(\theta + l_1 a_{13})\tilde{\xi}^2 = 0 \tag{3.79}$$

Which for l_1 chosen to satisfy $(\theta + l_1 a_{13})$<0 implies, $\lim_{t\to\infty}\tilde{\xi} = \lim_{t\to\infty}\Delta\tilde{x}_3 = 0$. As $\theta < 0$ and $a_{13} < 0$ this is satisfied for any $l_1 \geq 0$.

3.3.3 Adaptive Law

In assigning the parameter estimation error dynamics (3.77), $\tilde{\xi}$ is used. As $\tilde{\xi}$ is unknown it can not be used for implementation. To solve this issue we define

$$\sigma = \theta + \eta(\Delta\widehat{x}_3), \tag{3.80}$$

where η is a function of known signals. Using $\dot{\theta} = 0$ the σ-dynamics can be written as

$$\dot{\sigma} = \frac{\partial\eta}{\partial\Delta\widehat{x}_3}\Delta\dot{\widehat{x}}_3, \tag{3.81}$$

where $\Delta\dot{\widehat{x}}_3$ can be found by differentiating (3.70) w.r.t. time which gives

$$\Delta\dot{\widehat{x}}_3 = \dot{\widehat{\xi}} - l_1\Delta\dot{x}_1. \tag{3.82}$$

Inserting this into (3.81) gives

$$\dot{\sigma} = \frac{\partial\eta}{\partial\Delta\widehat{x}_3}(\dot{\widehat{\xi}} - l_1\Delta\dot{x}_1). \tag{3.83}$$

Inserting (3.66) for $\Delta\dot{x}_1$ gives

$$\begin{aligned}\dot{\sigma} &= \frac{\partial\eta}{\partial\Delta\widehat{x}_3}(\dot{\widehat{\xi}} - l_1(a_{13}\Delta x_3 + b_{11}\Delta u_1)) \\ &= -l_1a_{13}\Delta x_3\frac{\partial\eta}{\partial\Delta\widehat{x}_3} + (\dot{\widehat{\xi}} - l_1b_{11}\Delta u_1)\frac{\partial\eta}{\partial\Delta\widehat{x}_3},\end{aligned} \tag{3.84}$$

where both Δu_1 and $\dot{\widehat{\xi}}$ are known signals. An estimate $\widehat{\theta}$ of θ can be constructed as

$$\dot{\widehat{\sigma}} = -l_1a_{13}\Delta\widehat{x}_3\frac{\partial\eta}{\partial\Delta\widehat{x}_3} + (\dot{\widehat{\xi}} - l_1b_{11}\Delta u_1)\frac{\partial\eta}{\partial\Delta\widehat{x}_3} \tag{3.85}$$

$$\widehat{\theta} = \widehat{\sigma} - \eta(\Delta\widehat{x}_3). \tag{3.86}$$

Using (3.80) and (3.86) the estimation error can be expressed as

$$\begin{aligned}\tilde{\theta} &= \theta - \widehat{\theta} && (3.87)\\ &= \sigma - \eta - (\widehat{\sigma} - \eta) && (3.88)\\ &= \sigma - \widehat{\sigma} && (3.89)\\ &= \tilde{\sigma} && (3.90)\end{aligned}$$

Using (3.84), (3.85) and (3.72) the dynamics of the estimation error is

$$\begin{aligned}\dot{\tilde{\theta}} &= \dot{\sigma} - \dot{\widehat{\sigma}} \\ &= -l_1a_{13}\Delta\tilde{x}_3\frac{\partial\eta}{\partial\Delta\widehat{x}_3} \\ &= -l_1a_{13}\frac{\partial\eta}{\partial\Delta\widehat{x}_3}\tilde{\xi}.\end{aligned} \tag{3.91}$$

Comparing (3.91) with (3.77) suggest

$$-l_1a_{13}\frac{\partial\eta}{\partial\Delta\widehat{x}_3} = -\gamma\Delta\widehat{x}_3. \tag{3.92}$$

There are several solutions $\eta(\Delta\widehat{x}_3)$ to this PDE, one simple solution is

$$\eta(\Delta\widehat{x}_3) = \frac{\gamma\Delta\widehat{x}_3^2}{2l_1a_{13}}. \tag{3.93}$$

3.3.4 Convergence of $\Delta \tilde{p}_{bit}$

The adaptive observer presented in the previous section guarantees that $\lim_{t\to\infty} \Delta\tilde{x}_3 = 0$. Defining the estimate of Δp_{bit} as, see (3.33),

$$\begin{aligned} \Delta\widehat{p}_{bit} &= C(t)\Delta x \\ &= c_1\Delta x_1 + c_2\Delta x_2 + \widehat{c}_3\Delta\widehat{x}_3, \end{aligned} \tag{3.94}$$

where $\widehat{c}_3 = 2(\frac{M_d}{M}\widehat{F}_a - \frac{M_a}{M}F_d)x_3^0$ from the definition of the C matrix in (3.30), and $\widehat{F}_a = \frac{-\widehat{\theta}M}{2x_3^0(t)} - F_d$ from the definition of θ. Expressing $\widehat{c}_3$ as a function of $\widehat{\theta}$ gives

$$\widehat{c}_3 = -\widehat{\theta}M_d - 2F_d x_3^0. \tag{3.95}$$

Using (3.63) and (3.94) the estimation error, $\Delta\tilde{p}_{bit}$, can be expressed as

$$\begin{aligned} \Delta\tilde{p}_{bit} &= \Delta p_{bit} - \Delta\widehat{p}_{bit} \\ &= c_3\Delta x_3 - \widehat{c}_3\Delta\widehat{x}_3 \\ &= (-\theta M_d - 2F_d x_3^0)\Delta x_3 - (-\widehat{\theta}M_d - 2F_d x_3^0)\Delta\widehat{x}_3 \\ &= -M_d(\theta\Delta x_3 - \widehat{\theta}\Delta\widehat{x}_3) - 2F_d x_3^0\Delta\tilde{x}_3. \end{aligned} \tag{3.96}$$

As $\theta\Delta x_3 - \widehat{\theta}\Delta\widehat{x}_3 = \theta\Delta\tilde{x}_3 + \tilde{\theta}\Delta\widehat{x}_3$ we get

$$\begin{aligned} \Delta\tilde{p}_{bit} &= -M_d(\theta\Delta\tilde{x}_3 + \tilde{\theta}\Delta\widehat{x}_3) - 2F_d x_3^0\Delta\tilde{x}_3 \\ &= \tilde{\theta}\Delta\widehat{x}_3 - (M_d\theta + 2F_d x_3^0)\Delta\tilde{x}_3. \end{aligned} \tag{3.97}$$

From the previous Lyapunov analysis $\lim_{t\to\infty} \Delta\tilde{x}_3 = 0$. Hence $\lim_{t\to\infty} \Delta\tilde{p}_{bit} = 0$ if $\lim_{t\to\infty} \tilde{\theta}\Delta\widehat{x}_3 = 0$. Looking at the error dynamics for $\tilde{\xi}$ in (3.74) we have

$$\begin{aligned} \lim_{t\to\infty} \dot{\tilde{\xi}} &= \lim_{t\to\infty} (\theta + l_1 a_{13})\tilde{\xi} + \lim_{t\to\infty} \tilde{\theta}\Delta\widehat{x}_3 \\ \lim_{t\to\infty} \dot{\tilde{\xi}} &= \lim_{t\to\infty} \tilde{\theta}\Delta\widehat{x}_3. \end{aligned} \tag{3.98}$$

Hence if $\lim_{t\to\infty} \dot{\tilde{\xi}} = 0$ then we have $\lim_{t\to\infty} \Delta\tilde{p}_{bit} = 0$. $\lim_{t\to\infty} \dot{\tilde{\xi}} = 0$ can be proved using Barbălat's lemma, see appendix A.5, and demanding uniform continuity of $\dot{\tilde{\xi}}$. The uniform continuity condition will be satisfied if Δx and Δu are bounded. The derivation for these results will not be shown here as they involve some tedious calculations. However similar derivations are shown later for the main result in this thesis, namely the adaptive observer based on the nonlinear model, derived in Chapter 4.

Before summarizing the adaptive observer a quick note on initial conditions. There are two initial conditions to be chosen. In (3.71) $\widehat{\xi}(0)$ must be chosen, and in (3.85) $\widehat{\sigma}(0)$ must be chosen. These should be chosen as

$$\widehat{\xi}(0) = \Delta\widehat{x}_3(0) + l_1\Delta x_1(0) \tag{3.99}$$

$$\widehat{\sigma}(0) = \widehat{\theta}(0) + \eta(\Delta\widehat{x}_3(0)), \tag{3.100}$$

where $\Delta x_1(0)$ is known since it is measured. The user can now simply specify the initial guess for $\widehat{\theta}(0)$ and $\Delta\widehat{x}_3(0)$ and then use relations (3.99) and (3.100) to find $\widehat{\xi}(0)$ and $\widehat{\sigma}(0)$. Table 3.3 summarizes the observer.

Table 3.3: Summary of adaptive observer based on linear model

Plant	$\Delta\dot{x} = A(t)\Delta x + B(t)\Delta u(t)$ $\Delta p_{bit} = C(t)\Delta x$ Δx_1 and Δx_2 are measured, Δx_3 unmeasured.
Observer	$\Delta\widehat{p}_{bit} = c_1\Delta x_1 + c_2\Delta x_2 - (\widehat{\theta}M_d + 2F_d x_3^0)\Delta\widehat{x}_3$ $\Delta\widehat{x}_3 = \widehat{\xi} - l_1\Delta x_1$ $\dot{\widehat{\xi}} = a_{31}\Delta x_1 - a_{31}\Delta x_2 + (\widehat{\theta} + l_1 a_{13})\Delta\widehat{x}_3 + l_1 b_{11}\Delta u_1$ $\widehat{\xi}(0) = \Delta\widehat{x}_3(0) + l_1\Delta x_1(0)$
Adaptive law	$\widehat{\theta} = \widehat{\sigma} - \eta(\Delta\widehat{x}_3)$ $\dot{\widehat{\sigma}} = -l_1 a_{13}\Delta\widehat{x}_3\frac{\partial\eta}{\partial\Delta\widehat{x}_3} + (\dot{\widehat{\xi}} - l_1 b_{11}\Delta u_1)\frac{\partial\eta}{\partial\Delta\widehat{x}_3}$ $\widehat{\sigma}(0) = \widehat{\theta}(0) + \eta(\Delta\widehat{x}_3(0))$ $\eta(\Delta\widehat{x}_3) = \frac{\gamma\Delta\widehat{x}_3^2}{2l_1 a_{13}}$ $\frac{\partial\eta}{\partial\Delta\widehat{x}_3} = \frac{\gamma\Delta\widehat{x}_3}{l_1 a_{13}}$
Design variables	Observer gain $l_1 > 0$ Adaption gain: $\gamma > 0$ Initial conditions: $\Delta\widehat{x}_3(0)$ and $\widehat{\theta}(0)$

3.3.5 Example, Adaptive Observer

To illustrate how the adaptive observer works a simulation was performed. In the simulation (3.62) and (3.63) with constant parameters was considered the true plant. The same operating point (x^0, u^0) and the same parameter values as in Section 3.2.3 were used, resulting in the following A, B and C matrices:

$$A = \begin{bmatrix} 0 & 0 & -495.1487 \\ 0 & 0 & 145.6320 \\ 0.0001 & -0.0001 & -0.8449 \end{bmatrix}$$

$$B = \begin{bmatrix} 495.1487 & 0 \\ 0 & 145.6320 \\ 0 & 0 \end{bmatrix} \quad C = \begin{bmatrix} 0.2184 \\ 0.7816 \\ -659.2337 \end{bmatrix}^T$$

The state estimation gain $l_1 = 5 \times 10^{-3}$ and the adaptation gain was chosen to be $\gamma = 10^4$. Initial conditions were, $\widehat{\theta}(0) = 1.5\theta$ and $\widehat{\xi}(0) = 0$. The simulation was carried out with the same input as in Section 3.2.3, see Figure 3.2(e). As before, the simulation has three parts. In part one, starting from the step in u_2 at $t = 2\ min$ we can see that the step leads to an increase in state estimation error for a short period of time, see Figure 3.2(b). This triggers the adaptation and leads to a decrease in parameter estimation error, Figure 3.2(c). Note that the Lyapunov function V is monotonically decreasing, Figure 3.2(f), as proved in Section 3.3.2. The second step, at $t = 8\ min$ shows similar responses. At $t = 14\ min$ a step is applied the main pump flow. This results in a large state estimation error and $\tilde{\theta} \to 0$. This shows that a change in the main pump flow has better effect on parameter estimation than a transient change in the choke flow. Figure 3.2(d) shows that $\Delta\widehat{p}_{bit}$ tracks Δp_{bit} well, only with small deviations when $\Delta\tilde{q}_{bit}$ moves away from zero.

3.3.6 Issues With Design Based On Linearized Model

From Section 3.3.5 we have seen that the adaptive observer based on a linear approach works well under the assumption the the true (nonlinear) plant can be approximated well with a linear model with a constant $\theta = \frac{-2(F_d+F_a)|x_3^0|}{M}$. This assumption is far from valid under realistic conditions as x_3^0 will vary with e.g., changes in pump flows which will occur frequently (e.g., during pipe connections). One could of course use the adaptive observer presented and hope for the best, but no proof of convergence can be stated. Furthermore a design based on the linear model is quite complex as the trajectory that the model is based on is changing and unknown, see equation (3.21). Due to these issues the preceding chapter should only be used as an introduction to adaptive observers and a motivation to why a design based on a nonlinear model i pursued.

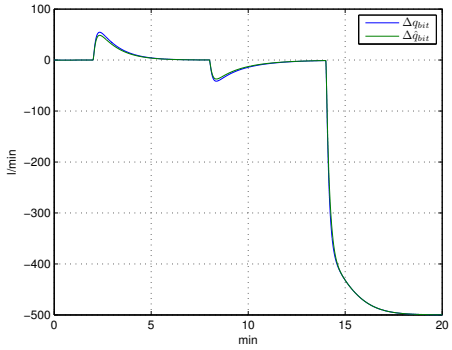

(a) Δq_{bit} and $\Delta\widehat{q}_{bit}$

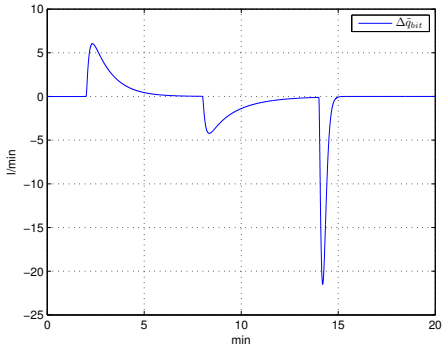

(b) $\Delta\tilde{q}_{bit} = \Delta q_{bit} - \Delta\widehat{q}_{bit}$

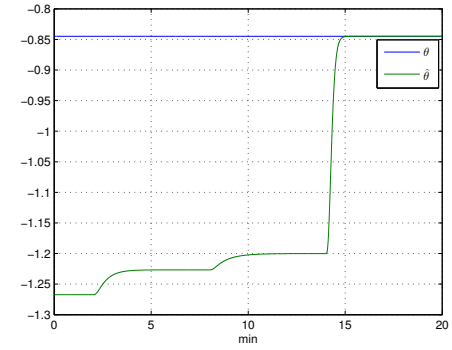

(c) θ and $\widehat{\theta}$

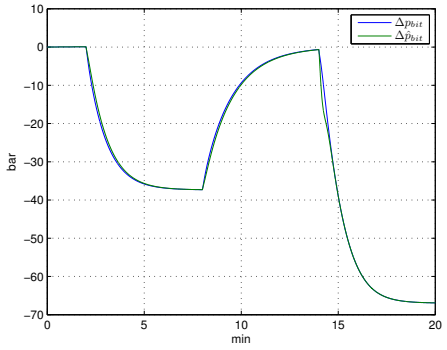

(d) Δp_{bit} and $\Delta\widehat{p}_{bit}$

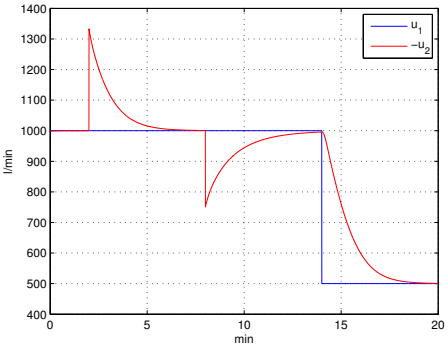

(e) Main pump flow u_1 and flow through choke $-u_2$

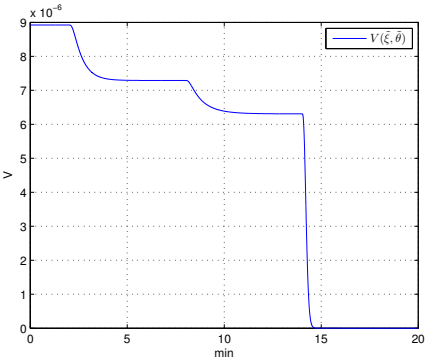

(f) Lyapunov function V defined in (3.75)

Figure 3.2: Simulation results adaptive observer

Chapter 4

Adaptive Observer Based On Nonlinear Model

The main goal of this chapter is to design an observer that estimates the bottomhole pressure, p_{bit}. This goal will be achieved by first designing an adaptive observer that estimates q_{bit} and certain unknown parameters, which is done in sections 4.2.1–4.2.4. Using the LaSalle-Yoshizawa theorem the error dynamics of the observer is shown to be uniformly bounded and the state estimation error is shown to converge to zero. Then in Section 4.2.5 an estimate of p_{bit} based on a measurement equation is shown to converge to p_{bit} under certain reasonable conditions. The observer and its properties are summarized in Section 4.2.6. In Section 4.3 a parameter estimator for the bulk modulus β_a is derived to facilitate for future control design. Due to the model complexity at $q_{bit} = 0$, commented on in Section 2.3.3, the results are only valid for $q_{bit} > 0$. In Section 4.4 a pragmatic approach to the case where $q_{bit} = 0$ is presented.

4.1 Model

The model that will be used for the observer design was derived in Chapter 2. Assumption 6, $q_{res} = 0$, will still be used. As commented in Section 2.3.3 there is a check valve in the drill bit which implies $q_{bit} \geq 0$. The check valve introduced a complicated expression for $\dot{q}_{bit}$ at $q_{bit} = 0$, see (2.44). This is further complicated by the fact that the switching condition is dependent on an unknown state, q_{bit}. Therefore we will make the following assumption for the observer design presented in this chapter.

Assumption 8. $q_{bit} > 0$

This will limit the proved performance of the observer during pipe connections. However a pragmatic solution to the case where $q_{bit} = 0$ will be presented later in this chapter.

Under assumptions 6 and 8 the model used for observer and parameter estimator design is:

$$\dot{p}_p = -a_1 q_{bit} + b_1 u_p \tag{4.1}$$
$$\dot{q}_{bit} = a_2(p_p - p_c) - \theta_1 |q_{bit}| q_{bit} + \theta_2 v_3 \tag{4.2}$$
$$\dot{p}_c = \frac{\theta_3}{v_1}(a_3 q_{bit} + u + v_2) \tag{4.3}$$

Where p_p and p_c are measured, u_p is the known speed of the main pump and $u = b_2 u_b - q_{choke}$ is the known combined flow through the back pressure pump and the choke valve. The constants are $a_1 = \frac{\beta_d}{V_d}$, $b_1 = \frac{\beta_d}{V_d} K_p$, $a_2 = \frac{1}{M}$,$a_3 = \frac{1}{1000}$, $b_2 = K_b$ and they are all known. Note that a_3 appears due to numerical conditioning, see appendix A.2. There are three known time-varying terms, $v_1(t) = V_a(t) \geq c > 0$, $v_2(t) = -\dot{V}_a(t)$, $v_3(t) = h_{bit}(t)$. And three unknown constant/slowly varying parameters, F_a, ρ_a and β_a that are lumped into:

$$\theta_1 = \frac{F_d + F_a}{M} > 0 \Rightarrow F_a = M\theta_1 - F_d \tag{4.4}$$
$$\theta_2 = \frac{(\bar{\rho}_d - \bar{\rho}_a)g}{M} \Rightarrow \bar{\rho}_a = \bar{\rho}_d - \frac{M}{g}\theta_2 \tag{4.5}$$
$$\theta_3 = \beta_a > 0 \tag{4.6}$$

The pressure at the bit p_{bit} is given by the measurement equation, (2.41), using assumptions 6 and 8:

$$p_{bit} = p_c + M_a \dot{q}_{bit} + F_a |q_{bit}| q_{bit} + \bar{\rho}_a g v_3 \tag{4.7}$$
$$= p_c + M_a(a_2(p_p - p_c) - \theta_1 |q_{bit}| q_{bit} + \theta_2 v_3) + (M\theta_1 - F_d)|q_{bit}| q_{bit} + (\bar{\rho}_d g - M\theta_2) v_3 \tag{4.8}$$

In the choice of the unknown parameter θ_2 certain assumptions have been made. The reason for choosing θ_2 as an unknown is because ρ_a is encumbered with uncertainty. From (2.35) one can see that M_a is linearly dependent on ρ_a. This implies that $M = M_a + M_d$ will also depend on ρ_a. In our choice of unknows this dependency has been neglected. The motivation for neglecting the dependency comes from reducing complexity of the observer. Neglecting the dependency can be justified by two observations. First M_a does not affect the system in steady state and second the sensitivity of M w.r.t. changes in ρ_a is small as M_d is typically larger than M_a. Figure 4.1 plots $\frac{M_d + M_a(\rho_a)}{M_d + M_{a_{nom}}}$ vs. $\frac{\rho_a}{\rho_d}$ for a typical well, defined later in Table 5.1, where $M_{a_{nom}} = M_a(\rho_d)$. The figure shows that variations of 20% in ρ_a gives variations less than 5% in M.

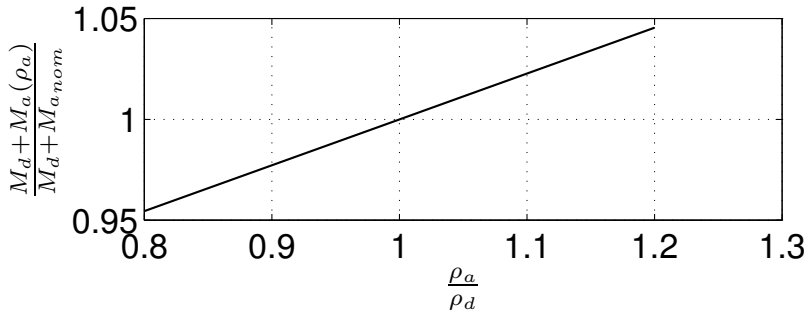

Figure 4.1: Sensitivity of M to changes in ρ_a

4.2 Adaptive Observer for p_{bit}

The goal for this section is to design an observer that estimates p_{bit} and adapts to unknown θ_1 and θ_2. The estimated states and estimated parameters will be denoted with a hat. We will assume that all signals in (4.1) and (4.2) are bounded.

Assumption 9. All signals in (4.1) - (4.2) are bounded $\Leftrightarrow$ $p_p, p_c, q_{bit}, u_p, v_3 \in \mathcal{L}_\infty$

Considering that the system is stable and v_3 is the vertical depth of the well this assumption is mild.

4.2.1 Error Dynamics

Using a similar procedure as in Section 3.3.1, motivated by (Tan et al. 1998), define the following change of coordinates

$$\xi_1 = q_{bit} + l_1 p_p,$$

where l_1 is a feedback gain. One might ask the question why injection from the p_c measurement is not used, the reason for this is the unknown θ_3 appearing in (4.3) which complicates the analysis. If θ_3 was known p_c could be included as an extension to the design presented here. The dynamics for ξ_1 is

$$\begin{aligned}\dot{\xi}_1 &= \dot{q}_{bit} + l_1 \dot{p}_p \\ &= a_2(p_p - p_c) - \theta_1 |q_{bit}| q_{bit} + \theta_2 v_3 + l_1(-a_1 q_{bit} + b_1 u_p) \\ &= -l_1 a_1 q_{bit} - \theta_1 |q_{bit}| q_{bit} + \theta_2 v_3 + a_2(p_p - p_c) + l_1 b_1 u_p.\end{aligned}$$

An observer for q_{bit} is

$$\dot{\widehat{\xi}}_1 = -l_1 a_1 \widehat{q}_{bit} - \widehat{\theta}_1 |\widehat{q}_{bit}| \widehat{q}_{bit} + \widehat{\theta}_2 v_3 + a_2(p_p - p_c) + l_1 b_1 u_p \tag{4.9}$$

$$\widehat{q}_{bit} = \widehat{\xi}_1 - l_1 p_p. \tag{4.10}$$

The state estimation error is

$$\tilde{\xi}_1 = \xi_1 - \widehat{\xi}_1 = \tilde{q}_{bit}, \tag{4.11}$$

which is driven by the differential equation

$$\begin{aligned}\dot{\tilde{\xi}}_1 &= \dot{\xi}_1 - \dot{\widehat{\xi}}_1 \\ &= -l_1 a_1 \tilde{q}_{bit} - (\theta_1 |q_{bit}|q_{bit} - \widehat{\theta}_1 |\widehat{q}_{bit}|\widehat{q}_{bit}) + \tilde{\theta}_2 v_3\end{aligned} \tag{4.12}$$

Noticing that

$$\begin{aligned}\theta_1 |q_{bit}|q_{bit} - \widehat{\theta}_1 |\widehat{q}_{bit}|\widehat{q}_{bit} &= \theta_1 |q_{bit}|q_{bit} - \theta_1 |\widehat{q}_{bit}|\widehat{q}_{bit} + \theta_1 |\widehat{q}_{bit}|\widehat{q}_{bit} - \widehat{\theta}_1 |\widehat{q}_{bit}|\widehat{q}_{bit} \\ &= \theta_1 (|q_{bit}|q_{bit} - |\widehat{q}_{bit}|\widehat{q}_{bit}) + \tilde{\theta}_1 |\widehat{q}_{bit}|\widehat{q}_{bit},\end{aligned}$$

which implies that (4.12) can be written as

$$\begin{aligned}\dot{\tilde{\xi}}_1 &= -l_1 a_1 \tilde{q}_{bit} - (\theta_1 (|q_{bit}|q_{bit} - |\widehat{q}_{bit}|\widehat{q}_{bit}) + \tilde{\theta}_1 |\widehat{q}_{bit}|\widehat{q}_{bit}) + \tilde{\theta}_2 v_3 \\ &= -l_1 a_1 \tilde{q}_{bit} - \theta_1 (|q_{bit}|q_{bit} - |\widehat{q}_{bit}|\widehat{q}_{bit}) - \tilde{\theta}_1 |\widehat{q}_{bit}|\widehat{q}_{bit} + \tilde{\theta}_2 v_3.\end{aligned} \tag{4.13}$$

Let the parameter errors be denoted as $\tilde{\theta} = \begin{bmatrix} \tilde{\theta}_1 \\ \tilde{\theta}_2 \end{bmatrix}$ and the regressor as

$$\phi(\widehat{q}_{bit}, v_3) = \begin{bmatrix} -|\widehat{q}_{bit}|\widehat{q}_{bit} \\ v_3 \end{bmatrix}. \tag{4.14}$$

Using this and $\tilde{\xi}_1 = \tilde{q}_{bit}$ from (4.11) gives

$$\dot{\tilde{\xi}}_1 = -l_1 a_1 \tilde{\xi}_1 - \theta_1 (|q_{bit}|q_{bit} - |\widehat{q}_{bit}|\widehat{q}_{bit}) + \tilde{\theta}^T \phi, \tag{4.15}$$

4.2.2 Lyapunov Analysis

For the error system $\begin{bmatrix} \tilde{\xi}_1 \\ \tilde{\theta} \end{bmatrix}$ with $\tilde{\xi}_1$ dynamics described by (4.15) and $\tilde{\theta}$ dynamics to be found, consider the candidate Lyapunov function

$$U_1(\tilde{\xi}_1, \tilde{\theta}) = \frac{1}{2}\tilde{\xi}_1^2 + \frac{1}{2}\tilde{\theta}^T \Gamma^{-1} \tilde{\theta}, \tag{4.16}$$

where $\Gamma = \Gamma^T > 0$ is the adaptation gain matrix. The time derivative of U_1 is, using (4.15),

$$\begin{aligned}\dot{U}_1 &= \tilde{\xi}_1 [-l_1 a_1 \tilde{\xi}_1 - \theta_1 (|q_{bit}|q_{bit} - |\widehat{q}_{bit}|\widehat{q}_{bit}) + \tilde{\theta}^T \phi] + \tilde{\theta^T} \Gamma^{-1} \dot{\tilde{\theta}} \\ &= -l_1 a_1 \tilde{\xi}_1^2 - \theta_1 (|q_{bit}|q_{bit} - |\widehat{q}_{bit}|\widehat{q}_{bit}) \tilde{\xi}_1 + \tilde{\theta}^T (\phi \tilde{\xi}_1 + \Gamma^{-1} \dot{\tilde{\theta}}).\end{aligned}$$

Choosing the $\tilde{\theta}$ dynamics to be

$$\dot{\tilde{\theta}} = -\Gamma\phi\tilde{\xi}_1 \tag{4.17}$$

gives

$$\dot{U}_1 = -l_1 a_1 \tilde{\xi}_1^2 - \theta_1(|q_{bit}|q_{bit} - |\widehat{q}_{bit}|\widehat{q}_{bit})\tilde{\xi}_1. \tag{4.18}$$

Defining

$$\begin{aligned} f_q(q_{bit}, \widehat{q}_{bit}) &= (|q_{bit}|q_{bit} - |\widehat{q}_{bit}|\widehat{q}_{bit})\tilde{\xi}_1 \\ &= (|q_{bit}|q_{bit} - |\widehat{q}_{bit}|\widehat{q}_{bit})(q_{bit} - \widehat{q}_{bit}), \end{aligned} \tag{4.19}$$

and noticing that

$$\begin{aligned} q_{bit} - \widehat{q}_{bit} = \tilde{\xi}_1 = 0 \Rightarrow f_q(q_{bit}, \widehat{q}_{bit}) = 0 \\ q_{bit} - \widehat{q}_{bit} = \tilde{\xi}_1 \neq 0 \Rightarrow f_q(q_{bit}, \widehat{q}_{bit}) > 0 \end{aligned}$$

implies that $f_q(q_{bit}, \widehat{q}_{bit})$ is positive semidefinite w.r.t. $\tilde{\xi}$. Using this and $\theta_1 > 0$ gives

$$\dot{U}_1 \leq -l_1 a_1 \tilde{\xi}_1^2. \tag{4.20}$$

Since $a_1 > 0$ choosing $l_1 > 0$ gives $\dot{U}(\tilde{\xi}, \tilde{\theta}) \leq 0$. Noticing that $\tilde{\xi}_1 = \tilde{\theta} = 0$ is an equilibrium point for the system defined by (4.15) and (4.17). And that the system is locally Lipschitz in $(\tilde{\xi}, \tilde{\theta})$, uniformly in t under assumption 9. For details see appendix A.3. Using these properties we can conclude, by using LaSalle-Yoshizawa theorem (see appendix A.4) that all solutions to (4.15) and (4.17) are uniformly bounded. Furthermore

$$\begin{aligned} &\lim_{t\to\infty} -l_1 a_1 \tilde{\xi}_1^2 = 0 \\ \Rightarrow &\lim_{t\to\infty} \tilde{\xi}_1 = 0, \end{aligned}$$

which implies that $\widehat{q}_{bit} \to q_{bit}$ as $t \to \infty \ \forall \ q_{bit} > 0$. There is no guarantee that the parameter estimates converge to their true values. The results derived hold $\forall \ (\tilde{\xi}_1, \tilde{\theta}) \in \mathbf{R}^3$ but only for $q_{bit} > 0 \ \forall \ t$[1]. The limitation in q_{bit} is a consequence of the complex model dynamics at $q_{bit} = 0$.

[1] $q_{bit} > 0$ can be slightly relaxed as the model (4.2) for $\dot{q}_{bit}$ is sometimes valid at $q_{bit} = 0$, more on this in Section 4.4

4.2.3 Adaptive Law

In (4.17) $\tilde{\xi}$ is unknown which implies that the adaptive law, $\dot{\widehat{\theta}} = -\dot{\tilde{\theta}}$ can not be implemented, as-is. This problem will be dealt with now. Define

$$\sigma = \theta + \eta(\widehat{q}_{bit}, v_3), \tag{4.21}$$

where η is a function of known/measured signals that is to be designed to assign σ desired dynamics. Differentiating σ with respect to time (remembering that $\dot{\theta} = 0$)

$$\dot{\sigma} = \frac{\partial \eta}{\partial \widehat{q}_{bit}} \dot{\widehat{q}}_{bit} + \frac{\partial \eta}{\partial v_3} \dot{v}_3,$$

where $\dot{\widehat{q}}_{bit}$ can be found by differentiating (4.10) w.r.t. time giving

$$\dot{\widehat{q}}_{bit} = \dot{\widehat{\xi}}_1 - l_1 \dot{p}_p \tag{4.22}$$

This gives

$$\begin{aligned}
\dot{\sigma} &= \frac{\partial \eta}{\partial \widehat{q}_{bit}} (\dot{\widehat{\xi}} - l_1 \dot{p}_p) + \frac{\partial \eta}{\partial v_3} \dot{v}_3 \\
&= -l_1 \frac{\partial \eta}{\partial \widehat{q}_{bit}} \dot{p}_p + \frac{\partial \eta}{\partial \widehat{q}_{bit}} \dot{\widehat{\xi}} + \frac{\partial \eta}{\partial v_3} \dot{v}_3 \\
&= -l_1 \frac{\partial \eta}{\partial \widehat{q}_{bit}} (-a_1 q_{bit} + b_1 u_p) + \frac{\partial \eta}{\partial \widehat{q}_{bit}} \dot{\widehat{\xi}} + \frac{\partial \eta}{\partial v_3} \dot{v}_3,
\end{aligned} \tag{4.23}$$

where $\dot{\widehat{\xi}}$ is known from (4.9). From here assumption 10 is made.

Assumption 10. $\dot{v}_3$ is a known signal.

Using the assumption implies that only q_{bit} in (4.23) is unknown. To deal with this an estimate $\dot{\widehat{\sigma}}$ is used

$$\dot{\widehat{\sigma}} = -l_1 \frac{\partial \eta}{\partial \widehat{q}_{bit}} (-a_1 \widehat{q}_{bit} + b_1 u_p) + \frac{\partial \eta}{\partial \widehat{q}_{bit}} \dot{\widehat{\xi}} + \frac{\partial \eta}{\partial v_3} \dot{v}_3 \tag{4.24}$$

$$\widehat{\theta} = \widehat{\sigma} - \eta(\widehat{q}_{bit}, v_3). \tag{4.25}$$

The estimation error, using (4.21) and (4.25), can be expressed as

$$\begin{aligned}
\tilde{\theta} &= \theta - \widehat{\theta} \\
&= \sigma - \eta - (\widehat{\sigma} - \eta) \\
&= \sigma - \widehat{\sigma} \\
&= \tilde{\sigma}.
\end{aligned}$$

The dynamics of the estimation error is, using (4.23), (4.24) and $\tilde{\xi}_1 = \tilde{q}_{bit}$,

$$\begin{aligned}\dot{\tilde{\theta}} &= \dot{\tilde{\sigma}} \\ &= l_1 a_1 \frac{\partial \eta}{\partial \widehat{q}_{bit}} \tilde{\xi}_1. \end{aligned} \tag{4.26}$$

Comparing (4.26) to (4.17), suggest

$$-l_1 a_1 \frac{\partial \eta(\widehat{q}_{bit}, v_3)}{\partial \widehat{q}_{bit}} = \Gamma \phi. \tag{4.27}$$

There are several solutions $\eta(\widehat{q}_{bit}, v_3)$ to this partial differential equation. Simplicity will be the motivating factor when selecting one. Remembering that the regressor is $\phi(\widehat{q}_{bit}, v_3) = \begin{bmatrix} -|\widehat{q}_{bit}|\widehat{q}_{bit} \\ v_3 \end{bmatrix}$ and integrating w.r.t $\widehat{q}_{bit}$ gives

$$\eta(\widehat{q}_{bit}, v_3) = \Gamma \begin{bmatrix} \frac{|\widehat{q}_{bit}|^3}{3 l_1 a_1} \\ -\frac{v_3 \widehat{q}_{bit}}{l_1 a_1} \end{bmatrix}.$$

The partial derivatives of $\eta(\widehat{q}_{bit}, v_3)$ are

$$\begin{aligned}\frac{\partial \eta}{\partial \widehat{q}_{bit}} &= \Gamma \begin{bmatrix} \frac{|\widehat{q}_{bit}|\widehat{q}_{bit}}{l_1 a_1} \\ -\frac{v_3}{l_1 a_1} \end{bmatrix} \\ \frac{\partial \eta}{\partial v_3} &= \Gamma \begin{bmatrix} 0 \\ -\frac{\widehat{q}_{bit}}{l_1 a_1} \end{bmatrix}. \end{aligned}$$

4.2.4 Initial Conditions

There are two initial conditions that needs to be set. One is $\widehat{\xi}_1(0)$ in (4.9) and the other is $\widehat{\sigma}(0)$ in (4.24). The initial conditions should be constructed by using the relationships

$$\widehat{\xi}(0) = \widehat{q}_{bit}(0) + l_1 p_p(0) \tag{4.28}$$

$$\widehat{\sigma}(0) = \widehat{\theta}(0) + \eta(\widehat{q}_{bit}(0), v_3(0)), \tag{4.29}$$

where $p_p(0)$ and $v_3(0)$ are known since they are measured. The user can now come up with estimates of $\widehat{q}_{bit}(0)$ and $\widehat{\theta}(0)$ and then use relations (4.28) and (4.29) to find $\widehat{\xi}(0)$ and $\widehat{\sigma}(0)$.

4.2.5 Convergence of $\tilde{p}_{bit}$

The goal of Section 4.2 was to design an observer so that the estimated BHP $\widehat{p}_{bit}$ tracks p_{bit}. In section 4.2.1 – 4.2.4 an observer for the unmeasured state q_{bit} was designed. In this section convergence properties of $\tilde{p}_{bit}$ will be proved. The measurement equation for p_{bit} stated in (4.8) is

$$\begin{aligned} p_{bit} &= p_c + M_a(a_2(p_p - p_c) - \theta_1|q_{bit}|q_{bit} + \theta_2 v_3) \\ &\quad + (M\theta_1 - F_d)|q_{bit}|q_{bit} + (\rho_d g - M\theta_2)v_3, \end{aligned}$$

where p_c, v_3 are measured and M_a, M, a_2, F_d and ρ_d are known. An estimate of p_{bit} is

$$\begin{aligned} \widehat{p}_{bit} &= p_c + M_a(a_2(p_p - p_c) - \widehat{\theta}_1|\widehat{q}_{bit}|\widehat{q}_{bit} + \widehat{\theta}_2 v_3) \\ &\quad + (M\widehat{\theta}_1 - F_d)|\widehat{q}_{bit}|\widehat{q}_{bit} + (\rho_d g - M\widehat{\theta}_2)v_3. \end{aligned}$$

The error in the estimate is

$$\begin{aligned} \tilde{p}_{bit} &= p_{bit} - \widehat{p}_{bit} \\ &= M_a(-(\theta_1|q_{bit}|q_{bit} - \widehat{\theta}_1|\widehat{q}_{bit}|\widehat{q}_{bit}) + \tilde{\theta}_2 v_3) + M(\theta_1|q_{bit}|q_{bit} - \widehat{\theta}_1|\widehat{q}_{bit}|\widehat{q}_{bit}) \\ &\quad - F_d(|q_{bit}|q_{bit} - |\widehat{q}_{bit}|\widehat{q}_{bit}) - M\tilde{\theta}_2 v_3. \end{aligned}$$

Using $M = M_a + M_d$ this can be rewritten as

$$\tilde{p}_{bit} = M_d(\theta_1|q_{bit}|q_{bit} - \widehat{\theta}_1|\widehat{q}_{bit}|\widehat{q}_{bit}) - F_d(|q_{bit}|q_{bit} - |\widehat{q}_{bit}|\widehat{q}_{bit}) - M_d\tilde{\theta}_2 v_3 \tag{4.30}$$

$$\begin{aligned} &= M_d(\theta_1(|q_{bit}|q_{bit} - |\widehat{q}_{bit}|\widehat{q}_{bit}) + \tilde{\theta}_1|\widehat{q}_{bit}|\widehat{q}_{bit} - \tilde{\theta}_2 v_3) - F_d(|q_{bit}|q_{bit} - |\widehat{q}_{bit}|\widehat{q}_{bit}) \\ &= M_d(\theta_1(|q_{bit}|q_{bit} - |\widehat{q}_{bit}|\widehat{q}_{bit}) - \tilde{\theta}^T\phi) - F_d(|q_{bit}|q_{bit} - |\widehat{q}_{bit}|\widehat{q}_{bit}). \end{aligned} \tag{4.31}$$

From the error equation (4.31) and remembering that $(q_{bit} - \widehat{q}_{bit}) \to 0$ from the previous Lyapunov analysis it can be seen that if $\tilde{\theta}^T\phi \to 0$ then $\tilde{p}_{bit} \to 0$. Conditions for $\tilde{\theta}^T\phi \to 0$ will now be derived.

The error system $\begin{bmatrix} \tilde{\xi}_1 \\ \tilde{\theta} \end{bmatrix}$ has the following dynamics, from (4.15) and (4.17)

$$\dot{\tilde{\xi}}_1 = -l_1 a_1 \tilde{\xi}_1 - \theta_1(|q_{bit}|q_{bit} - |\widehat{q}_{bit}|\widehat{q}_{bit}) + \tilde{\theta}^T\phi \tag{4.32}$$

$$\dot{\tilde{\theta}} = -\Gamma\phi\tilde{\xi}_1. \tag{4.33}$$

From the Lyapunov analysis it is known that $\tilde{\xi}_1 = (q_{bit} - \widehat{q}_{bit}) \to 0$ which implies by (4.33) that $\dot{\tilde{\theta}} \to 0$. Hence, as ϕ is bounded, the adaptation will slow down and stop as

the state estimation error goes to zero. Furthermore if it can be proved that $\dot{\tilde{\xi}}_1 \to 0$ then from (4.32)

$$\tilde{\theta}^T \phi \to 0.$$

Using Barbălat's lemma, see appendix A.5, $\dot{\tilde{\xi}}_1 \to 0$ will be proved. Let

$$\begin{aligned} \varphi(t) &= \dot{\tilde{\xi}}_1(t) \\ &= -l_1 a_1 \tilde{\xi}_1 - \theta_1(|q_{bit}|q_{bit} - |\widehat{q}_{bit}|\widehat{q}_{bit}) + \tilde{\theta}^T \phi. \end{aligned} \tag{4.34}$$

Using $\lim_{t\to\infty} \tilde{\xi}_1(t) = 0$ we then have

$$\begin{aligned} \lim_{t\to\infty} \int_0^t \varphi(t) d\tau &= \lim_{t\to\infty} (\tilde{\xi}_1(t) - \tilde{\xi}_1(0)) \\ &= -\tilde{\xi}(0). \end{aligned}$$

Hence $\lim_{t\to\infty} \int_0^t \varphi(t) d\tau$ exists and is finite. Assume that $\varphi(t)$ is uniformly continuous. Then, by Barbălat's Lemma

$$\lim_{t\to\infty} \varphi(t) = 0.$$

Hence, under the assumption that $\varphi(t)$ is uniformly continuous $\lim_{t\to\infty} \varphi(t) = \lim_{t\to\infty} \dot{\tilde{\xi}}_1 = 0$.

According to (Ioannou & Sun 1996) $\dot{\varphi}(t) \in \mathcal{L}_\infty$ implies uniform continuity of $\varphi(t)$. From (4.34) one can find

$$\begin{aligned} \dot{\varphi}(t) =& \ddot{\tilde{\xi}}_1(t) \\ =& - l_1 a_1 \dot{\tilde{\xi}}_1 - \theta_1(2|q_{bit}|\dot{q}_{bit} - 2|\widehat{q}_{bit}|\dot{\widehat{q}}_{bit}) + \tilde{\theta}^T \dot{\phi} + \dot{\tilde{\theta}}^T \phi. \end{aligned}$$

Inserting (4.32), (4.2), (4.22), (4.33) and the derivative w.r.t. time of the regressor defined in (4.14) gives

$$\begin{aligned} \dot{\varphi}(t) =& - l_1 a_1(-l_1 a_1 \tilde{\xi}_1 - \theta_1(|q_{bit}|q_{bit} - |\widehat{q}_{bit}|\widehat{q}_{bit}) + \tilde{\theta}^T \phi) \\ & - \theta_1 \left[2q_{bit}(a_2(p_p - p_c) - \theta_1 |q_{bit}|q_{bit} + \theta_2 v_3) - 2\widehat{q}_{bit}(\dot{\hat{\xi}}_1 - l_1 \dot{p}_p) \right] \\ & + \tilde{\theta}^T \begin{bmatrix} -|\widehat{q}_{bit}|\dot{\widehat{q}}_{bit} \\ \dot{v}_3 \end{bmatrix} - \phi^T \Gamma \phi \tilde{\xi}_1. \end{aligned}$$

Finally, inserting (4.9), (4.1) and remembering that $\dot{\hat{q}} = w\dot{h}\xi_1 - l_1\dot{p}_p$ gives

$$\begin{aligned}
\dot{\varphi}(t) = &- l_1a_1(-l_1a_1\tilde{\xi}_1 - \theta_1(|q_{bit}|q_{bit} - |\widehat{q}_{bit}|\widehat{q}_{bit}) + \tilde{\theta}^T\phi) \\
&- \theta_1\left[2q_{bit}(a_2(p_p - p_c) - \theta_1|q_{bit}|q_{bit} + \theta_2 v_3)\right] \\
&+ \theta_1 2\widehat{q}_{bit}\Big[(-l_1a_1\widehat{q}_{bit} - \widehat{\theta}_1|\widehat{q}_{bit}|\widehat{q}_{bit} + \widehat{\theta}_2 v_3 \\
&+a_2(p_p - p_c) + l_1b_1u_p) - l_1(-a_1q_{bit} + b_1u_p)\Big] \\
&+ \tilde{\theta}^T\begin{bmatrix} -\widehat{q}_{bit}\left[(-l_1a_1\widehat{q}_{bit} - \widehat{\theta}_1|\widehat{q}_{bit}|\widehat{q}_{bit} + \widehat{\theta}_2 v_3 + a_2(p_p - p_c) + l_1b_1u_p)\right] \\ \dot{v}_3 \end{bmatrix} \\
&+ \tilde{\theta}^T\begin{bmatrix} \widehat{q}_{bit}l_1(-a_1q_{bit} + b_1u_p) \\ 0 \end{bmatrix} \\
&- \begin{bmatrix} -|\widehat{q}_{bit}|\widehat{q}_{bit} & v_3 \end{bmatrix}\Gamma\begin{bmatrix} -|\widehat{q}_{bit}|\widehat{q}_{bit} \\ v_3 \end{bmatrix}\tilde{\xi}_1.
\end{aligned}$$

Hence, under the conditions on the signals in $\dot{\varphi}(t)$ found in Table 4.1, $\dot{\phi}(t) \in \mathcal{L}_\infty$.

Table 4.1: Conditions on signals for uniform continuity

Condition	Comment
$p_p(t), q_{bit}(t), p_c(t), u_p(t) \in \mathcal{L}_\infty$	Should be provided by the controller, se assumption 9
$\widehat{q}_{bit}(t), \widehat{\theta} \in \mathcal{L}_\infty$	Satisfied by the observer if the states are bounded
$v_3(t), \dot{v}_3(t) \in \mathcal{L}_\infty$	Condition on v_3 is satisfied by assumption 9
	For the condition on $\dot{v}_3$ see below

$\dot{v}_3 \in \mathcal{L}_\infty \Leftrightarrow \dot{h}_{bit} \in \mathcal{L}_\infty$, where h_{bit} is the vertical depth of the bit, see Figure 2.1. From physical considerations one can assume that the vertical speed of the bit is bounded, therefore the condition is not unrealistic.

The proof for $\tilde{p}_{bit} \to 0$ is summarized below:

- $\dot{\varphi}(t) \in \mathcal{L}_\infty \Rightarrow \varphi(t)$ uniformly continuous
- $\varphi(t)$ uniformly continuous and Barbălat's lemma $\Rightarrow \lim_{t\to\infty}\dot{\tilde{\xi}}_1 = 0$
- $\Rightarrow \lim_{t\to\infty}\tilde{\theta}^T\phi = 0$
- $\Rightarrow \lim_{t\to\infty}\tilde{p}_{bit} = 0$

What can be said about parameter estimatation error from the previous analysis? We have $\lim_{t\to\infty}\tilde{\theta}^T\phi = 0$ which only implies that

$$-|\widehat{q}_{bit}(t)|\widehat{q}_{bit}(t)\tilde{\theta}_1(t) + v_3(t)\tilde{\theta}_2(t) \to 0. \tag{4.35}$$

It might be possible to come up with conditions on the signals in (4.35) to achieve persistent excitation (PE) and $\tilde{\theta}(t) \to 0$. Due to time constraints a mathematical analysis of this has not been pursued in this thesis. However (4.35) is used later on to decide when to turn on/off the adaption to get good parameter estimates.

4.2.6 Summary Adaptive Observer

The adaptive observer summarized in table Table 4.2, has the following properties:

- All solutions to (4.15), (4.17) are uniformly bounded.
- $\lim_{t\to\infty} \tilde{q}_{bit} = 0$
- $\lim_{t\to\infty} \dot{\hat{\theta}} = 0$

Furthermore, if the signal conditions in Table 4.1 are satisfied, then the observer has the following additional properties:

- $\lim_{t\to\infty} \tilde{\theta}^T \phi = 0$
- $\lim_{t\to\infty} \tilde{p}_{bit} = 0$

The properties are valid for $q_{bit} > 0$. This limitation is a result of the switched dynamics at $q_{bit} = 0$.

Table 4.2: Summary of adaptive observer based on nonlinear model

Plant	$\dot{p}_p = -a_1 q_{bit} + b_1 u_p$ $\dot{q}_{bit} = a_2(p_p - p_c) - \theta_1 \lvert q_{bit}\rvert q_{bit} + \theta_2 v_3$ $\dot{p}_c = \frac{\theta_3}{v_1}(a_3 q_{bit} + u + v_2)$ $p_{bit} = p_c + M_a(a_2(p_p - p_c) - \theta_1 \lvert q_{bit}\rvert q_{bit} + \theta_2 v_3)$ $+(M\theta_1 - F_d)\lvert q_{bit}\rvert q_{bit} + (\rho_d g - M\theta_2)v_3$ p_p and p_c are measured
Observer	$\widehat{p}_{bit} = p_c + M_a(a_2(p_p - p_c) - \widehat{\theta}_1 \lvert \widehat{q}_{bit}\rvert \widehat{q}_{bit} + \widehat{\theta}_2 v_3)$ $+(M\widehat{\theta}_1 - F_d)\lvert \widehat{q}_{bit}\rvert \widehat{q}_{bit} + (\rho_d g - M\widehat{\theta}_2)v_3$ $\widehat{q}_{bit} = \widehat{\xi}_1 - l_1 p_p$ $\dot{\widehat{\xi}}_1 = -l_1 a_1 \widehat{q}_{bit} - \widehat{\theta}_1 \lvert \widehat{q}_{bit}\rvert \widehat{q}_{bit} + \widehat{\theta}_2 v_3 + a_2(p_p - p_c) + l_1 b_1 u_p$ $\widehat{\xi}_1(0) = \widehat{q}_{bit}(0) + l_1 p_p(0)$
Adaptive law	$\widehat{\theta} = \widehat{\sigma} - \eta(\widehat{q}_{bit}, v_3)$ $\dot{\widehat{\sigma}} = -l_1 \frac{\partial \eta}{\partial \widehat{q}_{bit}}(-a_1 \widehat{q}_{bit} + b_1 u_p) + \frac{\partial \eta}{\partial \widehat{q}_{bit}} \dot{\widehat{\xi}}_1 + \frac{\partial \eta}{\partial v_3} \dot{v}_3$ $\widehat{\sigma}(0) = \widehat{\theta}(0) + \eta(\widehat{q}_{bit}(0), v_3(0))$ $\eta(\widehat{q}_{bit}, v_3) = \Gamma \begin{bmatrix} \frac{\lvert \widehat{q}_{bit}\rvert^3}{3 l_1 a_1} \\ -\frac{v_3 \widehat{q}_{bit}}{l_1 a_1} \end{bmatrix}$ $\frac{\partial \eta}{\partial \widehat{q}_{bit}} = \Gamma \begin{bmatrix} \frac{\lvert \widehat{q}_{bit}\rvert \widehat{q}_{bit}}{l_1 a_1} \\ -\frac{v_3}{l_1 a_1} \end{bmatrix}$ $\frac{\partial \eta}{\partial v_3} = \Gamma \begin{bmatrix} 0 \\ -\frac{\widehat{q}_{bit}}{l_1 a_1} \end{bmatrix}$
Design variables	Observer gain $l_1 > 0$ Adaption gain: $\Gamma = \Gamma^T > 0$ Initial conditions: $\widehat{q}_{bit}(0)$ and $\widehat{\theta}(0)$

4.3 θ_3 parameter estimator

As the bulk modulus $\beta_a = \theta_3$ is encumbered with high uncertainty it will be estimated too. β_a does not enter in the analysis for the observer derived in Section 4.2, but it will prove useful for later control design. It might also prove useful for detecting gas influx from the reservoir (i.e. $q_{res} > 0$) as gas in the annulus will change the bulk modulus.

Define the error variable

$$\tilde{\xi}_2 = p_c - \widehat{p}_c,$$

where $\widehat{p}_c$ is the solution to

$$\dot{\widehat{p}}_c = \frac{a_3 \widehat{\theta}_3 \widehat{q}_{bit}}{v_1} + \frac{\widehat{\theta}_3 (u + v_2)}{v_1} + l_2 \tilde{\xi}_2, \tag{4.36}$$

with $\widehat{p}_c(0) = p_c(0)$. $\dot{\widehat{p}}_c$ is similar to $\dot{p}_c$ in (4.3), with estimates of the unknown state and the unknown parameter and in addition an injection term $l_2\tilde{\xi}_2$ for stabilization. Note that $\tilde{\xi}_2$ is a known signal as p_c is measured.

4.3.1 Error Dynamics

The dynamics of the error $\tilde{\xi}_2$ is governed by

$$\dot{\tilde{\xi}}_2 = \dot{p}_c - \dot{\widehat{p}}_c. \tag{4.37}$$

Inserting (4.3) and (4.36) gives

$$\begin{aligned} \dot{\tilde{\xi}}_2 &= \frac{a_3}{v_1}(\theta_3 q_{bit} - \widehat{\theta}_3 \widehat{q}_{bit}) + \frac{\tilde{\theta}_3}{v_1}(u + v_2) - l_2 \tilde{\xi}_2 \\ &= \frac{a_3}{v_1}(\theta_3 \tilde{q}_{bit} + \tilde{\theta}_3 \widehat{q}_{bit}) + \frac{\tilde{\theta}_3}{v_1}(u + v_2) - l_2 \tilde{\xi}_2 \\ &= \frac{a_3}{v_1}\theta_3 \tilde{\xi}_1 + \frac{\tilde{\theta}_3}{v_1}(a_3 \widehat{q}_{bit} + u + v_2) - l_2 \tilde{\xi}_2, \end{aligned} \tag{4.38}$$

where $\tilde{q}_{bit} = \tilde{\xi}_1$ from (4.11) has been used. Defining the regressor

$$\phi_3(\widehat{q}_{bit}, u, v_1, v2) = \frac{a_3 \widehat{q}_{bit} + u + v_2}{v_1}, \tag{4.39}$$

gives

$$\dot{\tilde{\xi}}_2 = \frac{a_3}{v_1}\theta_3 \tilde{\xi}_1 + \tilde{\theta}_3 \phi_3 - l_2 \tilde{\xi}_2. \tag{4.40}$$

4.3.2 Lyapunov Analysis

Consider the Lyapunov function candidate

$$U(\tilde{\xi}_1, \tilde{\xi}_2, \tilde{\theta}_1, \tilde{\theta}_2, \tilde{\theta}_3) = U_1(\tilde{\xi}_1, \tilde{\theta}_1, \tilde{\theta}_2) + U_2(\tilde{\xi}_2, \tilde{\theta}_3), \tag{4.41}$$

where U_1 is taken as (4.16) and U_2 is

$$U_2(\tilde{\xi}_2, \tilde{\theta}_3) = \frac{1}{2}\tilde{\xi}_2^2 + \frac{1}{2\gamma_3}\tilde{\theta}_3^2. \tag{4.42}$$

Differentiating U_2 w.r.t. time and inserting (4.40) yields

$$\begin{aligned}\dot{U}_2 &= (\frac{a_3}{v_1}\theta_3\tilde{\xi}_1 + \tilde{\theta}_3\phi_3 - l_2\tilde{\xi}_2)\tilde{\xi}_2 + \frac{1}{\gamma_3}\tilde{\theta}_3\dot{\tilde{\theta}}_3 \\ &= -l_2\tilde{\xi}_2^2 + \frac{a_3\theta_3}{v_1}\tilde{\xi}_1\tilde{\xi}_2 + \tilde{\theta}_3(\phi_3\tilde{\xi}_2 + \frac{1}{\gamma_3}\dot{\tilde{\theta}}_3),\end{aligned}$$

suggests choosing the adaptive law as

$$\dot{\tilde{\theta}}_3 = -\dot{\hat{\theta}}_3 = -\gamma_3\phi_3\tilde{\xi}_2, \tag{4.43}$$

where all signals and parameters are known. Hence $\dot{\hat{\theta}}_3$ can be implemented as-is. This gives

$$\dot{U}_2 = -l_2\tilde{\xi}_2^2 + \frac{a_3\theta_3}{v_1}\tilde{\xi}_1\tilde{\xi}_2.$$

Using completion of squares $\tilde{\xi}_1\tilde{\xi}_2 \leq \frac{1}{2}(\tilde{\xi}_1^2 + \tilde{\xi}_2^2)$ gives

$$\begin{aligned}\dot{U}_2 &\leq -l_2\tilde{\xi}_2^2 + \frac{a_3\theta_3}{v_1}\frac{1}{2}(\tilde{\xi}_1^2 + \tilde{\xi}_2^2) \\ &= (-l_2 + \frac{a_3\theta_3}{2v_1})\tilde{\xi}_2^2 + \frac{a_3\theta_3}{2v_1}\tilde{\xi}_1^2,\end{aligned} \tag{4.44}$$

where an unwanted $\tilde{\xi}_1^2$ appears at the end. This term will be dealt with by using the previous Lyapunov analysis for U_1. Differentiating (4.41) w.r.t. time gives

$$\dot{U} = \dot{U}_1 + \dot{U}_2.$$

Inserting $\dot{U}_1$ from (4.20) and $\dot{U}_2$ from (4.44) gives

$$\begin{aligned}\dot{U} &= \dot{U}_1 + \dot{U}_2 \\ &\leq -l_1a_1\tilde{\xi}_1^2 + (-l_2 + \frac{a_3\theta_3}{2v_1})\tilde{\xi}_2^2 + \frac{a_3\theta_3}{2v_1}\tilde{\xi}_1^2 \\ &= (-l_1a_1 + \frac{a_3\theta_3}{2v_1})\tilde{\xi}_1^2 + (-l_2 + \frac{a_3\theta_3}{2v_1})\tilde{\xi}_2^2.\end{aligned} \tag{4.45}$$

For compact notation define: $\tilde{x} = [\tilde{\xi}_1\ \tilde{\xi}_2\ \tilde{\theta}_1\ \tilde{\theta}_3\ \tilde{\theta}_3]$. Noticing that $x = 0$ is an equilibrium for the system described by (4.32), (4.33), (4.40) and (4.43). And that the system is Lipschitz in x, uniformly in t under assumption 9. We can conclude by LaSalle-Yoshizawa theorem that for l_1 and l_2 chosen such that $(-l_1 a_1 + \frac{a_3\theta_3}{2v_1}) < 0$ and $(-l_2 + \frac{a_3\theta_3}{2v_1}) < 0$ all solutions to (4.32), (4.33), (4.40) and (4.43) are uniformly bounded (note that v_1 is bounded from below). And that

$$\begin{aligned} &\lim_{t\to\infty}(-l_1 a_1 + \frac{a_3\theta_3}{2v_1})\tilde{\xi}_1^2 + (-l_2 + \frac{a_3\theta_3}{2v_1})\tilde{\xi}_2^2 = 0 \\ \Rightarrow &\lim_{t\to\infty}\tilde{\xi}_1 = \lim_{t\to\infty}\tilde{\xi}_2 = 0, \end{aligned}$$

which implies that $\widehat{q}_{bit} \to q_{bit}$ and $\widehat{p}_c \to p_c$ as $t \to \infty$.

4.3.3 Parameter Convergence

Using a similar approach as in Section 4.2.5 conditions for $\lim_{t\to\infty}\tilde{\theta}_3\phi_3 = 0$ will be found. From (4.40) and the previous Lyapunov analysis we have

$$\begin{aligned} \lim_{t\to\infty}\dot{\tilde{\xi}}_2 &= \lim_{t\to\infty}\left(\frac{a_3}{v_1}\theta_3\tilde{\xi}_1 + \tilde{\theta}_3\phi_3 - l_2\tilde{\xi}_2\right) \\ \lim_{t\to\infty}\dot{\tilde{\xi}}_2 &= \lim_{t\to\infty}\tilde{\theta}_3\phi_3. \end{aligned} \tag{4.46}$$

Hence, if we can find conditions for $\lim_{t\to\infty}\dot{\tilde{\xi}}_2 = 0$ we can state that $\lim_{t\to\infty}\tilde{\theta}_3\phi_3 = 0$. This can be done by using Barbălat's lemma and assuming uniform continuity of $\dot{\tilde{\xi}}_2$. As this leads to some tedious calculations an extension of Barbălat's lemma will be used instead. Using the following lemma found in (Lefeber 2000), slightly changed from the original in (Micaelli & Samson 1993).

Lemma 1. *(Micaelli and Samson, 1993) Let $f : \mathbb{R}_+ \to \mathbb{R}$ be any differentiable function. If $f(t)$ converges to zero as $t \to \infty$ and its derivative satisfies:*

$$\dot{f}(t) = f_0(t) + \eta(t) \qquad t \geq 0$$

where f_0 is a uniformly continuous function and $\eta(t)$ tends to zero as $t \to \infty$, then $\dot{f}(t)$ and $f_0(t)$ tend to zero as $t \to 0$.

Define:

$$\begin{aligned} \dot{f}(t) &= \dot{\tilde{\xi}}_2 \\ &= \frac{a_3}{v_1}\theta_3\tilde{\xi}_1 + \tilde{\theta}_3\phi_3 - l_2\tilde{\xi}_2 \\ &= f_0(t) + \eta(t) \end{aligned} \tag{4.47}$$

Where $f_0(t) = \tilde{\theta}_3\phi_3$ and $\eta(t) = \frac{a_3}{v_1}\theta_3\tilde{\xi}_1 - l_2\tilde{\xi}_2$. From the previous Lyapunov analysis the following is known:

- $f(t) = \tilde{\xi}_2 \to 0$
- $\eta(t) \to 0$

Hence, by Lemma 1 if $f_0(t)$ is uniformly continuous both $f_0(t)$ and $\dot{f}(t)$ will tend to zero as $t \to 0$. If $\dot{f}_0(t) \in \mathcal{L}_\infty$ then $f_0(t)$ is uniformly continuous, (Ioannou & Sun 1996).

$$\dot{f}_0(t) = \dot{\tilde{\theta}}_3\phi_3 + \tilde{\theta}_3\dot{\phi}_3 \tag{4.48}$$

$$= -\gamma_3\phi_3\tilde{\xi}_2\phi_3 + \tilde{\theta}_3\dot{\phi}_3, \tag{4.49}$$

where (4.43) has been inserted in the last equation. And

$$\dot{\phi}_3 = \frac{a_3\dot{\hat{q}}_{bit} + \dot{u} + \dot{v}_2}{v_1} + \frac{v_2}{v_1}\phi_3, \tag{4.50}$$

where $-\dot{v}_1 = v_2$ has been used. Table 4.3 summarize the conditions needed to ensure that $f_0(t)$ is uniformly continous which implies that $\lim_{t\to\infty}\dot{\tilde{\xi}}_2 = \lim_{t\to\infty}\tilde{\theta}_3\phi_3 = 0$.

Table 4.3: Conditions on signals for θ_3 estimator

Condition	Comment
$\tilde{\xi}_2, \tilde{\theta}_3 \in \mathcal{L}_\infty$	Proved in Lyapunov analysis
$\phi_3 \in \mathcal{L}_\infty$	True by assumption 9 and the Lyapunov analysis
$\dot{\phi}_3 \in \mathcal{L}_\infty$	True by assumption 9, $\phi_3 \in \mathcal{L}_\infty$ and in addition $\dot{u}, \dot{v}_2 \in \mathcal{L}_\infty$

The condition that $\dot{u}, \dot{v}_2 \in \mathcal{L}_\infty$ is quite strict. Remembering that $u = b_2u_b - q_{choke}$, one can assume that $\dot{u}$ is bounded by assuming some sort of dynamic behavior in both the back pressure pump and the choke valve. E.g., $\tau_c\dot{q}_{choke} = -q_{choke} + u_c$ where u_c is a bounded control input. This is reasonable to do in practice but will increase the complexity of a future control problem. The assumption that $\dot{v}_2 = -\ddot{V}_a(t)$ is bounded could be justified by the fact that inertia and elastic deformation will limit acceleration in the volume.

The result that $\lim_{t\to\infty}\tilde{\theta}_3\phi_3 = 0$ under the signal conditions in Table 4.3 tells us that $\tilde{\theta}_3$ only converges to zero if the regressor ϕ_3 is sufficiently exciting. Practically this means that β_a can not be estimated as long as the system is in steady state. This is obvious in view of (4.3) as β_a only has an effect on transient behavior. Hence to get a good estimate of β_a the p_c dynamics must be excited.

4.3.4 Summary Parameter Estimator

Figure 4.2 shows the interconnection of the parameter estimator for θ_3 and the observer. The parameter estimator is summarized in Table 4.4 and the observer is summarized in Table 4.2.

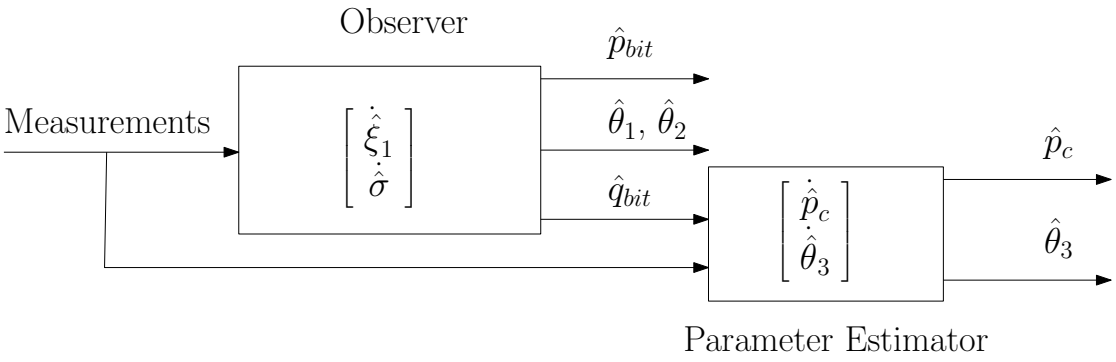

Figure 4.2: Interconnection of observer and parameter estimator

In addition to the properties of the adaptive observer summarized in Section 4.2.6, the interconnection has the following properties:

- All solutions to (4.40) and (4.43) are uniformly bounded.
- $\lim_{t\to\infty} \tilde{p}_c = 0$
- $\lim_{t\to\infty} \dot{\tilde{\theta}}_3 = 0$

Furthermore if the conditions in Table 4.3 are satisfied the estimator has the following additional property:

- $\lim_{t\to\infty} \tilde{\theta}_3 \phi_3 = 0$

All results are valid for $q_{bit} > 0$. The limitation is a result of the switched dynamics at $q_{bit} = 0$.

Table 4.4: Summary of parameter estimator

Plant	$\dot{p}_c = \frac{\theta_3}{v_1}(a_3 q_{bit} + u + v_2)$ p_c measured
Observer	$\tilde{\xi}_2 = p_c - \widehat{p}_c$ $\dot{\widehat{p}}_c = \frac{a_3 \widehat{\theta}_3 \widehat{q}_{bit}}{v_1} + \frac{\widehat{\theta}_3 (u+v_2)}{v_1} + l_2 \tilde{\xi}_2$ $\widehat{p}_c(0) = p_c(0)$
Parameter Estimator	$\dot{\widehat{\theta}}_3 = \gamma_3 \phi_3 \tilde{\xi}_2$ $\phi_3 = \frac{a_3 \widehat{q}_{bit} + u + v_2}{v_1}$
Design variables	Observer gain l_1 and l_2 chosen to satisfy: $(-l_1 a_1 + \frac{a_3 \theta_3}{2v_1}) < 0$ and $(-l_2 + \frac{a_3 \theta_3}{2v_1}) < 0$ Adaption gain: $\gamma_3 > 0$ Initial condition: $\widehat{\theta}_3(0)$

4.4 Pragmatic Approach to $q_{bit} = 0$

As the proved performance of the adaptive observer and parameter estimator is limited to $q_{bit} > 0$ two pragmatic approaches on how to deal with the case where $q_{bit} = 0$ will be presented. The approaches are based on practical intuition and thus do not provide proofs of performance. However, simulation results in chapter 5 shows promising performance of the approach suggested in section 4.4.2 and should therefore serve as a stepping stone for future work.

4.4.1 Observer as Before

As the observer dynamics are stable for all $\widehat{q}_{bit}$ one approach is to assume that the errors when using the observer at $q_{bit} = 0$ are so small that they may be neglected. Using (2.44) it is possible to analyze what affects the modeling error. Restating (2.44) using the notation introduced in the beginning of this chapter gives

$$\dot{q}_{bit} = \begin{cases} a_2(p_p - p_c) - \theta_1 |q_{bit}| q_{bit} + \theta_2 v_3 & q_{bit} > 0 \\ \max\left\{0, a_2(p_p - p_c) + \theta_2 v_3\right\} & q_{bit} = 0 \end{cases} . \tag{4.51}$$

As the observer is based on the top equation we will analyze what affects the modeling error if we assume that the top equation is valid for $q_{bit} = 0$ too. Looking at what

happens when $q_{bit} = 0 \Rightarrow \theta_1 |q_{bit}| q_{bit} = 0$ which gives the modeling error, e_{m0}, at $q_{bit} = 0$,

$$\begin{aligned} e_{m0} &= \max(0, a_2(p_p - p_c) + \theta_2 v_3) - (a_2(p_p - p_c) + \theta_2 v_3) \\ &= \begin{cases} 0 & (a_2(p_p - p_c) + \theta_2 v_3) \geq 0 \\ -(a_2(p_p - p_c) + \theta_2 v_3) & (a_2(p_p - p_c) + \theta_2 v_3) < 0 \end{cases} . \end{aligned} \tag{4.52}$$

As $a_2 = \frac{1}{M}$ and $\theta_2 = \frac{(\bar{\rho}_d - \bar{\rho}_a)g}{M}$ The condition $(a_2(p_p - p_c) + \theta_2 h_{bit}) < 0$ can be rewritten as

$$(p_p - p_c + (\bar{\rho}_d - \bar{\rho}_a) g v_3) = p_{bit_{ds}} - p_{bit_{as}} < 0, \tag{4.53}$$

where $p_{bit_{ds}} = p_p + \bar{\rho}_d g v_3$ is the static pressure on the drill string side of the bit and $p_{bit_{as}} = p_c + \bar{\rho}_a g v_3$ is the static pressure on the annulus side of the drill string. This implies that the modeling error is large when the differential pressure over the bit $\Delta p_{bit} = p_{bit_{ds}} - p_{bit_{as}} << 0$ which is logical as that is when the check valve has the most influence. If the condition (4.53) never occurred, or when it did it was small, one could argue that the modeling error could be neglected. Unfortunately this is not the case. As an example, consider a pipe connection procedure (zero flow, $p_p = 0$) with $\bar{\rho}_d = \bar{\rho}_a$. The condition (4.53) can then be written as $-p_c < 0$. As p_c usually is ramped up during pipe connections to counter loss of friction pressure p_c can be in the order of 10's of bars. This will lead to a very large modeling error.

As explained in Section 2.3.3 this modeling error affects q_{bit} but most important it will enter directly into the estimate of p_{bit}, see equation (4.7). As a consequence a more sophisticated approach is needed.

4.4.2 Modified Observer

Motivated by the previous modeling error analysis the observer will be implemented as before for $q_{bit} > 0$,but for the condition

$$q_{bit} = 0 \text{ and } (a_2(p_p - p_c) + \theta_2 v_3) < 0 \tag{4.54}$$

the following modifications will be made

$$\dot{\hat{\xi}}_1 = l_1 b_1 u_p \tag{4.55}$$

$$\widehat{p}_{bit} = p_c + (\rho_d g - M\widehat{\theta}_2) v_3, \tag{4.56}$$

where (4.55) is motivated by differentiating (4.10) w.r.t. time and setting $\dot{\widehat{q}}_{bit} = 0$ and $\widehat{q}_{bit} = 0$ and (4.56) is motivated by equation (4.7) with $\dot{q}_{bit} = 0$ and $q_{bit} = 0$. As the

condition (4.54) depends on the unmeasured state q_{bit} and the unknown parameter θ_2 it will be implemented as

$$\widehat{q}_{bit} = 0 \text{ and } (a_2(p_p - p_c) + \widehat{\theta}_2 v_3) < 0. \tag{4.57}$$

Furthermore in view of equation (4.2) the adaptation for θ_1 at low flows should be turned off since it becomes unobservable. It is also interesting to note that according to (4.35) for $\widehat{q}_{bit} = 0$ and $v_3 > 0$ we have $\tilde{\theta}_2 \to 0$ at steady state ($\dot{\tilde{\xi}}_1 = 0$). This implies that we could get a very good estimate for $\tilde{\theta}_2$ during pipe connections. Therefore θ_2 adaptation will be turned off permanently as soon as $\widehat{q}_{bit} = 0$ during the connection procedure.

The suggested approach raises issues of smoothness, which might affect parameter estimates. Also it is a pragmatic approach and does not provide any proofs. Therefore it should be seen as a starting point for future work and analysis.

Chapter 5

Simulations and Results

To analyze the performance of the adaptive observer presented in Chapter 4 several simulations were performed. First, to verify that the observer performs as proved, simulations were run to compare the observer estimates with output from the design model defined in (4.1)-(4.3) and (4.8). The results verify that the observer does indeed perform as proved. From the simulations interesting trends in which of the unknown parameters one can expect to estimate can be seen. Then, to see how the observer performs in more realistic scenarios, simulations with drill string movements (swab and surge) and pipe connection procedures were performed. The observer has no difficulties with surge and swab scenarios. For the pipe connection scenario both of the pragmatic approaches in Section 4.4 are simulated. The results show that the modified observer proposed in section 4.4.2 gives a much better estimates than simply ignoring the modeling error at zero flow. To test the robustness of the observer to unmodeled dynamics the observer was also tested on a data set from a pipe connection scenario simulated with WeMod. WeMod is a simulator designed by the International Research Institute of Stavanger (IRIS) for simulating drilling operations, (Nygaard & Gravdal 2007). It is based on a distributed parameter model for describing the well dynamics. For $q_{bit} > 0$ both of the approaches presented in section 4.4 show good estimates of p_{bit}, but at low flow the modified observer proposed in section 4.4.2 shows the best performance. Finally the modified observer was tested on a dataset collected from the Grane field. Due to unmodeled events at Grane the observer is only tested without adaptation and with adaptation of the friction parameter θ_1. In both cases the observer shows promising behavior (especially during steady state) but more work is needed to model certain manually controlled valves.

5.1 Simulations Verifying Proved Properties

In this section the model defined in (4.1)–(4.3) and (4.8) with q_{choke} defined in (2.13) is considered the true system. The model is numerically conditioned according to appendix A.2. Simulations were carried out using Matlab™and Simulink™. The observer was implemented with a fixed step solver.

The parameters used in the model where found by fitting the low order model to a dataset from a WeMod simulation, see (Imsland 2007) and (Nygaard 2007). The parameters were adjusted for numerical conditioning and are presented in Table 5.1. Note that $V_a(t)$, $h_{bit}(t)$ and $l_{bit}(t)$ are allowed to change with time. All other parameters are constant, see figure 2.1 for explanation of notation.

Table 5.1: Parameter values for simulation

Parameter	Value	Description
V_d	28.2743	Volume drill string (m^3)
β_d	14000	Bulk modulus drill string (bar)
β_a	14000	Bulk modulus annulus (bar)
K_c	0.0046	Choke valve constant
p_0	1	Pressure outside system (bar)
$\bar{\rho}_a$	0.0125	Density annulus ($10^{-5} \times \frac{kg}{m^3}$)
$\bar{\rho}_d$	0.0125	Density drill string ($10^{-5} \times \frac{kg}{m^3}$)
F_d	0.1650	Friction factor drill string
F_a	0.0208	Friction factor annulus
M_a	1.6009	($10^{-8} \times \frac{kg}{m^4}$)
M_d	5.7296	($10^{-8} \times \frac{kg}{m^4}$)
L_{dN}	3600	Total length drill string
V_a^0	96.1327	Volume (m^3) annulus at $t = 0$
h_{bit}^0	2000	Vertical depth (m) of bit at $t = 0$
l_{bit}^0	3600	Length of well at $t = 0$

5.1.1 Simulation 1, step input one unknown

In the first simulation the observer estimates are compared to the low order model to see how well the observer performes with only one unknown parameter, θ_1. The design variables are defined in Table 5.2. The input, shown in Figure 5.1(d), consists of a constant main pump flow $q_p = 1000\frac{l}{min}$, zero back pressure pump flow and a low-pass filtered step in the choke opening z_c from 0.07 to 0.12 at $t = 60s$. From figures 5.1(a), 5.1(b) and 5.1(c) one can see that the state estimation error $\tilde{q}_{bit}$, the output estimation error $\tilde{p}_{bit}$ and the parameter estimation error $\tilde{\theta}$ all converge to zero within approximately

$10s$. All estimation errors remain at zero throughout the step in the choke opening. The results are in accordance with the proved properties of the observer. $\tilde{q}_{bit}$ was proved to converge to zero in the Lyapunov analysis in Section 4.2.2 while $\tilde{p}_{bit} \to 0$ was proved in Section 4.2.5. The fact that $\widehat{\theta}$ converges to θ_1 in this case is easily explained by equation (4.35) which tells us that if θ_2 is known and $\widehat{q}_{bit} \neq 0$ then $\tilde{\theta}_1 \to 0$.

Table 5.2: Design variables simulation 1

Variable	Description
$l_1 = 1$	State estimation gain
$\gamma_1 = 10^{-5}$	Adaptation gain
$\widehat{q}_{bit}(0) = 400\frac{l}{min}$	Initial condition
$\widehat{\theta}_1(0) = 2\theta_1$	Initial condition

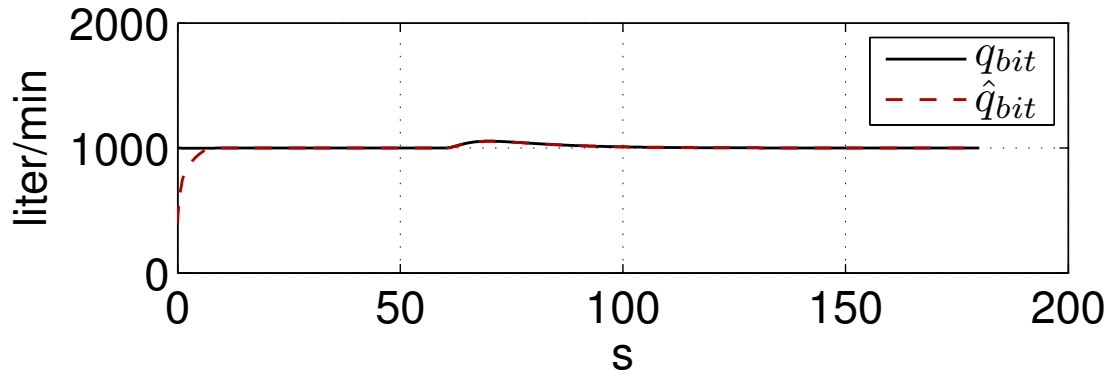

(a) q_{bit} and $\widehat{q}_{bit}$

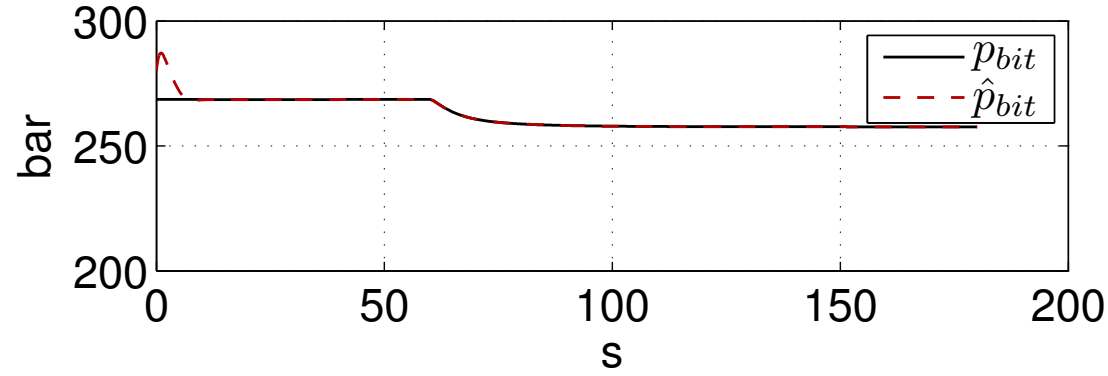

(b) p_{bit} and $\widehat{p}_{bit}$

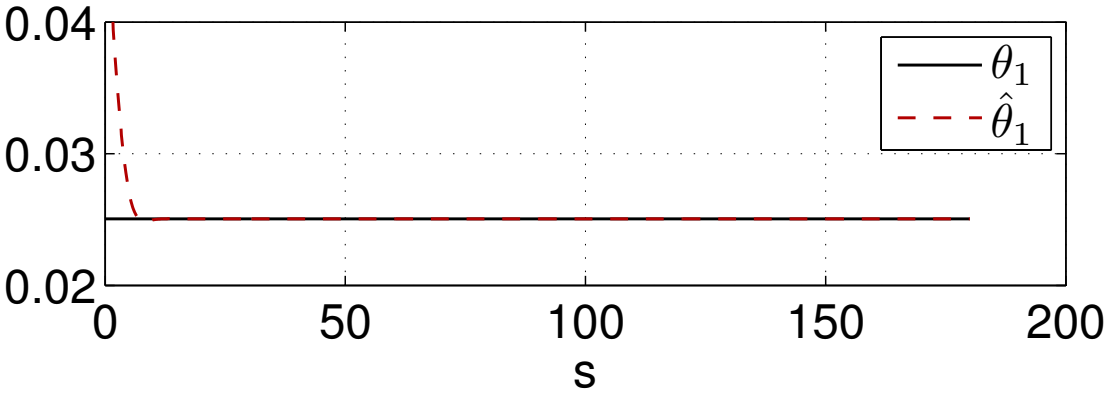

(c) θ and $\widehat{\theta}$

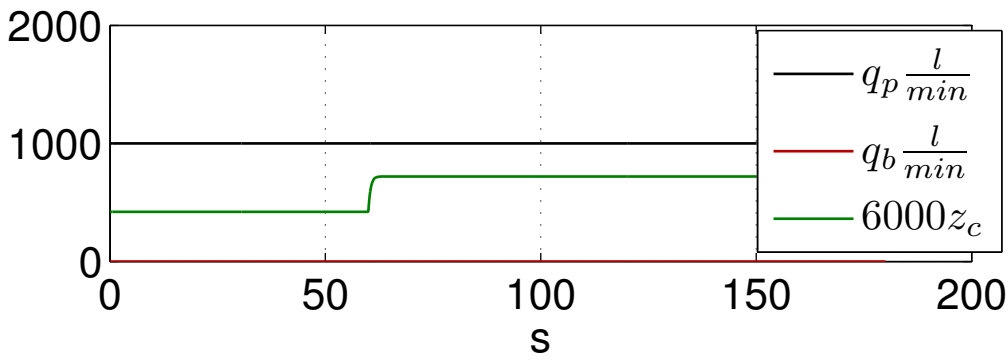

(d) Flows q_p, q_b and choke opening z_c

Figure 5.1: Simulation results simulation 1

5.1.2 Simulation 2, Step Input Two Unknowns

In the second simulation both θ_1 and θ_2 are unknown. The design variables are presented in Table 5.3. As $\bar{\rho}_a = \bar{\rho}_d$ in Table 5.1, $\theta_2 = 0$. The initial condition is $\widehat{\theta}_2(0) = -0.0083$ which corresponds to $\widehat{\bar{\rho}}_a = 1.5\bar{\rho}_a$. The same input as in the previous simulation was used, see Figure 5.1(d).

From figures 5.2(a) and 5.2(b) one can see that the state and output estimation errors converge to zero. This is as expected from the previous Lyapunov analysis. There are strong transient effects during the first five seconds in both $\widehat{q}_{bit}$ and $\widehat{p}_{bit}$ due to the adaptation. Figure 5.2(c) shows this for $\widehat{p}_{bit}$. Note that the transient effect can be made less aggressive (but it will take longer to pass) by tuning down the adaptation gains. Figures 5.3(a) and 5.3(b) show that the parameter errors do not converge to zero. According to (4.35) this can happen as only $\tilde{\theta}^T\phi \to 0$ is guaranteed, Figure 5.3(c) shows that $\tilde{\theta}^T\phi \to 0$. As the parameter estimation errors do not converge to zero the Lyapunov function U_1 defined in (4.16) will not converge to zero either. This is shown in Figure 5.3(d). As U_1 is non-increasing it is possible that during a transient one parameter estimation error becomes larger while the other one decreases. This effect can be seen around $t = 60s$ in figures 5.3(a) and 5.3(b).

Table 5.3: Design variables simulation 2

Variable	Description
$l_1 = 1$	State estimation gain
$\gamma_1 = 10^{-5}$	Adaptation gain, $\widehat{\theta}_1$
$\gamma_2 = 10^{-6}$	Adaptation gain, $\widehat{\theta}_2$
$\widehat{q}_{bit}(0) = 400\frac{l}{min}$	Initial condition
$\widehat{\theta}_1(0) = 2\theta_1$	Initial condition
$\widehat{\theta}_2(0) = -0.0083$	Initial condition

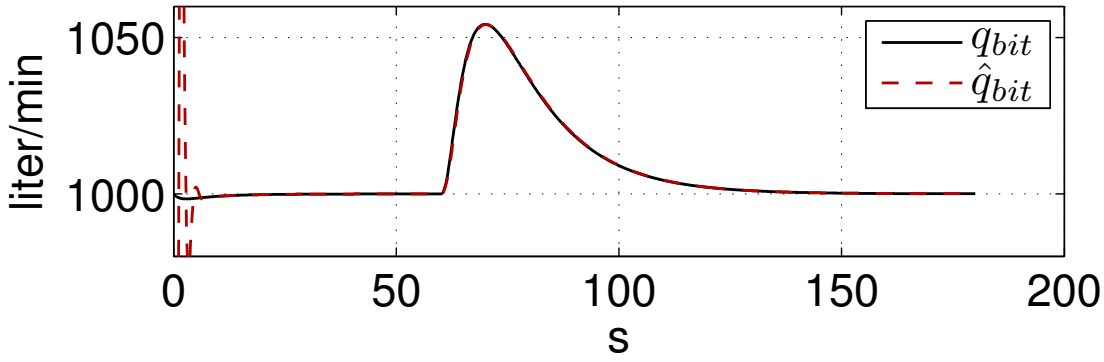

(a) q_{bit} and $\widehat{q}_{bit}$

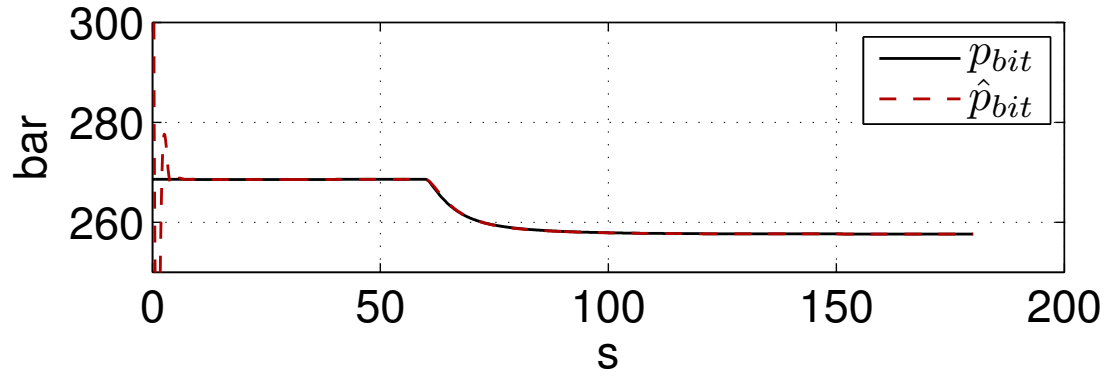

(b) p_{bit} and $\widehat{p}_{bit}$

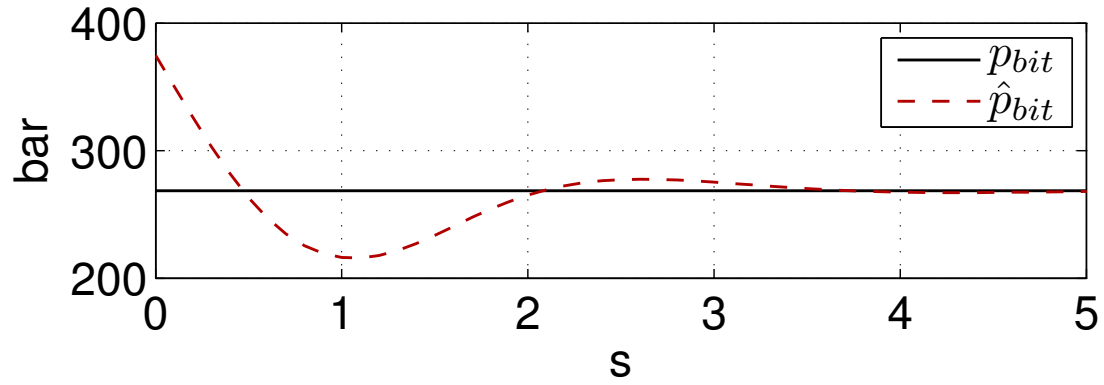

(c) p_{bit} and $\widehat{p}_{bit}$, transient behavior during the first five seconds.

Figure 5.2: Simulation results simulation 2

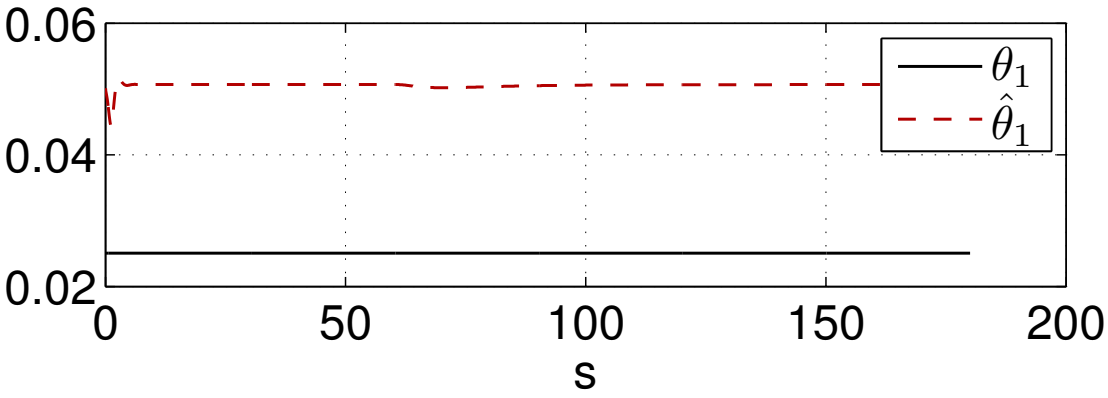

(a) θ_1 and $\widehat{\theta}_1$

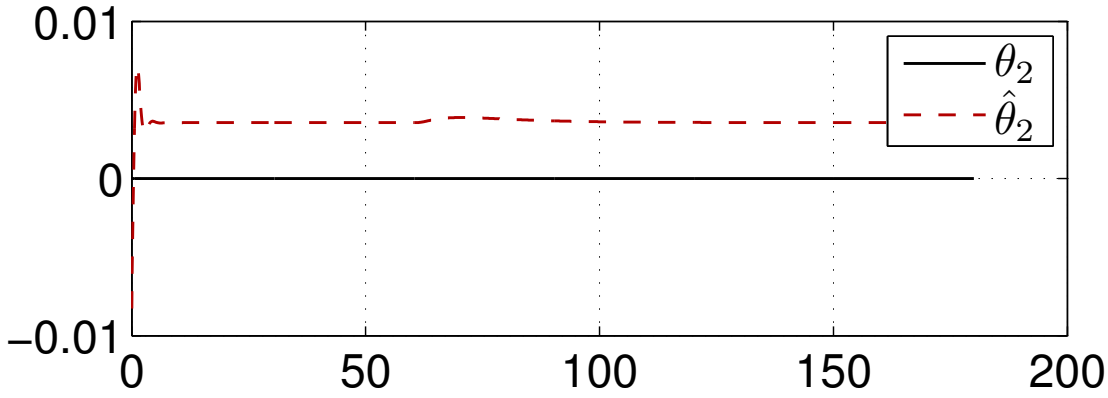

(b) θ_2 and $\widehat{\theta}_2$

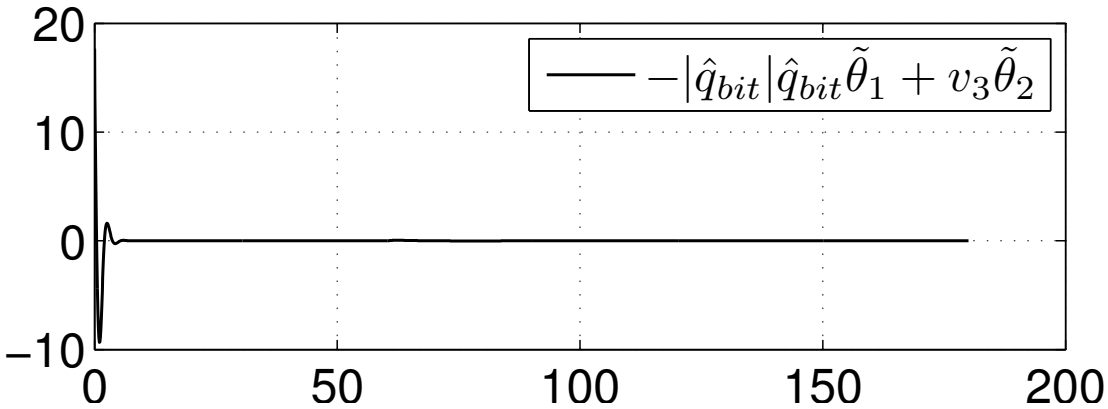

(c) Plot of $\tilde{\theta}^T\phi$

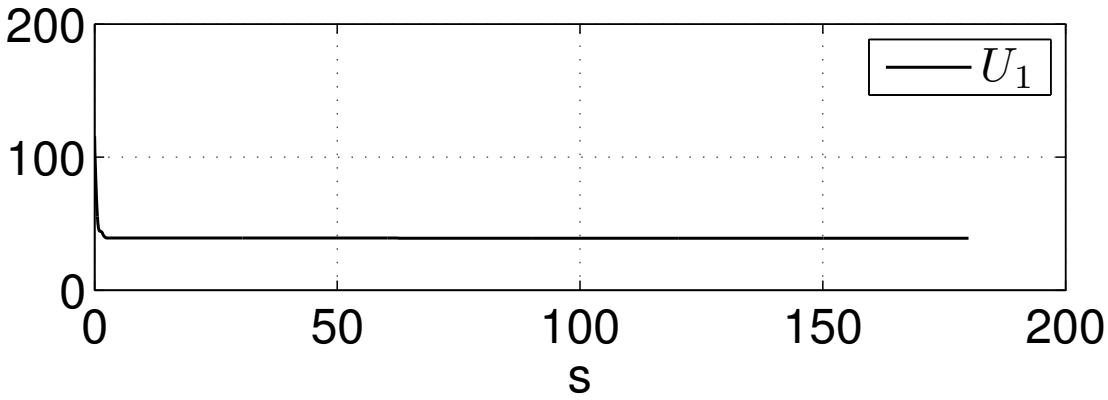

(d) Lyapunov function U_1

Figure 5.3: Simulation results simulation 2

5.1.3 Simulation 3, θ_3 Estimator

To see how the θ_3 estimator performs a third simulation was carried out. The design variables are summarized in Table 5.4, the gains were chosen to satisfy the conditions summarized in Table 4.4. As no information about θ_3 can be obtained at steady state ($\dot{p}_c = 0$), see equation (4.3), it is hard to estimate. It was necessary to choose the adaption gain γ_3 quite large to get $\tilde{\theta}_3 \to 0$. The size of the gain is also related to the fact that the θ_3 parameter is several orders of magnitude larger than the other unknown parameters. As the θ_3 estimator is decoupled from the observer, see Figure 4.2, only plots of signals relevant to $\widehat{\theta}_3$ will be shown.

To excite the system the same step in the choke as in the two previous simulations was used, with additional steps in main pump flow and backpressure pump flow, see Figure 5.4(c). From Figure 5.4(b) it can be seen that $\widehat{p}_c$ tracks p_c very well. This makes the adaptation hard as it is $\tilde{p}_c$ that drives the adaptation, see equation (4.43). The l_2 gain, which controls the rate of convergence for $\tilde{p}_c$, was chosen just large enough to satisfy the condition imposed by the Lyapunov design to give the adaptation more time. From Figure 5.4(a) it can be seen that $\tilde{\theta}_3$ comes close to zero towards the end but diverges slightly at $t = 380s$. Looking at only one part of the Lyapunov function, namely U_2, defined in (4.42) might lead to the conclusion that this contradicts the Lyapunov based proof. But as it is $U = U_1 + U_2$, defined in (4.41), that is nondecreasing, U_2 can increase if U_1 decreases. Although not shown here, this is what happens. This illustrates that the estimate is sensitive to changes as long as $U > 0$. For the same simulation only with θ_2 known the results are significantly better. Figure 5.4(d) shows this. For comparison the end of the simulation with unknown θ_2, $\tilde{\theta}_3 \approx -140$ which is about 1% of θ_1 while at the end of the second simulation $\tilde{\theta}_3 \approx 7$ which is twenty times less.

Table 5.4: Design variables simulation 3

Variable	Description
$l_1 = 1$	q_{bit} estimation gain
$l_2 = 0.1$	p_c estimation gain
$\gamma_1 = 10^{-5}$	Adaptation gain, $\widehat{\theta}_1$
$\gamma_2 = 10^{-6}$	Adaptation gain, $\widehat{\theta}_2$
$\gamma_3 = 10^{8}$	Adaptation gain, $\widehat{\theta}_3$
$\widehat{q}_{bit}(0) = 400\frac{l}{min}$	Initial condition
$\widehat{\theta}_1(0) = 2\theta_1$	Initial condition
$\widehat{\theta}_2(0) = -0.0083$	Initial condition
$\widehat{\theta}_3(0) = 0.9\theta_3$	Initial condition

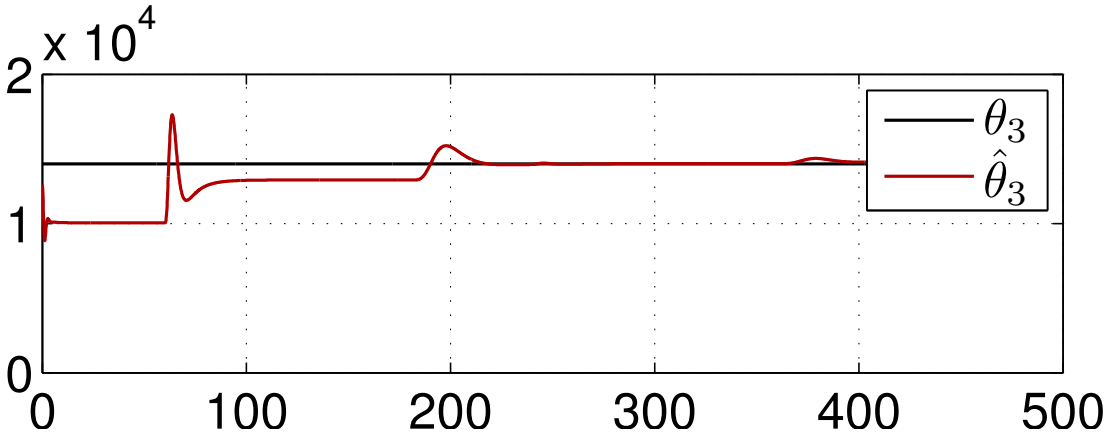

(a) θ_3 and $\widehat{\theta}_3$, θ_2 unknown

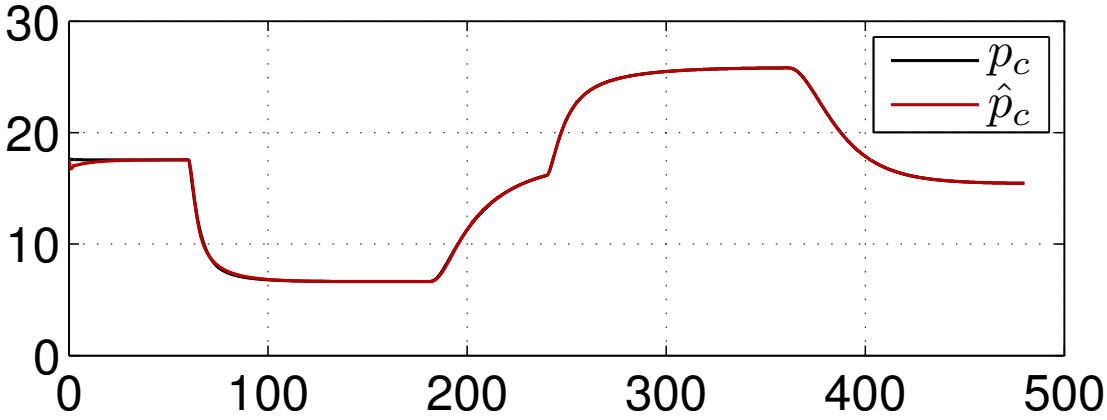

(b) p_c and $\widehat{p}_c$

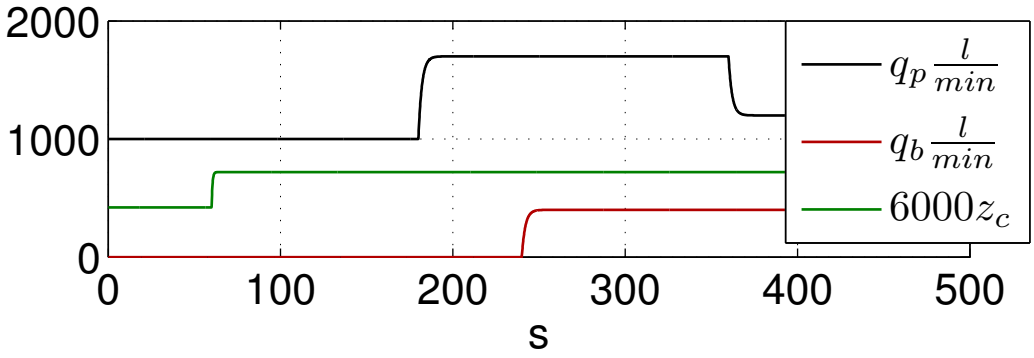

(c) Flows q_p, q_b and choke opening z_c

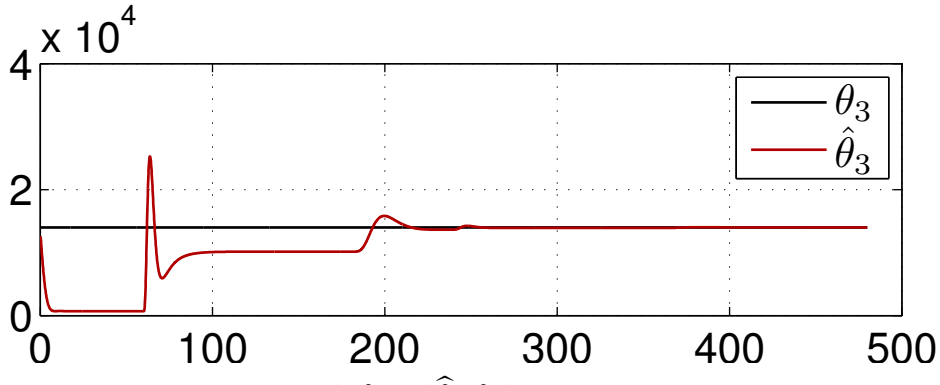

(d) θ_3 and $\widehat{\theta}_3$, θ_2 known

Figure 5.4: Simulation results simulation 3

5.2 Simulation Results Operational Scenarios

To see how the observer works during more realistic scenarios two simulation cases were performed. The first case was a surge and swab case which includes movement in the drill string. The second one was a pipe connection procedure where the main difficulty lies in $q_{bit} = 0$ during the actual procedure. The model parameters used are defined in Table 5.1.

5.2.1 Surge and Swab

Simulations were carried out to see how the observer performs in the presence of drill string movements. Specifically surge (moving the drill string into the well) and swab(moving the drill string out from the well) scenarios where simulated. Drill string movements affect p_{bit} through changes in volume in the annulus. The design variables were the same as in the previous simulation, defined in Table 5.4. The main and back pressure pump flows were kept constant at $1000\frac{l}{min}$ and $200\frac{l}{min}$ respectively, and the choke opening was $z_c = 0.070$. The drill string was first moved out (swab) starting at $t \approx 200$. The speed was chosen to be $18\frac{m}{min}$ which is high. Approximately 27m of pipe was moved, which corresponds to the length of one drill pipe. At $t = 400s$ the reverse procedure (surge) takes place. Figure 5.5(c) shows the changes in volume in the annulus and vertical depth. Figure 5.5(a) shows that $\widehat{p}_{bit}$ tracks p_{bit} well after some initial transients. The same can be seen for $\widehat{q}_{bit}$ in 5.5(b). The operation does not affect $\widehat{\theta}_1$ or $\widehat{\theta}_2$ much, see figures 5.6(a) and 5.6(b). However, it is very interesting to see that $\widehat{\theta}_3$ improves significantly during the operation compared to the previous simulation. Compare Figure 5.6(c) with 5.4(a) and 5.4(d). In view of equation (4.3) it seems reasonable that changes in the volume $V_a = v_1$ and $v_2 = -\dot{v}_1$ gives good excitation for estimating θ_3.

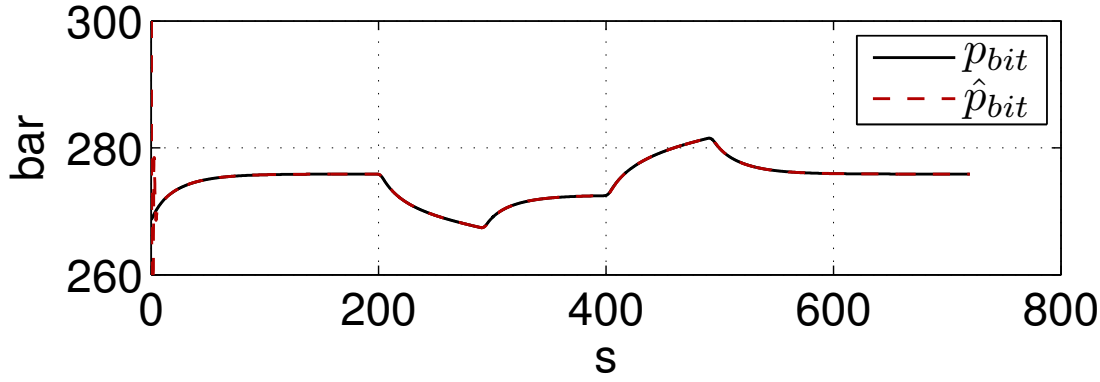

(a) p_{bit} and $\widehat{p}_{bit}$

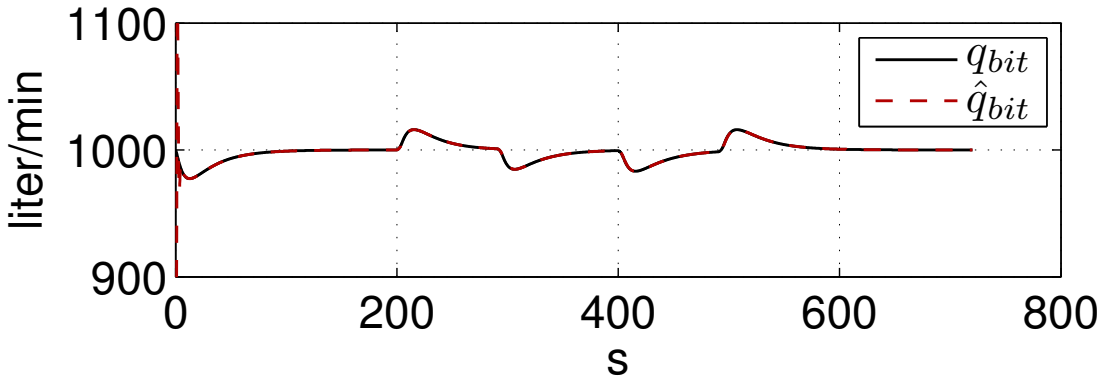

(b) q_{bit} and $\widehat{q}_{bit}$

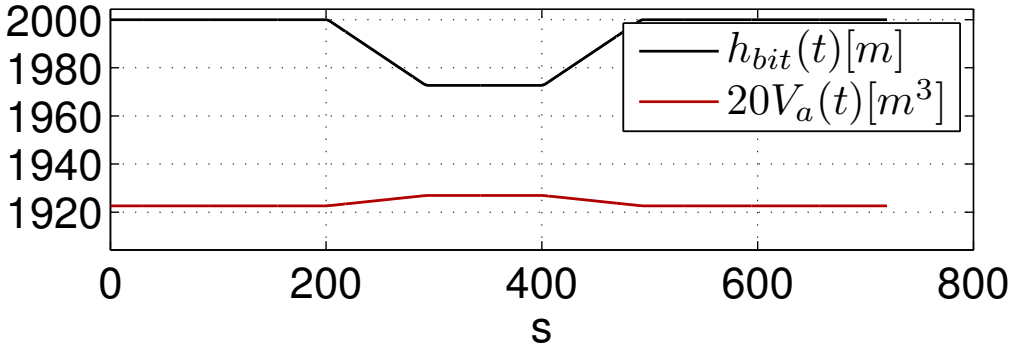

(c) Time varying signals $h_{bit}(t)$ and $V_a(t)$

Figure 5.5: Simulation results surge and swab

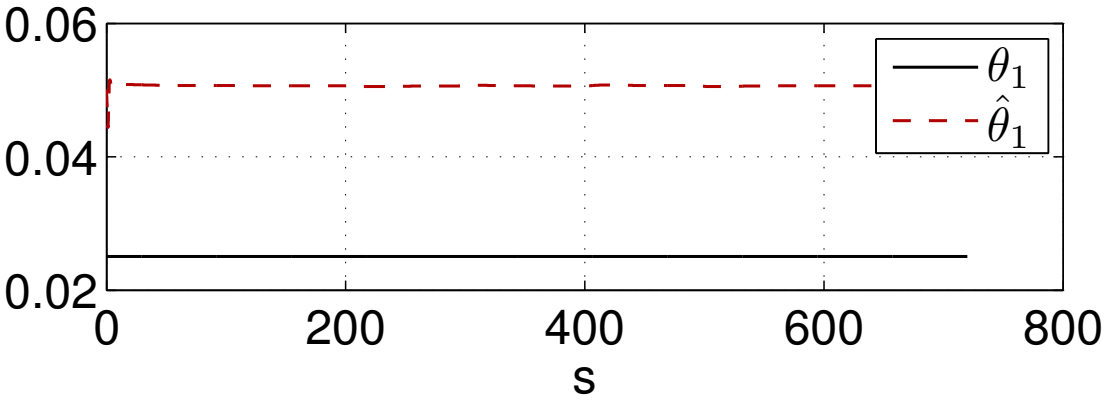

(a) θ_1 and $\widehat{\theta}_1$

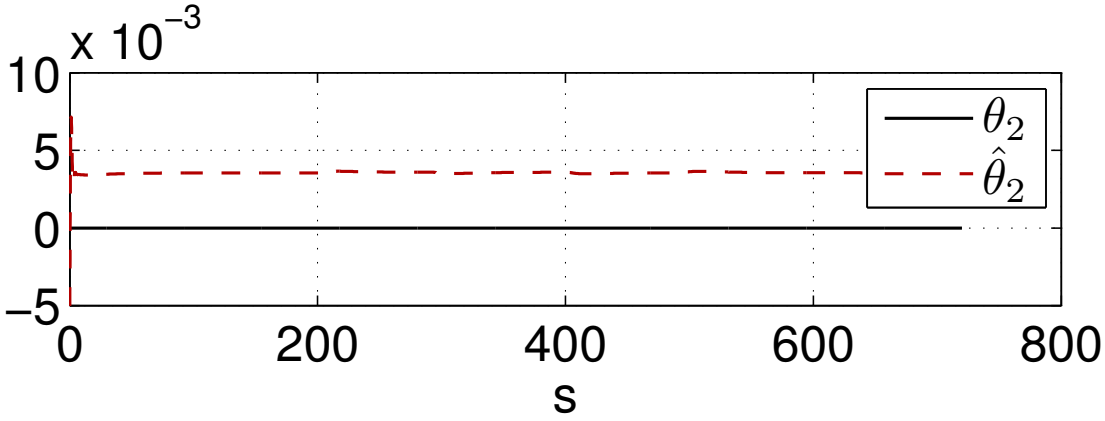

(b) θ_2 and $\widehat{\theta}_2$

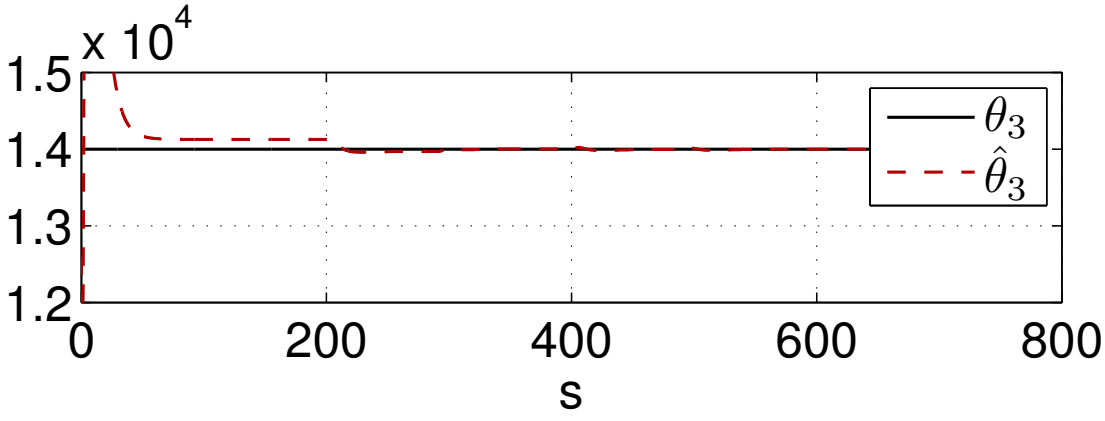

(c) θ_3 and $\widehat{\theta}_3$

Figure 5.6: Simulation results case 5

5.2.2 Pipe Connection

Pipe connection is a common scenario during drilling. For every drilled $27m$ a new drill pipe needs to be connected to the drill string. For the new drill pipe to be connected, the main pump must be shut down resulting in zero flow, $q_{pump} = 0$. Furthermore excess fluid in the drill string is bled off through a valve and returned to the mud tanks to reduce the main pump pressure to zero barg before the pump is disconnected. The procedure takes about 10 minutes to complete. As mentioned earlier zero flow is a problem since the observer is based on a model that is only valid for $q_{bit} > 0$.

Simulation results for the two approaches presented in Section 4.4 will be presented here. To achieve a realistic condition where the check valve is active, a proportional-integral (PI) controller will be used to increase p_c to compensate for friction loss. In addition the p_p pressure will be bled off which corresponds to reality. The PI controller is

$$z_c = K_p e + K_i e \tag{5.1}$$

$$e = p_c - p_{c_{ref}}, \tag{5.2}$$

where $p_{c_{ref}}$ is 6 bar step that compensates for loss of friction pressure in the annulus.

The increase in drill string volume V_d as a new pipe is connected is ignored both in the true system and in the observer to reduce complexity.

Pipe Connection 1

The first pipe connection simulation was carried out using the observer as it was derived, ignoring the modeling error due to the check valve. The design variables used are defined in Table 5.5. Figure 5.7(d) shows the inputs to the system during the pipe connection. The main pump flow (q_p) is reduced to zero while the back pressure pump flow (q_b) is increased to $400\frac{l}{min}$. The choke valve is tightened by the PI controller increasing p_c by 6 bar to compensate for the pressure loss caused by zero circulation. Note the negative q_p which is the simulated bleed off to reduce p_p to one bar.

From Figure 5.7(a) it can be seen that after initial transients $\widehat{p}_{bit}$ tracks p_{bit} as long as $q_{bit} > 0$. From $t \approx 790s$ to $t \approx 900s$ when $q_{bit} = 0$ there is a small (4 bar) error until the bleed off starts. During the bleed off the error grows to around 30 bar. Note that throughout the simulation $\widehat{q}_{bit}$ tracks q_{bit} quite well, see Figure 5.7(b). There are small damped oscillations as $\widehat{q}_{bit} \to 0$, see Figure 5.7(c). The 4 bar error in the p_{bit} estimate from $t \approx 790s$ to $t \approx 900s$ is mainly caused by the error in the θ_2 estimate, see Figure 5.8(c). This can be seen as the modeling error in ignoring the check valve is small at this stage since p_p is close to p_c, see Figure 5.8(a) and equation (4.52). And as $\widehat{q}_{bit} \approx q_{bit} = 0$ hence $\tilde{p}_{bit} \approx -M_d \tilde{\theta}_2 v_3$, see equation (4.30). The large error in the p_{bit} estimate from $t = 900s$ is due to the modeling error commented on in Section 4.4.

Figures 5.8(b) - 5.8(d) show that none of the estimated parameters converge to the true values.

Table 5.5: Design variables pipe connection

Variable	Description
$l_1 = 1$	q_{bit} estimation gain
$l_2 = 1$	p_c estimation gain
$\gamma_1 = 10^{-5}$	Adaptation gain, $\widehat{\theta}_1$
$\gamma_2 = 10^{-6}$	Adaptation gain, $\widehat{\theta}_2$
$\gamma_3 = 10^{8}$	Adaptation gain, $\widehat{\theta}_3$
$\widehat{q}_{bit}(0) = 400\frac{l}{min}$	Initial condition
$\widehat{\theta}_1(0) = 2\theta_1$	Initial condition
$\widehat{\theta}_2(0) = -0.0083$	Initial condition
$\widehat{\theta}_3(0) = 0.9\theta_3$	Initial condition
$K_p = 0.0025$	Proportional gain
$K_i = 0.0005$	Integral gain

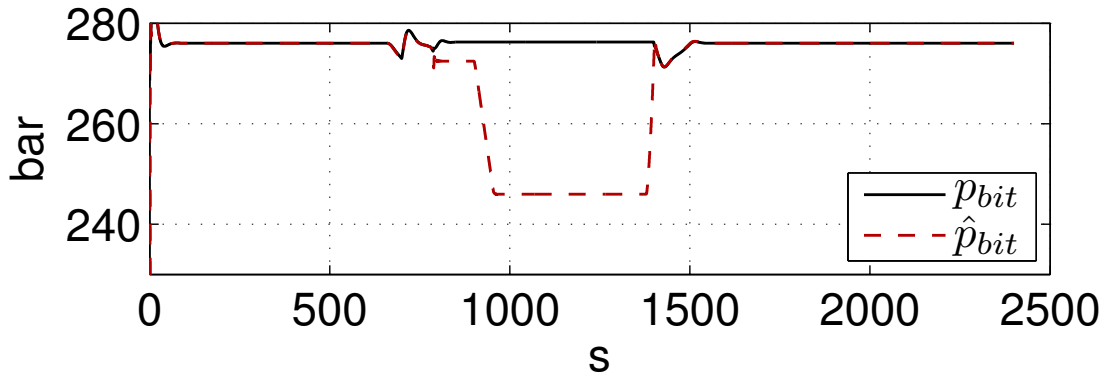

(a) p_{bit} and $\widehat{p}_{bit}$

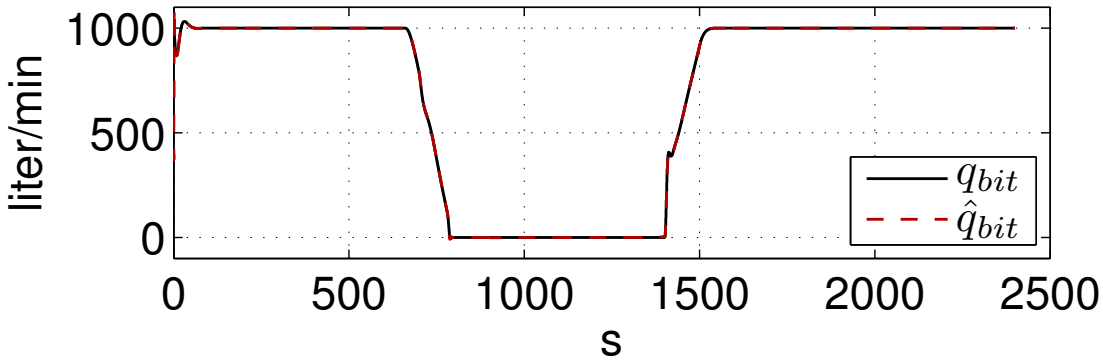

(b) q_{bit} and $\widehat{q}_{bit}$

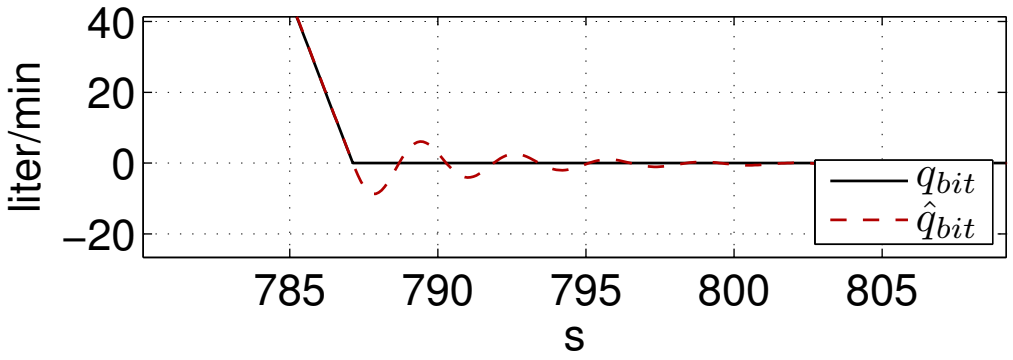

(c) q_{bit} and $\widehat{q}_{bit}$ enlarged

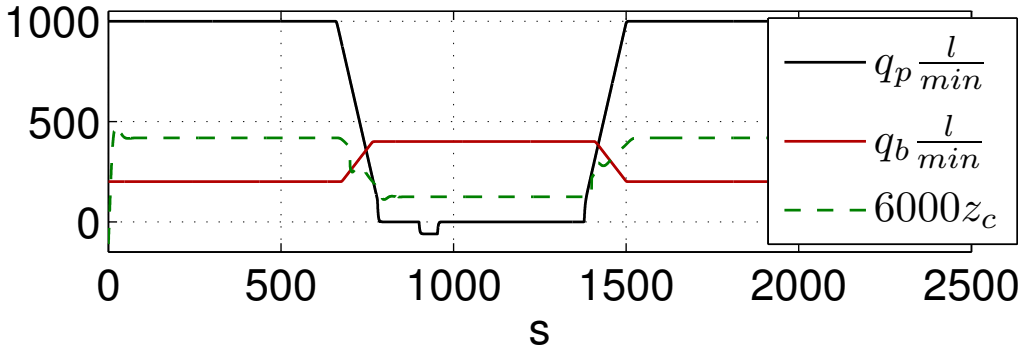

(d) Flows q_p, q_b and choke opening z_c

Figure 5.7: Simulation results pipe connection 1

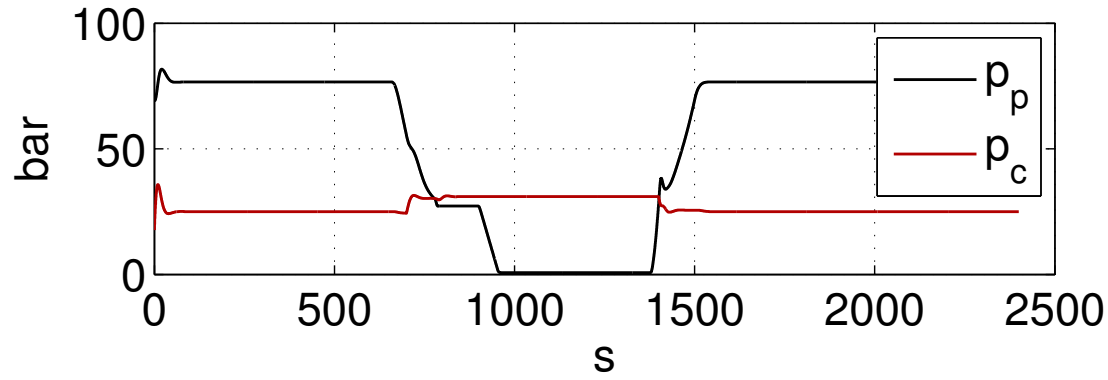

(a) p_p and p_c

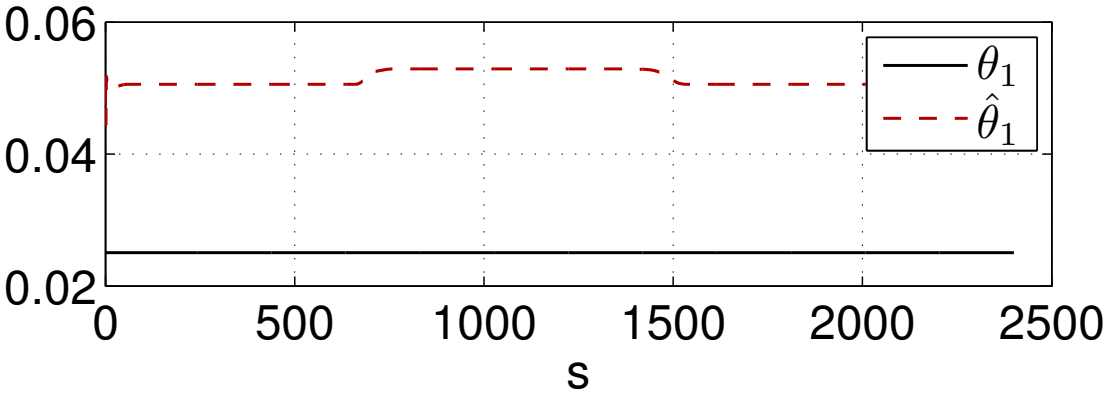

(b) θ_1 and $\widehat{\theta_1}$

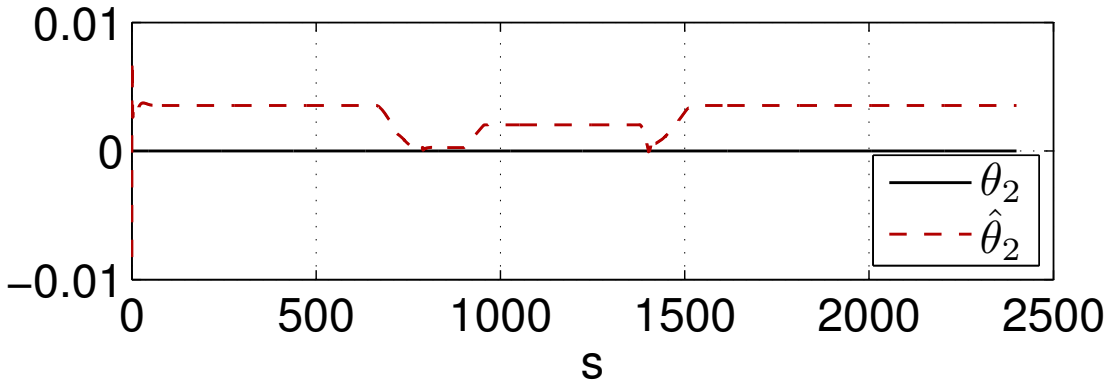

(c) θ_2 and $\widehat{\theta_2}$

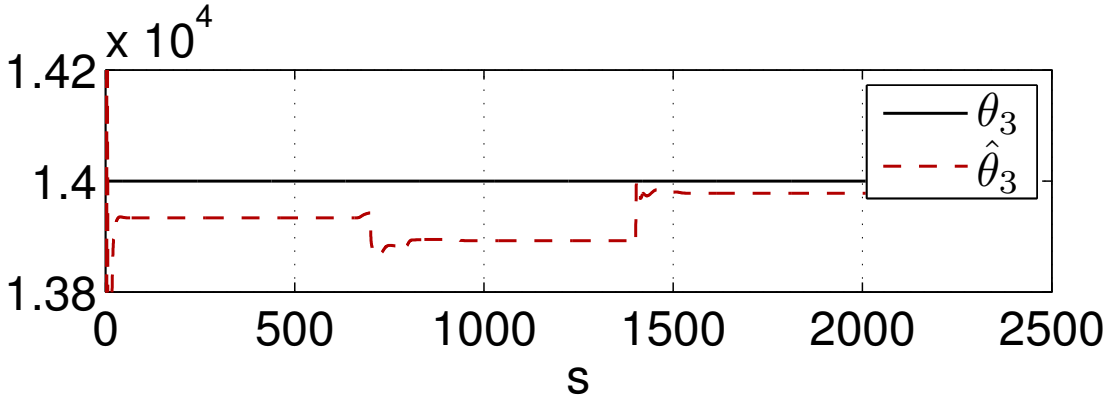

(d) θ_3 and $\widehat{\theta_3}$

Figure 5.8: Simulation results pipe connection 1

Pipe Connection 2

To illustrate that the modified observer presented in Section 4.4.2 outperforms simply ignoring the modeling error a second pipe connection simulation was performed. The same input as in the previous simulation was used only this simulation consists of two pipe connections. Figure 5.9(c) shows the inputs to the system. As commented on in Section 4.4.2 the θ_2 adaption is stopped permanently as $\widehat{q} \approx 0$ and the θ_1 and θ_2 adaptations were turned off at low flows (less than $200\frac{l}{min}$). Figure 5.9(a) shows that $\widehat{p}_{bit}$ tracks p_{bit} well until the end of the first pipe connection. The figure shows that $\widehat{p}_{bit}$ diverges from p_{bit} around $t = 1400s$, the reason for this is that the θ_1 adaptation is turned on again. From Figure 5.10(c) it can be seen that the θ_2 adaptation is stopped at the right time. This again leads to a very good estimate of θ_1 after the pipe connection, see Figure 5.10(b). As both the θ_1 and θ_2 estimates are very good after the first pipe connection $\widehat{p}_{bit}$ tracks p_{bit} very well during the second pipe connection. Furthermore $\widehat{\theta}_3$ does not show the strong transient behavior it showed during the first pipe connection, see Figure 5.10(d). Note that $\widehat{q}_{bit}$ tracks q_{bit} very well throughout the simulation, see Figure 5.9(b). The simulation shows that the performance of the modified observer is much better than the performance of the observer ignoring the modeling error.

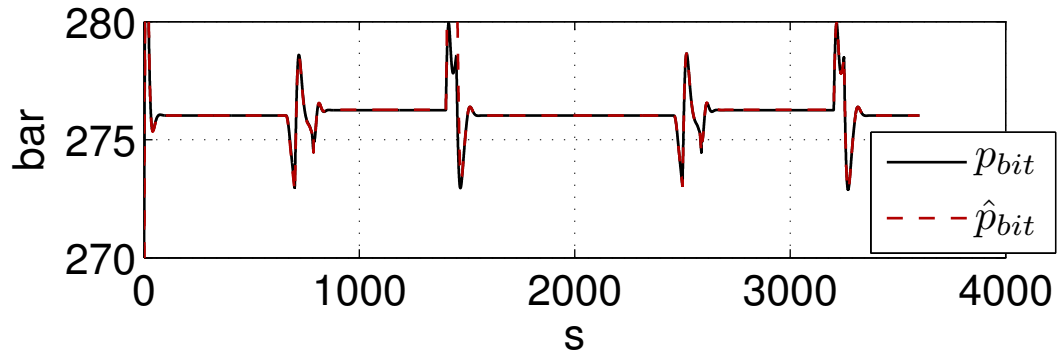

(a) p_{bit} and $\widehat{p}_{bit}$

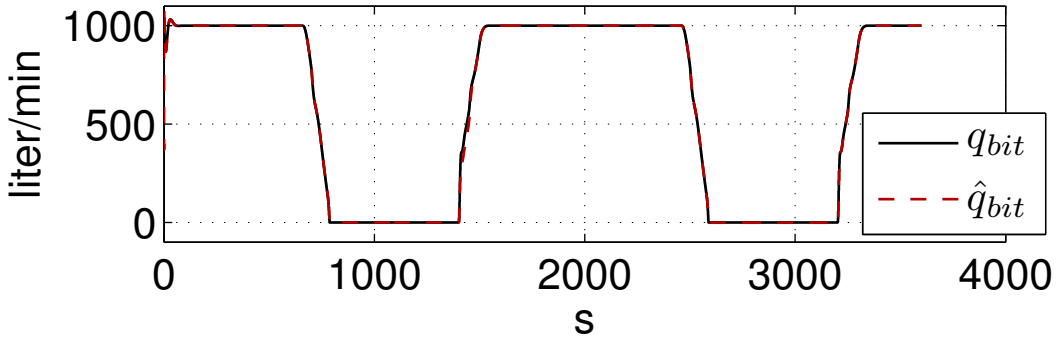

(b) q_{bit} and $\widehat{q}_{bit}$

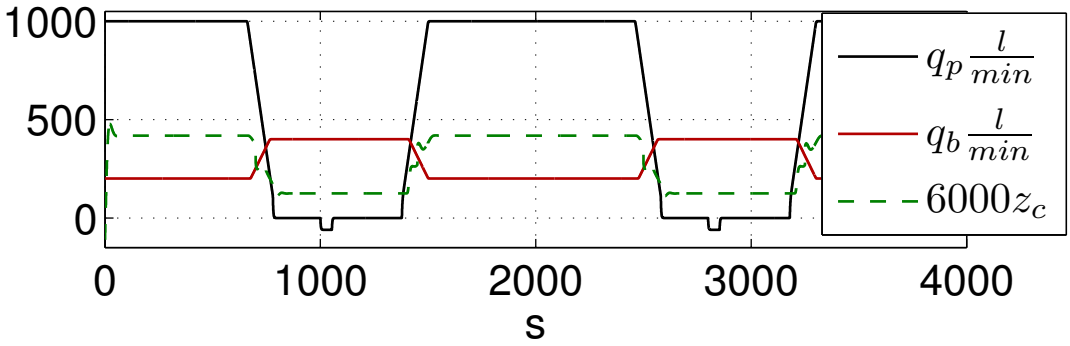

(c) Flows q_p, q_b and choke opening z_c

Figure 5.9: Simulation results pipe connection 2

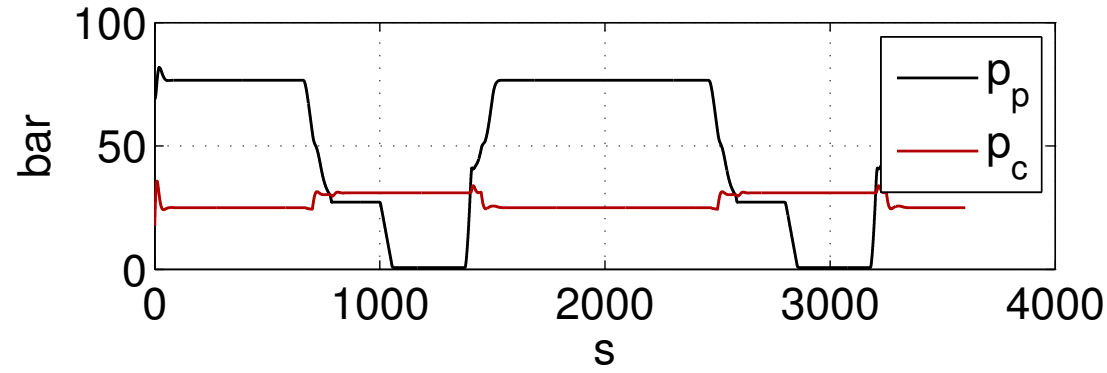

(a) p_p and p_c

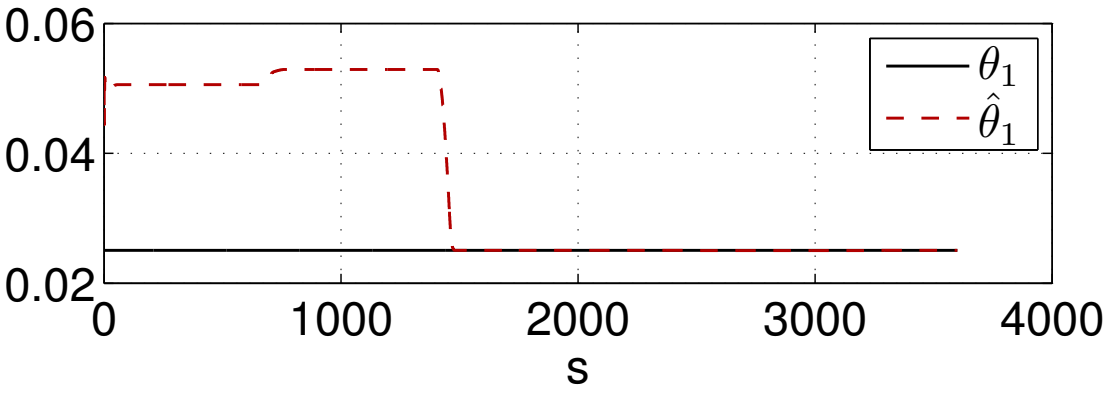

(b) θ_1 and $\widehat{\theta}_1$

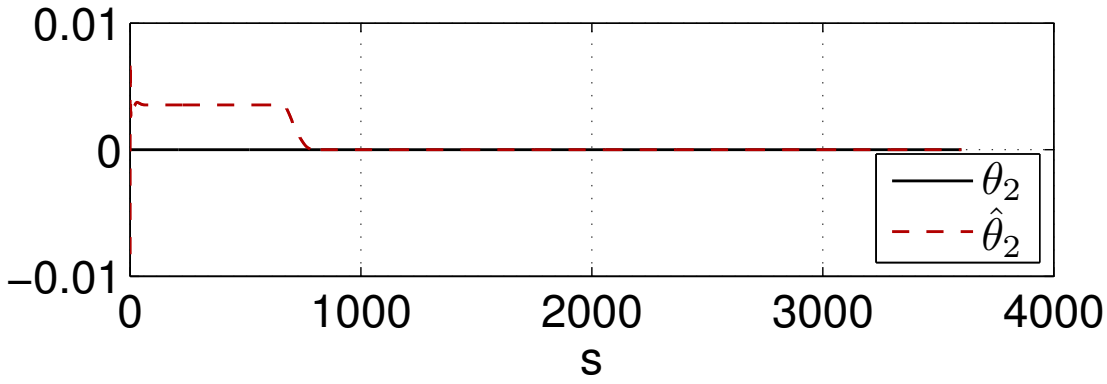

(c) θ_2 and $\widehat{\theta}_2$

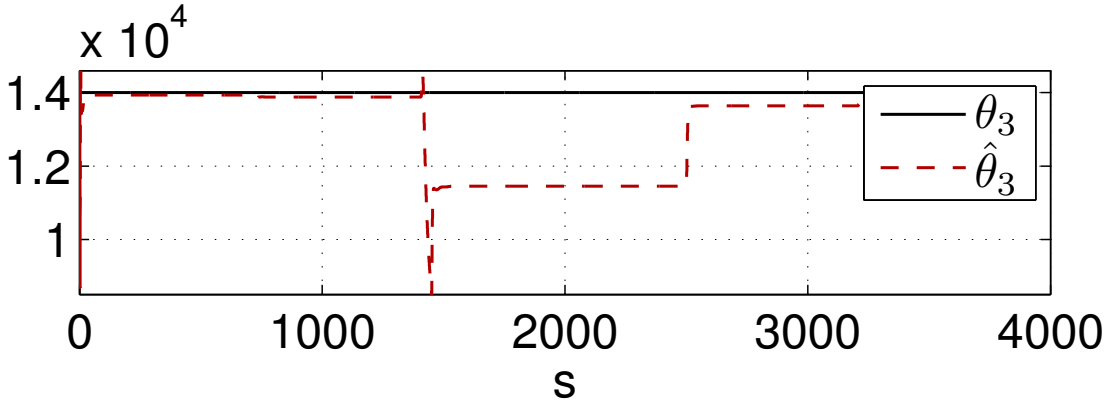

(d) θ_3 and $\widehat{\theta}_3$

Figure 5.10: Simulation results pipe connection 2

5.3 WeMod Simulations, Pipe Connection

To see how robust the observer is w.r.t unmodeled dynamics the observer was tested on a data set from a pipe connection simulation in WeMod, (Nygaard & Gravdal 2007). First the third order model was fitted to the data generated by WeMod. Table 5.6 summarizes the parameters found.

Table 5.6: Parameter values for WeMod simulation

Parameter	Value	Description
V_d	26.7131	Volume drill string (m^3)
β_d	13050	Bulk modulus drill string (bar)
β_a	7317	Bulk modulus annulus (bar)
K_c	0.0045	Choke valve constant
p_0	0	Pressure outside system (barg)
$\bar{\rho}_a$	0.0125	Density annulus ($10^{-5} \times \frac{kg}{m^3}$)
$\bar{\rho}_d$	0.0125	Density drill string ($10^{-5} \times \frac{kg}{m^3}$)
F_d	40.1700	Friction factor drill string
F_a	0.0158	Friction factor annulus
M_a	1.6215	($10^{-8} \times \frac{kg}{m^4}$)
M_d	6.0644	($10^{-8} \times \frac{kg}{m^4}$)
L_{dN}	3600	Total length drill string
V_a^0	99.9088	Volume (m^3) annulus at $t = 0$
h_{bit}^0	2014	Vertical depth (m) of bit at $t = 0$
l_{bit}^0	3600	Length of well at $t = 0$

The pipe connection was simulated by reducing the pump flow to zero and increasing the back pressure pump flow. The choke opening was kept constant at 0.04. To release excessive pressure in the drill string after $q_{bit} = 0$ the pressure was reduced to approximately 2barg by having a negative q_p. Both the approaches presented in Section 4.4 where simulated. First simply using the observer as it was derived ignoring the modeling error and then the observer considering the modeling error in a pragmatic manner.

5.3.1 WeMod Simulation 1

The design variables for the first WeMod simulation is presented in Table 5.7. Three solutions are compared. The results from the WeMod simulation, results from simulating the low order model including the check valve dynamics and the results from the observer. Figure 5.11(a) shows that after initial transients p_{bit} is estimated well by $\widehat{p}_{bit}$ between the pipe connections. During zero flow there is a steady state error which is

caused by neglecting the check valve. When it comes to the parameter estimation, $\widehat{\theta}_1$ and $\widehat{\theta}_2$ show promising behavior in figures 5.12(a) and 5.12(b) as they gradually converge to their true values. $\widehat{\theta}_3$ comes close to its true value during transients but drifts off during zero flow.

Table 5.7: Design variables WeMod simulation 1

Variable	Description
$l_1 = 1$	q_{bit} estimation gain
$l_2 = 1$	p_c estimation gain
$\gamma_1 = 10^{-6}$	Adaptation gain, $\widehat{\theta}_1$
$\gamma_2 = 10^{-8}$	Adaptation gain, $\widehat{\theta}_2$
$\gamma_3 = 10^{7}$	Adaptation gain, $\widehat{\theta}_3$
$\widehat{q}_{bit}(0) = 50\frac{l}{min}$	Initial condition
$\widehat{\theta}_1(0) = 2\theta_1$	Initial condition
$\widehat{\theta}_2(0) = -0.0080$	Initial condition
$\widehat{\theta}_3(0) = 0.9\theta_3$	Initial condition

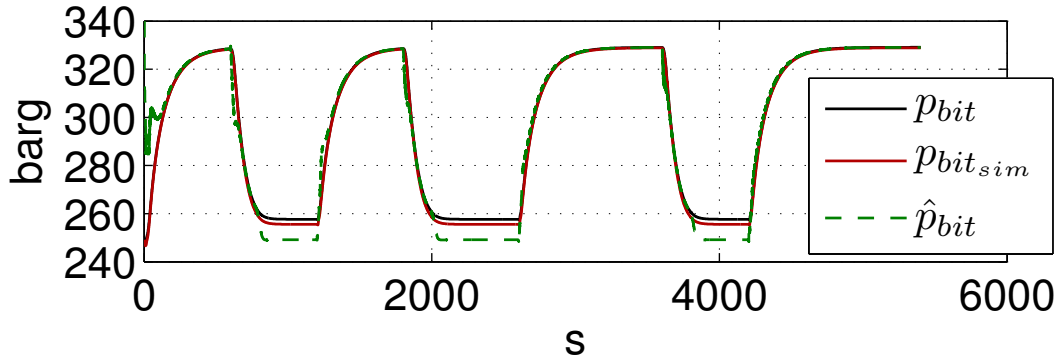

(a) p_{bit} and $\widehat{p}_{bit}$

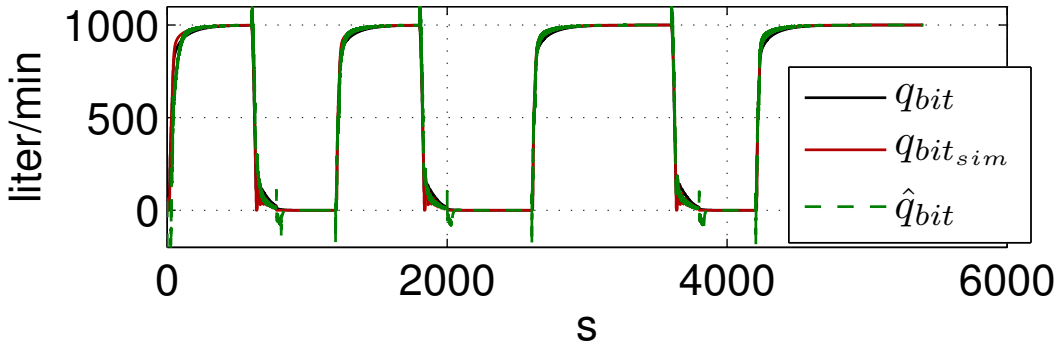

(b) q_{bit} and $\widehat{q}_{bit}$

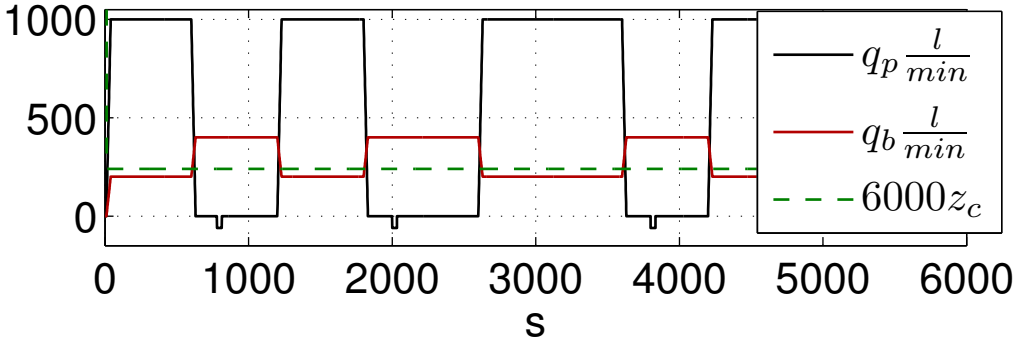

(c) Flows q_p, q_b and choke opening z_c

Figure 5.11: WeMod simulation 1, results

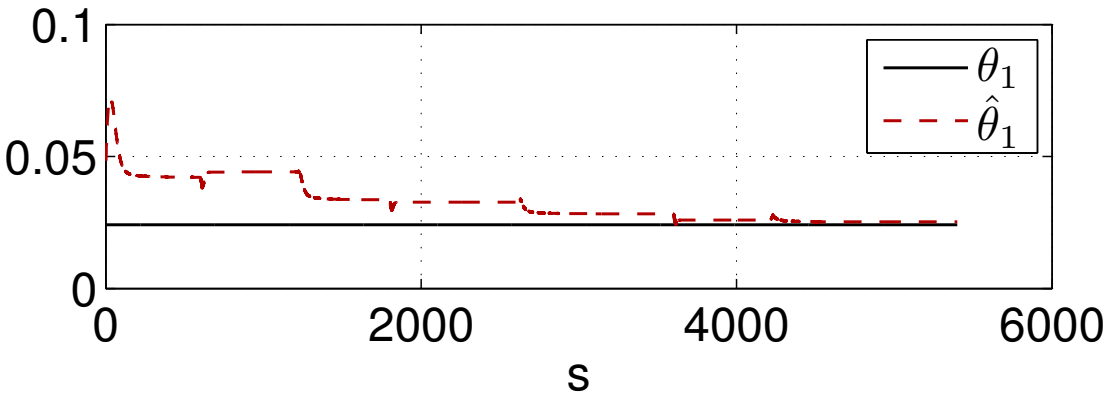

(a) θ_1 and $\widehat{\theta}_1$

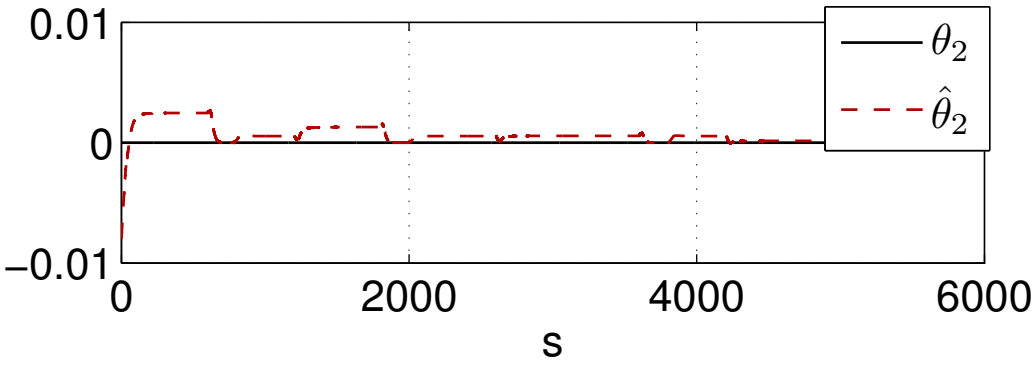

(b) θ_2 and $\widehat{\theta}_2$

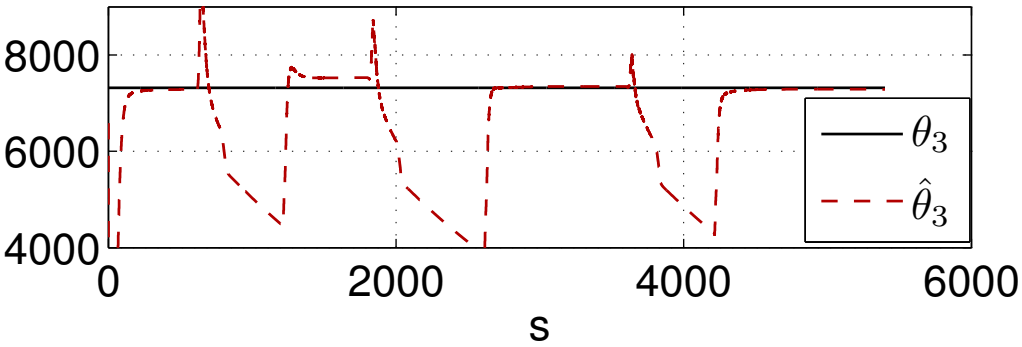

(c) θ_3 and $\widehat{\theta}_3$

Figure 5.12: WeMod simulation 1, results

5.3.2 WeMod Simulation 2

Using the same design parameters as in Table 5.7 the same simulation was performed using the modified observer presented in Section 4.4.2. Figure 5.13(a) shows much better tracking of p_{bit} during zero flow than in the previous case, see Figure 5.11(a). Furthermore $\widehat{\theta}_2$ is stopped at zero flow giving a very good estimate, see Figure 5.14(b). This again leads to much better estimates of θ_1 and θ_3, see figures 5.14(a) and 5.14(c). In Figure 5.14(a) it can be seen that the θ_1 estimate diverges during the pipe connection. Figures 5.15(a) and 5.15(b) show enlarged plots of q_{bit} and p_{bit} during the last pipe connection. The p_{bit} estimate is very accurate except for about $20 - 30$ seconds just as the pipe connection starts. The deviation can be seen in $\widehat{q}_{bit}$ too and should be seen in connection with the deviation in the θ_1 estimate. Closer analysis of this behavior is a topic for future work. Note that one solution to the problem is of course to turn off the θ_1 estimate after the first pipe connection. Figure 5.15(b) also shows interesting behavior in q_{bit} as the flow gets close to zero. It is believed that this behavior does not affect p_{bit} much as the pressure contribution due to friction, $\theta_1|q_{bit}|q_{bit}$, is very small at this stage. Therefore the accuracy provided in $\widehat{p}_{bit}$ should suffice.

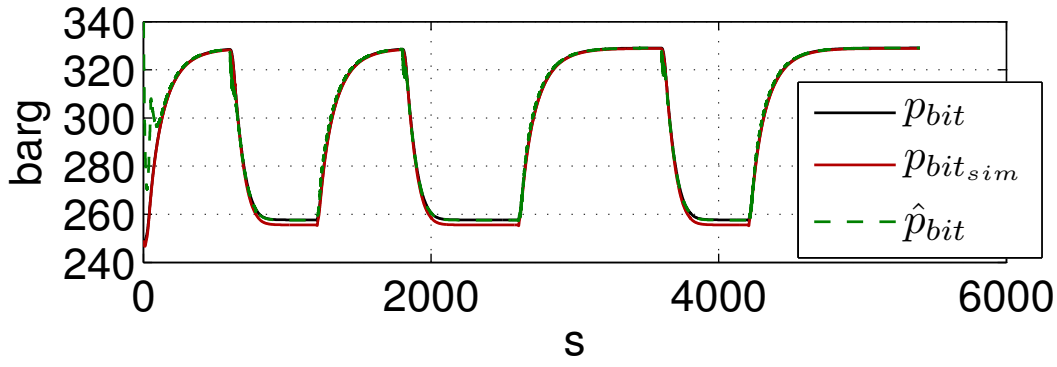

(a) p_{bit} and $\widehat{p}_{bit}$

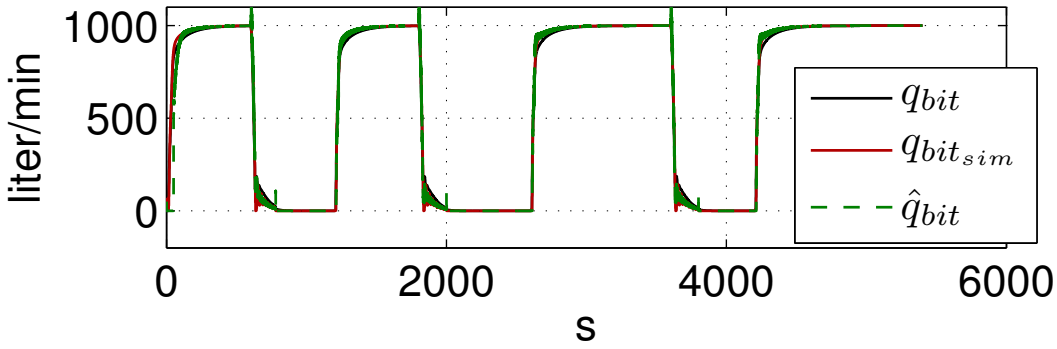

(b) q_{bit} and $\widehat{q}_{bit}$

Figure 5.13: WeMod simulation 2, results

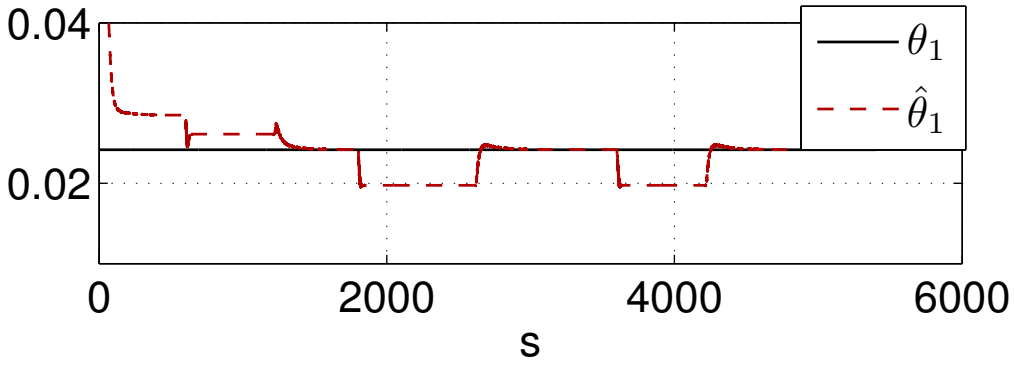

(a) θ_1 and $\widehat{\theta_1}$

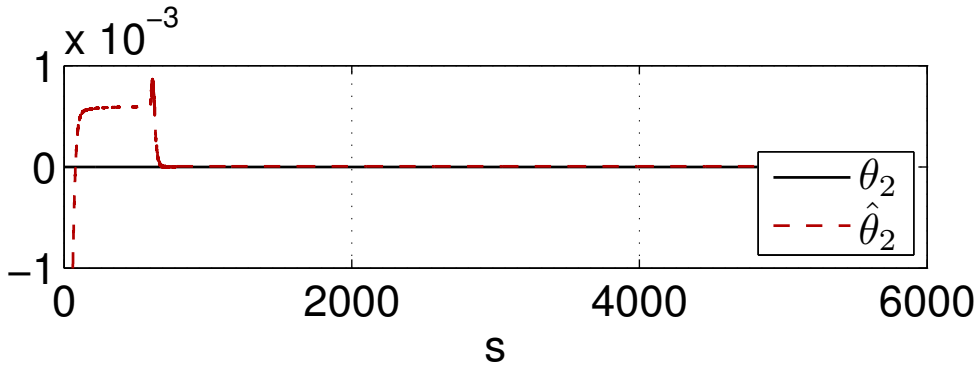

(b) θ_2 and $\widehat{\theta_2}$

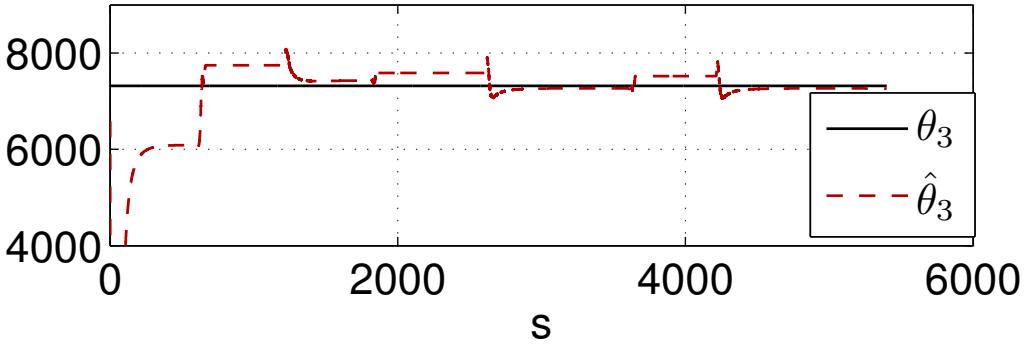

(c) θ_3 and $\widehat{\theta_3}$

Figure 5.14: WeMod simulation 2, results

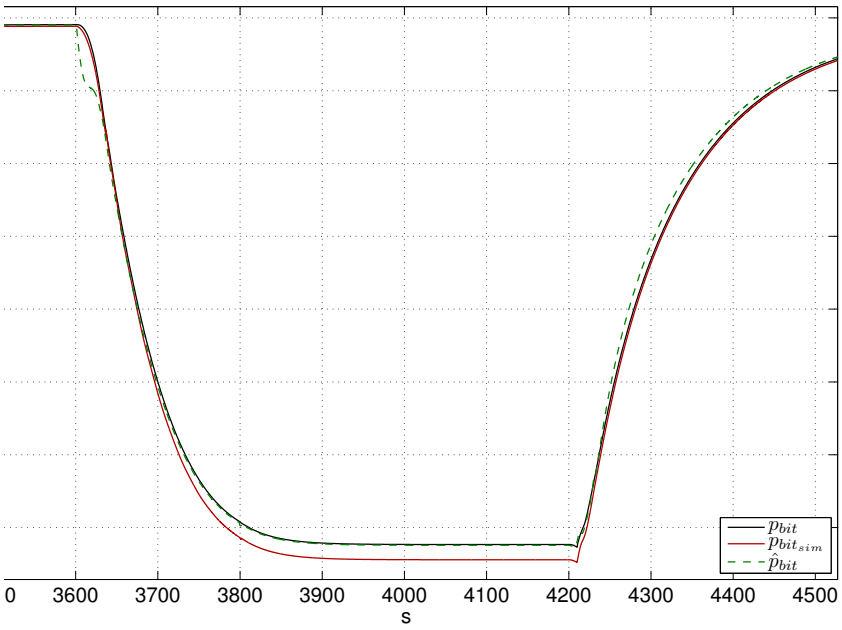

(a) p_{bit} and $\widehat{p}_{bit}$ enlarged, last pipe connection

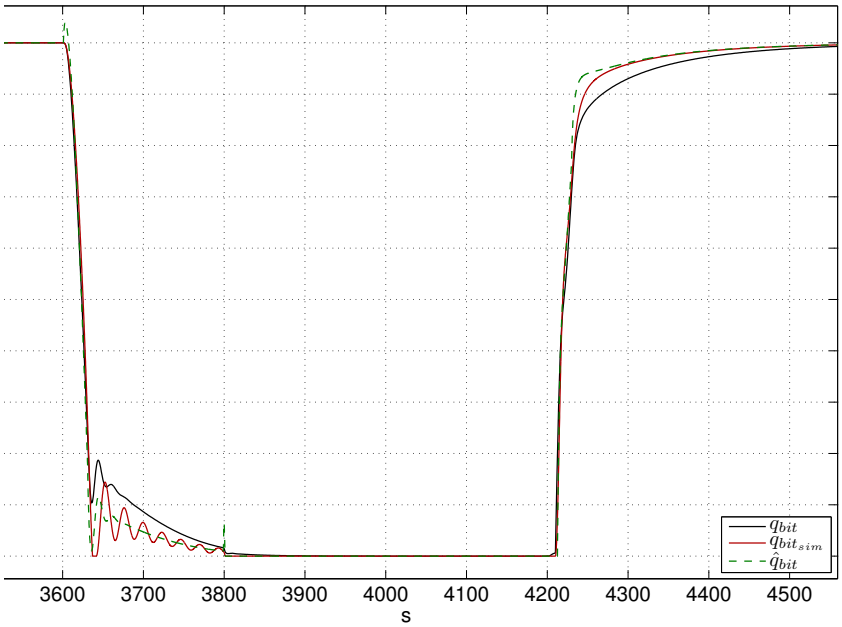

(b) q_{bit} and $\widehat{q}_{bit}$ enlarged, last pipe connection

Figure 5.15: WeMod simulation 2, results, enlarged

5.4 Pipe Connection, Grane Data

To see how well the observer performs in realistic scenarios, the observer was tested on log data from the Grane field provided by StatoilHydro. The data consists of two pipe connections. The input is shown in Figure 5.17(b) and the pressures are shown in Figure 5.17(a).

There where several unknown parameters β_a, K_c, $\bar{\rho}_a$, F_a, F_d and M_a that had to be fitted. No influx was assumed and the effect of cuttings in the drill mud in the annulus was neglected. Therefore the assumption $\beta_a = \beta_d$ and $\bar{\rho}_a = \bar{\rho}_d$ was made. All pressures were measured in barg and the pressure downstream the choke p_0 was assumed to be zero barg. Furthermore the orifice equation (2.13) was modified to:

$$q_{choke} = K_c g_c(z_c)\sqrt{p_c - p_0} \tag{5.3}$$

Where the $\sqrt{\frac{2}{\bar{\rho}_a}}$ has been lumped into K_c and the choke characteristic $g_c(z_c)$ was fitted to data and is shown in Figure 5.16.

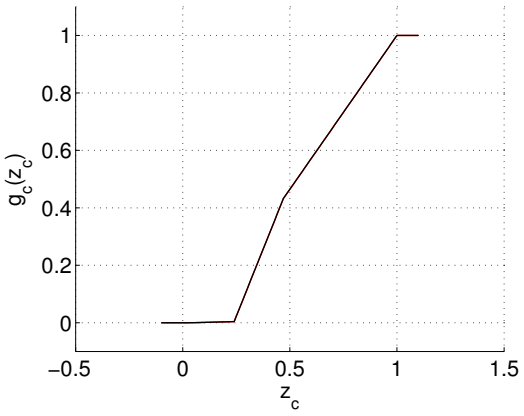

Figure 5.16: Choke characteristic

The remaining unknown parameters where found through the following relation-

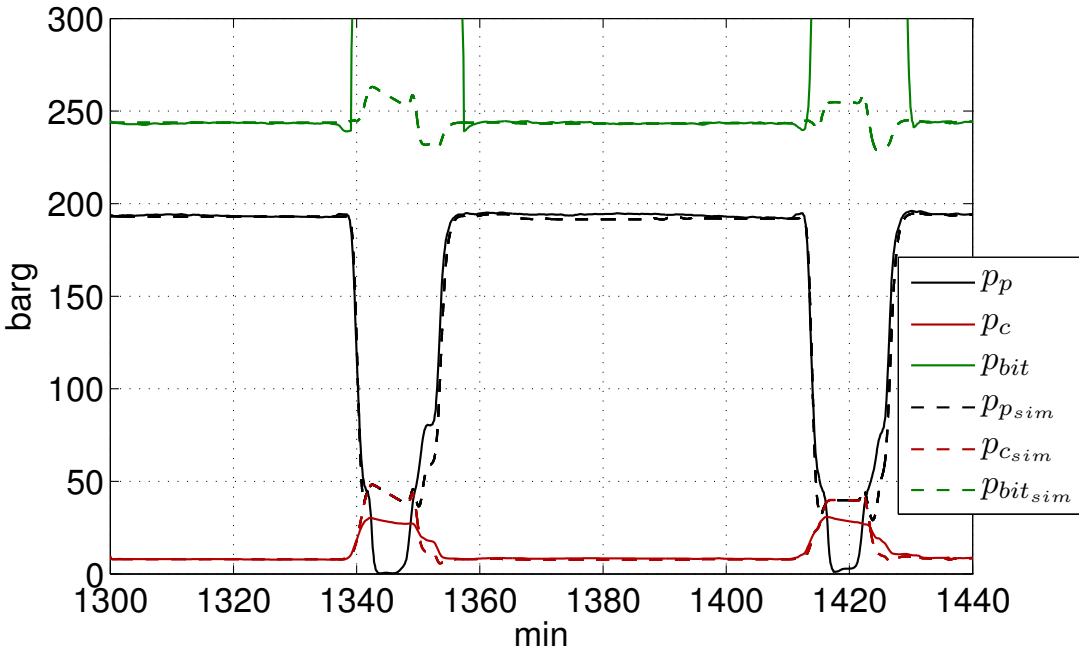

(a) Actual pressure measurements p_p, p_c, p_{bit}, and simulated pressures $p_{p_{sim}}$, $p_{c_{sim}}$, $p_{bit_{sim}}$

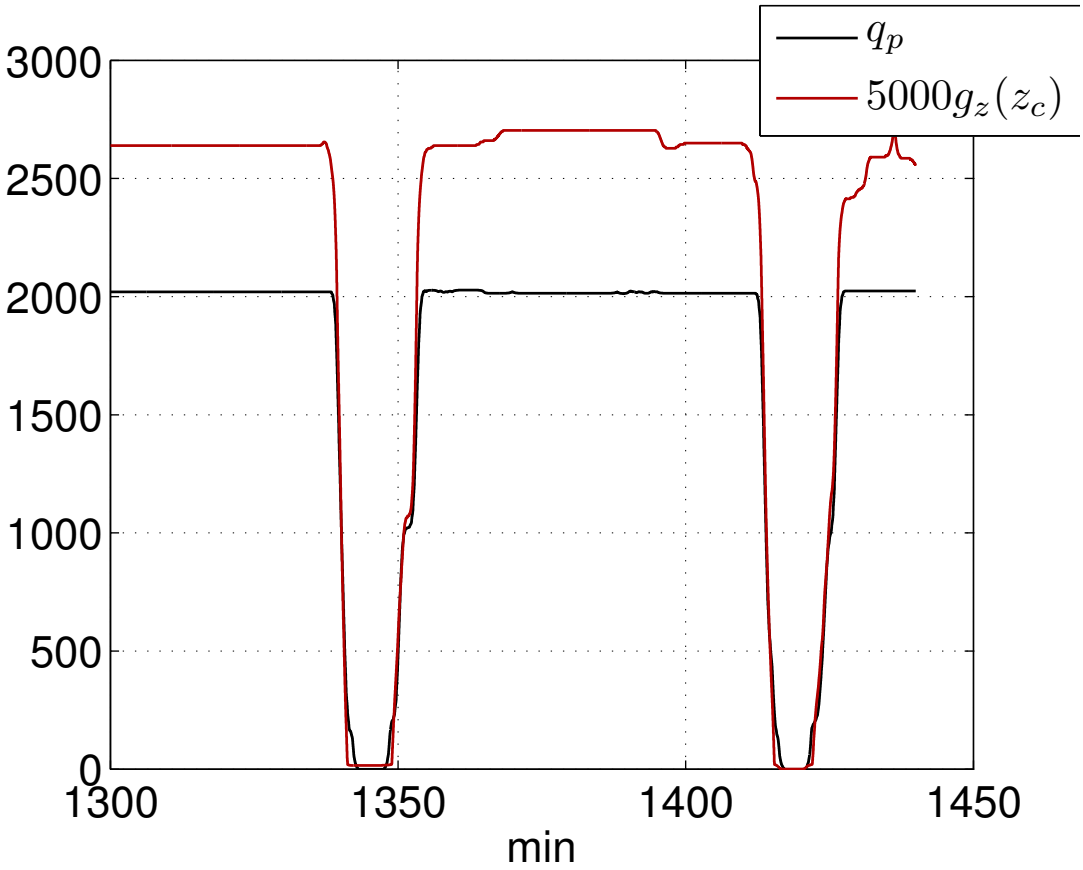

(b) Main pump flow q_p and choke opening $g_c(z_c)$

Figure 5.17: Grane data model fit

ships, using (2.39), (2.40), (2.41) and (5.3):

$$F = \frac{p_{p_{ss}} - p_{c_{ss}} + (\rho_d - \rho_a) g h_{bit}}{q^2_{bit_{ss}}} \tag{5.4}$$

$$F_d = \frac{-p_{bit_{ss}} + p_{p_{ss}} - \rho_d g h_{bit}}{q^2_{bit_{ss}}} \tag{5.5}$$

$$F_a = \frac{p_{bit_{ss}} - p_{c_{ss}} - \rho_a g h_{bit}}{q^2_{bit_{ss}}} \tag{5.6}$$

$$K_c = \frac{q_{bit_{ss}}}{g_c(z_{c_{ss}})\sqrt{p_{c_{ss}}}} \tag{5.7}$$

Where $*_{ss}$ denotes steady state value. Note that there is no back pressure pump on Grane. The model fit is shown in Figure 5.17(a) and the parameters for the well are summarized in Table 5.8. Some issues arose during the model fitting procedure. First there is an important unmodeled event that occurs before disconnecting the main pump. As the pressure p_p can be quite large at $q_{bit} = 0$ the remaining pressure is bled off through a valve releasing excessive fluid back into the drill fluid tank. From Figure 5.17(a) we can see that $p_{p_{sim}}$ does not go to zero as it should. This modeling error should be dealt with as part of the future work and is ignored here. Furthermore a more accurate choke characteristic $g_c(z_c)$ is needed to get a good simulation of p_c. Due to these modeling errors the performance of the observer will be degraded, especially during pipe connections. For all the tests the modified observer presented in Section 4.4.2 was used.

Table 5.8: Parameter values Grane data

Parameter	Value	Description
V_d	51.1825	Volume drill string (m^3)
β_d	14000	Bulk modulus drill string (bar)
β_a	14000	Bulk modulus annulus (bar)
$\bar{\rho}_a$	0.0120	Density annulus ($10^{-5} \times \frac{kg}{m^3}$)
$\bar{\rho}_d$	0.0120	Density drill string ($10^{-5} \times \frac{kg}{m^3}$)
K_c	0.0226	Choke valve constant
p_0	o	Pressure outside system (barg)
F_d	0.1448	Friction factor drill string
F_a	0.0184	Friction factor annulus
M_a	1.7828	($10^{-8} \times \frac{kg}{m^4}$)
M_d	4.9782	($10^{-8} \times \frac{kg}{m^4}$)
L_{dN}	4583	Total length drill string
V_a^0	145.1197	Volume (m^3) annulus at $t = 0$
h_{bit}^0	1825	Vertical depth (m) of bit at $t = 0$
l_{bit}^0	4681	Length of well at $t = 0$

5.4.1 No Adaptation

First the observer was tested on the Grane data without adaption. The design variables for the observer are summarized in Table 5.9. From Figure 5.18(a) we can see that both $\widehat{p}_{bit}$ and $p_{bit_{sim}}$ are close to p_{bit} during steady state. As the p_{bit} measurement is lost during pipe connection it is hard to evaluate how the observer performs. Considering the modeling error mentioned in the previous section it is reasonable to assume that the observer with feedback provides a better estimate during the pipe connection than the simulation/open-loop. The highly oscillatory behavior of $p_{bit_{sim}}$ during the pipe connection strengthens this argument as p_{bit} probably does not change much. Figure 5.18(b) is shown to illustrate that $\widehat{q}_{bit}$ shows a smooth and reasonable behavior.

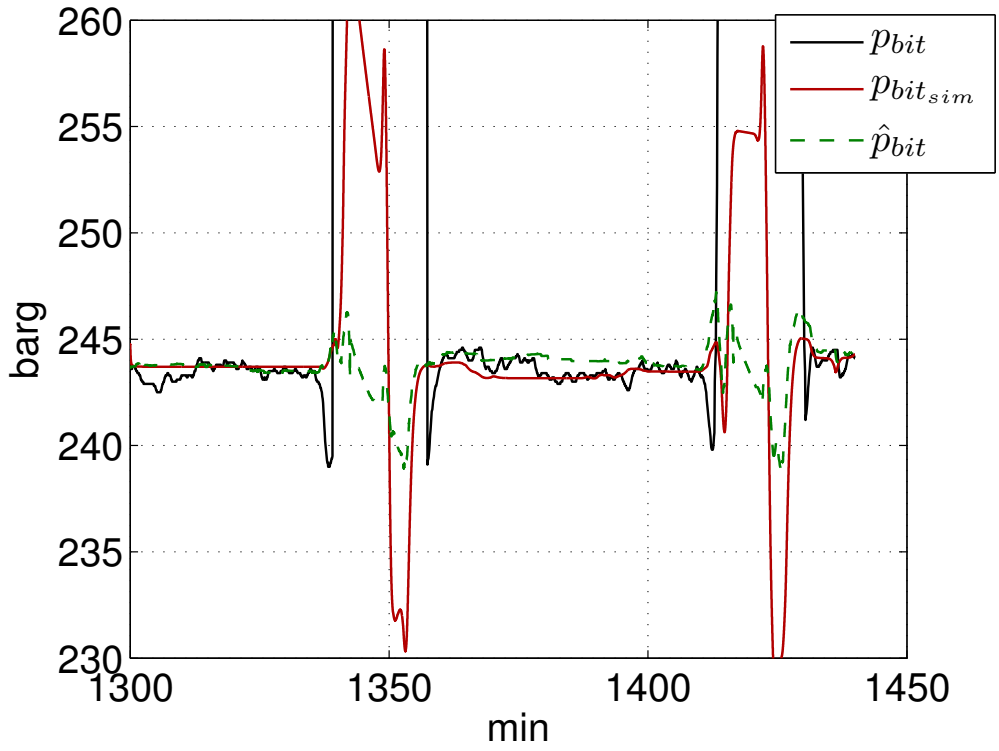

(a) p_{bit}, $p_{bit_{sim}}$ and $\widehat{p}_{bit}$

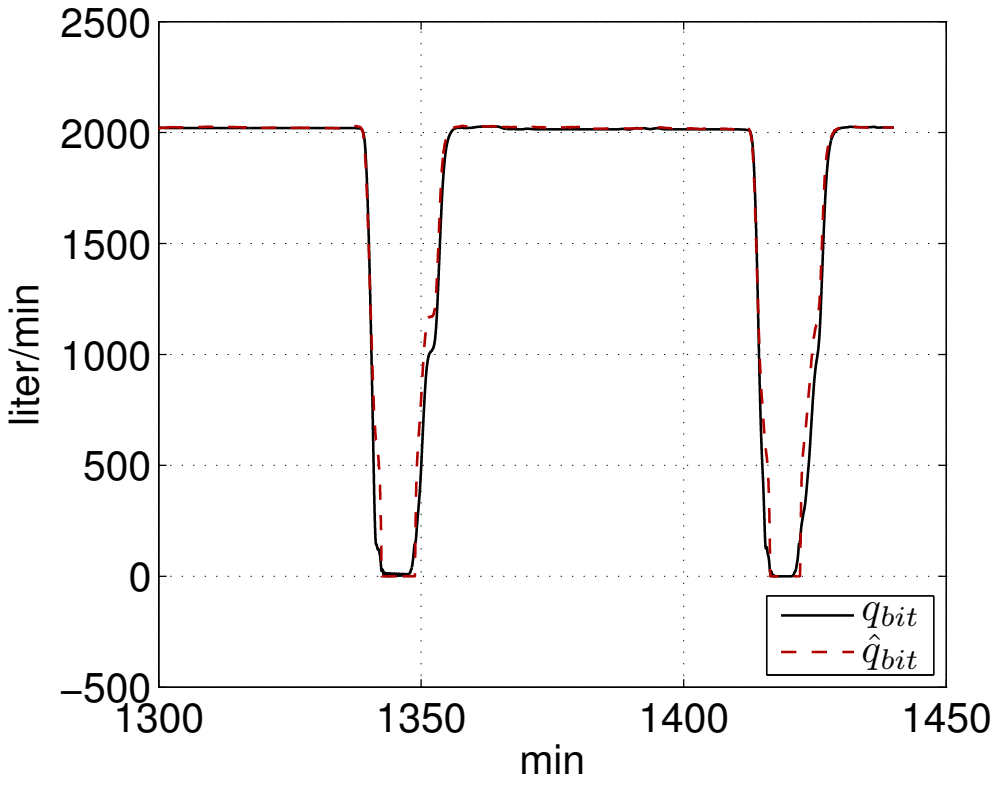

(b) $q_{bit_{sim}}$ and $\widehat{q}_{bit}$

Figure 5.18: Grane data simulation, no adaptation

Table 5.9: Design variables Grane simulation, no adaptation

Variable	Description
$l_1 = 0.1$	q_{bit} estimation gain
$l_2 = 0$	p_c estimation gain
$\gamma_1 = \gamma_2 = \gamma_3 = 0$	Adaptation gains
$\widehat{q}_{bit}(0) = 2020\frac{l}{min}$	Initial condition
$\widehat{\theta}_1(0) = \theta_1$	Initial condition
$\widehat{\theta}_2(0) = 0$	Initial condition
$\widehat{\theta}_3(0) = \theta_3$	Initial condition

5.4.2 Adaptation of θ_1

A second simulation was carried out to evaluate the performance of the observer in the presence of an unknown friction parameter. The initial condition $\widehat{q}_{bit}(0)$ was chosen unwisely. Table 5.10 summarizes the design variables. As the system considered is stable, a copy of the system constitutes an observer. Therefore simply simulating the low order model can actually give good results if all parameters are known. To illustrate that this approach does not work well in the pressence of parameter uncertainties both the low order model and the adaptive observer use an inital $\theta_1(0) = \frac{F_d+1.5F_a}{M}$, which corresponds to a 50% error in the initial estimate for F_a. The adaptive observer estimates θ_1 which gives a much better estimate of p_{bit}, than the estimate $p_{bit_{sim}}$ provided by simply simulating the low order model with a wrong θ_1. From Figure 5.19(a) it can be seen that the open loop simulation $p_{bit_{sim}}$ gives a steady state deviation due to the error in the friction estimate. Figure 5.19(c) shows that $\widehat{\theta}_1$ comes very close to θ_1 during steady state which gives a much better estimate of p_{bit} than $p_{bit_{sim}}$. Note that the θ_1 adaptation is turned off for $\widehat{q}_{bit} < 1800\frac{l}{min}$ to prevent drifting. From Figure 5.19(c) it can be seen that the θ_1 estimate drifts when the pipe connection procedure starts, this is similar to what was seen in the WeMod simulations, see Figure 5.14(a). The reason for the drift might be unmodeled dynamics and should be analyzed further as part of future work on this subject.

Table 5.10: Design variables Grane simulation, adaptation

Variable	Description
$l_1 = 0.1$	q_{bit} estimation gain
$l_2 = 0$	p_c estimation gain
$\gamma_1 = 10^{-7}$	Adaptation gain, $\widehat{\theta}_1$
$\gamma_2 = \gamma_3 = 0$	Adaptation gains
$\widehat{q}_{bit}(0) = 1000\frac{l}{min}$	Initial condition
$\widehat{\theta}_1(0) = \frac{F_d + 1.5F_a}{M}$	Initial condition
$\widehat{\theta}_2(0) = 0$	Initial condition
$\widehat{\theta}_3(0) = \theta_3$	Initial condition

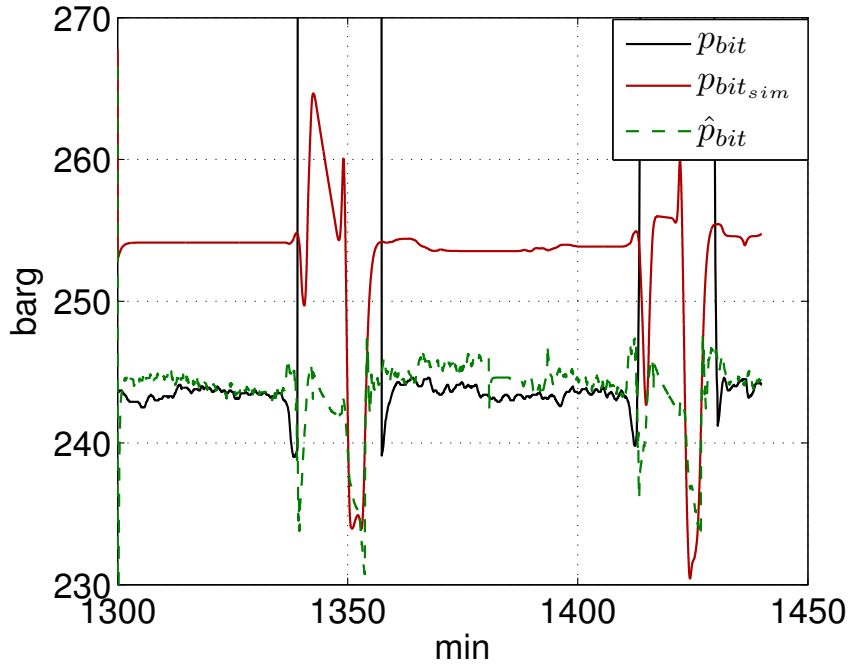

(a) p_{bit}, $p_{bit_{sim}}$ and $\widehat{p}_{bit}$

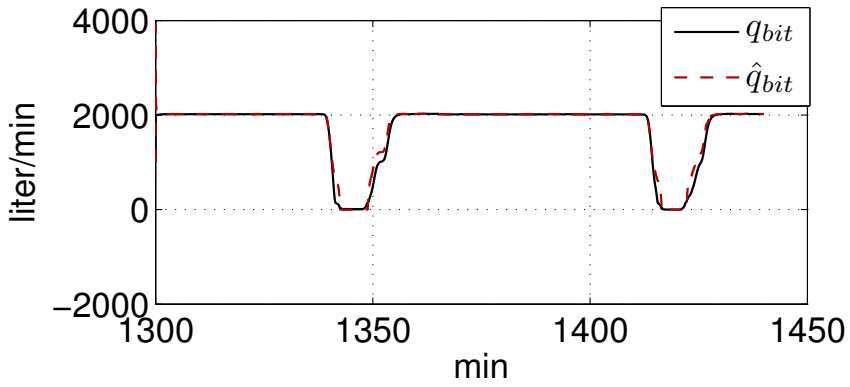

(b) $q_{bit_{sim}}$ and $\widehat{q}_{bit}$

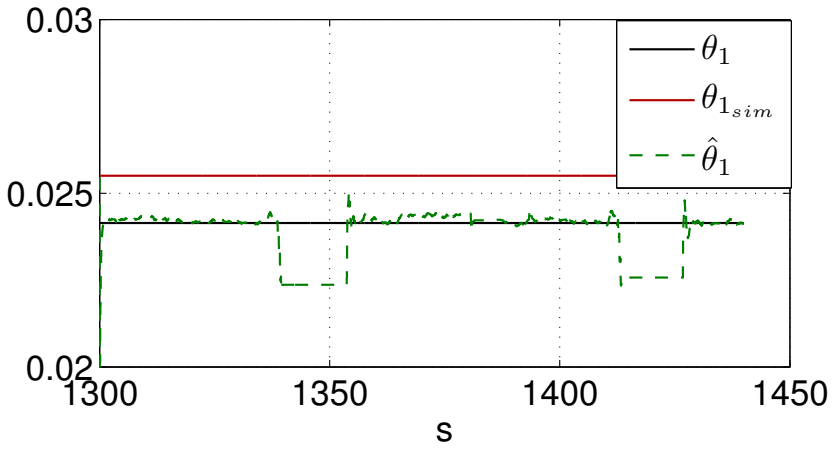

(c) θ_1,$\theta_{1_{sim}}$ and $\widehat{\theta}_1$

Figure 5.19: Grane data simulation, adaptation of friction parameter

Chapter 6

Conclusion, Contributions and Future work

6.1 Conclusion

1. An adaptive observer that fulfills the main goals stated in Section 1.4 has been developed in Chapter 4. The observer adapts to key unknown parameters and estimates the bottomhole pressure.

2. The observer design is based on rigid mathematical analysis and provides conditions for stability and convergence of the estimated bottomhole pressure and unknown parameters.

3. Simulation studies in Chapter 5 verifies the proved properties of the observer and show that the observer handles common scenarios during drilling such as, changes in choke valve opening, mud pump flow and drill string movements, very well.

4. Due to model complexity rigid proofs were not derived for zero flow conditions. As a starting point for future work a pragmatic solution during zero flow was proposed in Section 4.4. The proposed method shows promising behavior during during simulations.

6.2 Contributions

The main contributions to the drilling industry presented in this thesis is the adaptive observer developed in Chapter 4.

- The observer estimates the bottomhole pressure during drilling and adapts to unknown friction, density and bulk modulus.

- The extensions compared to existing results is that the design is based on a low order model and founded in rigid mathematical analysis which provide conditions for stability and convergence. As the design is based on a low order model it is simpler to implement and use compared to estimator designs based on distributed parameter models.
- Furthermore the results hold over a wide range of drilling operations. This has been demonstrated through simulation of common drilling scenarios.
- The results facilitate for future control design.

6.3 Future Work

Suggested future work is:

- Derive conditions for stability and convergence for the observer at zero flow based on the proposed approach in Section 4.4.
- Incorporate manually operated valves into the existing model.
- Remove the assumption of zero reservoir influx stated in Section 1.4.
- Analyze behavior of existing observer scheme with gas in the annulus. If needed extend the observer to two-phase flow, i.e. remove the fluid phase only assumption in Section 1.4.
- Include the p_{bit} measurement to achieve better performance.
- Try to get more log data of the bottomhole pressure measurement during typical drilling scenarios to test the observer.

Bibliography

Altermann, J., Bingham, B., Grayson, R., Linenberger, R., Mueller, F., Odelius, L. & Taylor, R. (2007), *Well Control Equipment and Procedures*, International Association of Drilling Contractors.

Brill, J. P. & Mukherjee, H. (1999), *Multiphase Flow in Wells*, Society of Petroleum Engineers Inc.

Egeland, O. & Gravdahl, J. T. (2002), *Modeling and Simulation for Automatic Control*, Marine Cybernetics AS.

Fischer, P. A. (2003), 'Real real-time drill pipe telemetry: A step-change in drilling', *World Oil* .

Fossil, B. & Sangesland, S. (2004), Managed pressure drilling for subsea applications; well control challenges in deep waters, *in* 'SPE/IADC Underbalanced Technology Conference and Exhibition, number SPE 91633'.

Gravdal, J. E., Lorentzen, R., Fjelde, K. & Vefring, E. (2005), Tuning of computer model parameters in managed-pressure drilling applications using an unscented kalman filter technique, *in* 'SPE Annual Technical Conference and Exhibition, number SPE 97028'.

Hannegan, D. (2006), Case studies - offshore managed pressure drilling, *in* 'SPE Annual Technical Conference and Exhibition, number SPE 101855, San Antonio, Texas'.

Hannegan, D., Todd, R. J., Pritchard, D. M. & Jonasson, B. (2004), Mpd - uniquely applicable to methane hydrate drilling, *in* 'SPE/IADC Underbalanced Techonlogy Conference and Exhibition, number SPE 91560'.

Hydro (2007), Technology outlook 2007 - efficient well construction, Technical report, Hydro.

Imsland, L. (2007), Mpd estimation, Technical report, Sintef.

Ioannou, P. A. & Sun, J. (1996), *Robust Adaptive Control*, Prentice Hall, Inc (out of print in 2003),.

Kaasa, G. O. (2007), A simple dynamic model of drilling for control, Technical report, StatoilHydro Resarch Centre Porsgrunn.

Key World Energy Statistics (2007), http://www.iea.org/Textbase/publications/free_new_Desc.asp?PUBS_ID=1199. Accessed 2007.17.12.

Khalil, H. K. (2002), *Nonlinear Systems*, Prentice-Hall.

Krstić, M., Kanellakopoulos, I. & Kokotović, P. (1995), *Nonlinear and Adaptive Control Design*, John Wiley & Sons, Inc.

Lage, A. C. V. M. (2000), Two-Phase Flow Models and Experiments for Low-Head and Underbalanced Drilling, PhD thesis, Stavanger University College.

Lefeber, A. A. J. (2000), Tracking Control of Nonlinear Mechanical Systems, PhD thesis, Universiteit Twente.

Manring, N. D. (2005), *Hydraulic Control Systems*, John Wiley & Sons, Inc.

Merrit, H. E. (1967), *Hydraulic Control Systems*, John Wiley & Sons, Inc.

Micaelli, A. & Samson, C. (1993), Trajectory tracking for unicycle-type and two-steering-wheels mobile robots, Technical report, Institut National de Recerche en Informatique et en Automatique.

Narendra, K. S. & Annaswamy, A. M. (1989), *Stable Adaptive Systems*, Prentice-Hall International Editions.

Nygaard, G. & Gravdal, J. E. (2007), WeModForMatlab user's guide, Technical Report Publ. nr. 2007/234, International Research Institute of Stavanger, Bergen, Norway.

Nygaard, G. H. (2007), Describing drilling case 1, Technical report, International Research Institute of Stavanger.

Nygaard, G. H., Johannessen, E., Gravdal, J. E. & Iversen, F. (2007), Automatic coordinated control of pump rates and choke valve for compensating pressure fluctuations during surge and swab operations, *in* 'IADC/SPE Managed Pressure Drilling and Underbalanced Operations Conference and Exhibition, number SPE 108344'.

Nygaard, G. H., Vefring, E. H., Fjelde, K.-K., Nævdal, G., Lorentzen, R. J. & Mylvaganam, S. (2004), Bottomhole pressure control during drilling operations in gas-dominant wells, *in* 'SPE/IADC Underbalanced Technology Conference and Exhibition, number SPE 91578'.

Nygaard, G., Imsland, L. & Johannessen, E. A. (2007), Using nmpc based on a low-order model for control pressure druing oil well drilling, *in* '8th International Symposium on Dynamics and Control of Process Systems,June 6-8'.

Nygaard, G. & Nævdal, G. (2006), 'Nonlinear model predictive control scheme for stabilizing annulus pressure during oil well drilling', *Journal of Prcess Control* **16**, 719–732.

Nygaard, O. G. H. (2006), Multivariable process control in high temperature and high pressure environment using non-intrusive multi sensor data fusion, PhD thesis, NTNU.

Skelton, R. E., Iwasaki, T. & Grigoriadis, K. M. (1998), *A Unified Algebraic Approach to Linear Control Design*, Taylor & Francis Ltd.

SPT Group (2007), http://www.sptgroup.com/olga/index.html. Accessed 2007.17.12.

Tan, Y., Kanellakopoulos, I. & Jiang, Z.-P. (1998), Nonlinear observer/controller design for a class of nonlinear systems, *in* 'Proceedings of the 37th IEEE Conference on Decision & Control'.

White, F. M. (1999), *Fluid Mechanics*, McGraw-Hill.

Appendix A

Appendix

A.1 Derivation of p_{bit}

Derivation of p_{bit} in equation (2.42) is based on (2.39) and (2.41):

$$\begin{aligned} M\dot{q}_{bit} &= p_p - p_c - F_d|q_{bit}|q_{bit} - F_a|q_{bit}+q_{res}|(q_{bit}+q_{res}) + (\bar{\rho}_d - \bar{\rho}_a)gh_{bit} \\ p_{bit} &= p_c + M_a\dot{q}_{bit} + F_a|q_{bit}+q_{res}|(q_{bit}+q_{res}) + \bar{\rho}_a g h_{bit} \end{aligned} \tag{A.1}$$

Inserting the top equation into the bottom gives:

$$\begin{aligned} M\dot{q}_{bit} &= p_p - p_c - F_d|q_{bit}|q_{bit} - F_a|q_{bit}+q_{res}|(q_{bit}+q_{res}) + (\bar{\rho}_d - \bar{\rho}_a)gh_{bit} \\ p_{bit} &= p_c + \frac{M_a}{M}(p_p - p_c - F_d|q_{bit}|q_{bit} - F_a|q_{bit}+q_{res}|(q_{bit}+q_{res}) + (\bar{\rho}_d - \bar{\rho}_a)gh_{bit}) \\ &\quad + F_a|q_{bit}+q_{res}|(q_{bit}+q_{res}) + \bar{\rho}_a g h_{bit} \\ &= \frac{M_a}{M}p_p + (1-\frac{M_a}{M})p_c + (1-\frac{M_a}{M})F_a|q_{bit}+q_{res}|(q_{bit}+q_{res}) \\ &\quad - \frac{M_a}{M}F_d|q_{bit}+q_{res}|(q_{bit}+q_{res}) + (1-\frac{M_a}{M})\bar{\rho}_a g h_{bit} + \frac{M_a}{M}\bar{\rho}_d g h_{bit} \\ &= \frac{M_a}{M}p_p + \frac{M_d}{M}p_c + (\frac{M_d}{M}F_a - \frac{M_a}{M}F_d)|q_{bit}+q_{res}|(q_{bit}+q_{res}) \\ &\quad + (\frac{M_d}{M}\bar{\rho}_a + \frac{M_a}{M}\bar{\rho}_d)g h_{bit} \end{aligned} \tag{A.2}$$

A.2 Numerical Conditioning

The states in (2.37)- (2.39) have units of pressures and volume flow. The SI unit for pressure is pascals (Pa) and for volume flow it is $\frac{m^3}{s}$, (White 1999). Standard operating

conditions will for the pressures be in the order of $0-400\text{bar} = (0-40)\times 10^6$ Pa and for the volume flow in the order of $0-6000\frac{l}{min} = 0-0.1\frac{\text{m}^3}{\text{s}}$. This will lead to a large spread in parameter values and signal sizes, which will make the model numerically ill-conditioned. Therefore the states should be normalized. An intuitive choice of units for flow and pressure is $\frac{l}{\text{s}}$ and bar. This conversion and the resulting signals and parameters will now be found. The signals and parameters after the conversion will be denoted with a bar.

$$\bar{q}_* = 1000 q_* \quad \bar{p}_* = \frac{p_*}{10^5}$$

First (2.37) can be used to find $\dot{\bar{p}}_p$:

$$\frac{10^5 V_d}{\beta_d}\dot{\bar{p}}_p = \frac{\bar{q}_{pump}}{1000} - \frac{\bar{q}_{bit}}{1000} \tag{A.3}$$

Using the unit bar for β_d gives:

$$\frac{V_d}{\bar{\beta}_d}\dot{\bar{p}}_p = \frac{\bar{q}_{pump}}{1000} - \frac{\bar{q}_{bit}}{1000} \tag{A.4}$$

Similar for (2.38), using assumption 6:

$$\begin{aligned}\frac{10^5 V_a}{\beta_a}\dot{\bar{p}}_c &= \frac{\bar{q}_{bit} + \bar{q}_{back} - \bar{q}_{choke}}{1000} - \dot{V}_a \\ \frac{V_a}{\bar{\beta}_a}\dot{\bar{p}}_c &= \frac{\bar{q}_{bit} + \bar{q}_{back} - \bar{q}_{choke}}{1000} - \dot{V}_a\end{aligned} \tag{A.5}$$

And for (2.39):

$$\frac{M}{1000}\dot{\bar{q}}_{bit} = 10^5(\bar{p}_p - \bar{p}_c) - (F_d + F_a)\frac{\bar{q}_{bit}|\bar{q}_{bit}|}{10^6} + (\bar{\rho}_d - \bar{\rho}_a)g h_{bit}$$

Denoting $\bar{\bar{\rho}}_a = \frac{\bar{\rho}_a}{10^5}$, gives:

$$\frac{M_d + M_a}{10^8}\dot{\bar{q}}_{bit} = \bar{p}_p - \bar{p}_c - (F_d + F_a)\frac{\bar{q}_{bit}|\bar{q}_{bit}|}{10^{11}} + (\bar{\bar{\rho}}_d - \bar{\bar{\rho}}_a)g h_{bit}$$

Denoting $\bar{M} = \frac{M}{10^8}$ and $\bar{F} = \bar{F}_d + \bar{F}_a = \frac{F_d + F_a}{10^{11}}$ gives:

$$\bar{M}\dot{\bar{q}}_{bit} = \bar{p}_p - \bar{p}_c - \bar{F}\bar{q}_{bit}|\bar{q}_{bit}| + (\bar{\bar{\rho}}_d - \bar{\bar{\rho}}_a)g h_{bit} \tag{A.6}$$

For the measurement equation (2.41) a similar approach gives:

$$\begin{aligned}10^5\bar{p}_{bit} &= 10^5\bar{p}_c + M_a\frac{\dot{\bar{q}}_{bit}}{1000} + F_a\frac{\bar{q}_{bit}|\bar{q}_{bit}|}{10^6} + \bar{\rho}_a g h_{bit} \\ \bar{p}_{bit} &= \bar{p}_c + M_a\frac{\dot{\bar{q}}_{bit}}{10^8} + F_a\frac{\bar{q}_{bit}|\bar{q}_{bit}|}{10^{11}} + \frac{\bar{\rho}_a}{10^5}g h_{bit} \\ &= \bar{p}_c + \bar{M}_a\dot{\bar{q}}_{bit} + \bar{F}_a\bar{q}_{bit}|\bar{q}_{bit}| + \bar{\bar{\rho}}_a g h_{bit}\end{aligned} \tag{A.7}$$

To summarize, the converted equations are:

$$\frac{V_d}{\bar{\beta}_d}\dot{\bar{p}}_p = \frac{\bar{q}_{pump}}{1000} - \frac{\bar{q}_{bit}}{1000} \tag{A.8}$$

$$\frac{V_a}{\bar{\beta}_a}\dot{\bar{p}}_c = \frac{\bar{q}_{bit} + \bar{q}_{back} - \bar{q}_{choke}}{1000} - \dot{V}_a \tag{A.9}$$

$$\bar{M}\dot{\bar{q}}_{bit} = \bar{p}_p - \bar{p}_c - \bar{F}\bar{q}_{bit}|\bar{q}_{bit}| + (\bar{\bar{\rho}}_d - \bar{\bar{\rho}}_a)gh_{bit} \tag{A.10}$$

$$\bar{p}_{bit} = \bar{p}_c + \bar{M}_a\dot{\bar{q}}_{bit} + \bar{F}_a\bar{q}_{bit}|\bar{q}_{bit}| + \bar{\bar{\rho}}_a g h_{bit} \tag{A.11}$$

Where the Table A.1 summarizes the conversions

Table A.1: Converted units

Old Signal/parameter	Old Unit	Conversion Factor	New Signal/parameter	New Unit
p_p,p_c, p_{bit}	Pa	$\frac{1}{10^5}$	$\bar{p}_p$,$\bar{p}_c$, $\bar{p}_{bit}$	Bar
q_{bit}	$\frac{\mathrm{m}^3}{\mathrm{s}}$	10^3	$\bar{q}_{bit}$	$\frac{\mathrm{liter}}{\mathrm{s}}$
β_d, β_a	Pa	$\frac{1}{10^5}$	$\bar{\beta}_d$, $\bar{\beta}_a$	Bar
M_d, M_a	$\frac{\mathrm{kg}}{\mathrm{m}^4}$	$\frac{1}{10^8}$	$\bar{M}_d$, $\bar{M}_a$	$\frac{\mathrm{kg}}{10^8\mathrm{m}^4}$
F_d, F_a	-	$\frac{1}{10^{11}}$	$\bar{F}_d$, $\bar{F}_a$	-
$\bar{\rho}_d$, $\bar{\rho}_a$	$\frac{\mathrm{kg}}{\mathrm{m}^3}$	$\frac{1}{10^5}$	$\bar{\bar{\rho}}_d$, $\bar{\bar{\rho}}_a$	$\frac{\mathrm{kg}}{10^5\mathrm{m}^3}$

A.3 Lipschitz Properties and Equilibrium Points

In this section equilibrium points and Lipschitz properties for the error system described by (4.15) and (4.17) are analyzed. First the following assumptions are made.

Assumption 11. $q_{bit}(t)$ is continuous and $0 \leq q_{bit}(t) \leq c < \infty$

Assumption 12. $v_3(t)$ is continuous and $0 \leq v_3(t) \leq c < \infty$

$$\dot{\tilde{\xi}}_1 = -l_1 a_1 \tilde{\xi}_1 - \theta_1(|q_{bit}|q_{bit} - |\widehat{q}_{bit}|\widehat{q}_{bit}) + \tilde{\theta}^T\phi \tag{A.12}$$

$$\dot{\tilde{\theta}} = -\Gamma\phi\tilde{\xi}_1 \tag{A.13}$$

$\tilde{\theta} = \begin{bmatrix} \tilde{\theta}_1 \\ \tilde{\theta}_2 \end{bmatrix}$ and the regressor as $\phi(\widehat{q}_{bit}, v_3) = \begin{bmatrix} -|\widehat{q}_{bit}|\widehat{q}_{bit} \\ v_3 \end{bmatrix}$.

Rewriting (A.12)-(A.13) by using the relationship $\widehat{q}_{bit} = q_{bit} - \tilde{q}_{bit} = q_{bit} - \tilde{\xi}_1$

$$\dot{\tilde{\xi}}_1 = -l_1 a_1 \tilde{\xi}_1 - \theta_1 \Big[|q_{bit}(t)| q_{bit}(t) - |q_{bit}(t) - \tilde{\xi}_1| (q_{bit}(t) - \tilde{\xi}_1) \Big] \tag{A.14}$$
$$- |q_{bit}(t) - \tilde{\xi}_1| (q_{bit}(t) - \tilde{\xi}_1) \tilde{\theta}_1 + v_3(t) \tilde{\theta}_2$$
$$\dot{\tilde{\theta}}_1 = \gamma_1 |q_{bit}(t) - \tilde{\xi}_1| (q_{bit}(t) - \tilde{\xi}_1) \tilde{\xi}_1 \tag{A.15}$$
$$\dot{\tilde{\theta}}_2 = -\gamma_2 v_3(t) \tilde{\xi}_1 \tag{A.16}$$

Where $q_{bit}(t)$ and $v_3(t)$ are the external time-varying signals.

A.3.1 Equilibrium Points

The equilibrium points of (A.14) - (A.16) are given by setting the left hand side to zero:

$$0 = -l_1 a_1 \tilde{\xi}_1^{eq} - \theta_1 \Big[|q_{bit}(t)| q_{bit}(t) - |q_{bit}(t) - \tilde{\xi}_1^{eq}| (q_{bit}(t) - \tilde{\xi}_1^{eq}) \Big] \tag{A.17}$$
$$- |q_{bit}(t) - \tilde{\xi}_1^{eq}| (q_{bit}(t) - \tilde{\xi}_1^{eq}) \tilde{\theta}_1^{eq} + v_3 \tilde{\theta}_2^{eq}$$
$$0 = \gamma_1 |q_{bit}(t) - \tilde{\xi}_1^{eq}| (q_{bit}(t) - \tilde{\xi}_1^{eq}) \tilde{\xi}_1^{eq} \tag{A.18}$$
$$0 = -\gamma_2 v_3(t) \tilde{\xi}_1^{eq} \tag{A.19}$$

Equation (A.19) and assumption 12 gives:

$$\tilde{\xi}_1^{eq} = 0 \tag{A.20}$$

Inserting this into (A.17) gives:

$$\begin{aligned} 0 &= -\theta_1 \left[|q_{bit}(t)| q_{bit}(t) - |q_{bit}(t)| q_{bit}(t) \right] - |q_{bit}(t)| (q_{bit}(t)) \tilde{\theta}_1^{eq} + v_3(t) \tilde{\theta}_2^{eq} \\ &= -|q_{bit}(t)| q_{bit}(t) \tilde{\theta}_1^{eq} + v_3(t) \tilde{\theta}_2^{eq} \\ \Rightarrow \tilde{\theta}_2^{eq} &= \frac{|q_{bit}(t)| q_{bit}(t) \tilde{\theta}_1^{eq}}{v_3(t)} \end{aligned} \tag{A.21}$$

From (A.20) and (A.21) it is obvious that $\tilde{\xi}_1 = \tilde{\theta}_1 = \tilde{\theta}_2 = 0$ is an equilibrium (although not unique) for the error system (A.14) -(A.16).

A.3.2 Lipschitz

In this section local Lipschitz properties for the system (A.14) -(A.16) will be proved. Lemma 3.2 in (Khalil 2002) will be used. Denoting, see (A.14) -(A.16):

$$\dot{\tilde{\xi}}_1 = f_1(\tilde{\xi}, \tilde{\theta}_1, 3\tilde{\theta}_2, t) \tag{A.22}$$
$$\dot{\tilde{\theta}}_1 = f_2(\tilde{\xi}, t) \tag{A.23}$$
$$\dot{\tilde{\theta}}_2 = f_3(\tilde{\xi}, t) \tag{A.24}$$

f_* is continuous. Using the relationship:

$$\frac{\partial |q_{bit}(t) - \tilde{\xi}_1|(q_{bit}(t) - \tilde{\xi}_1)}{\partial \tilde{\xi}_1} = \begin{cases} \frac{\partial (q_{bit}(t) - \tilde{\xi}_1)^2}{\partial \tilde{\xi}_1} & q_{bit}(t) \geq \tilde{\xi}_1 \\ -\frac{\partial (q_{bit}(t) - \tilde{\xi}_1)^2}{\partial \tilde{\xi}_1} & q_{bit}(t) < \tilde{\xi}_1 \end{cases}$$

$$= \begin{cases} -2(q_{bit}(t) - \tilde{\xi}_1) & q_{bit}(t) \geq \tilde{\xi}_1 \\ 2(q_{bit}(t) - \tilde{\xi}_1) & q_{bit}(t) < \tilde{\xi}_1 \end{cases}$$

$$= -2|q_{bit}(t) - \tilde{\xi}_1| \tag{A.25}$$

The Jacobian for (A.22)-(A.24) can be calculated to be:

$$\frac{\partial f_1}{\partial \tilde{\xi}_1} = -l_1 a_1 - 2\theta_1 |q_{bit}(t) - \tilde{\xi}_1| + 2|q_{bit}(t) - \tilde{\xi}_1|\tilde{\theta}_1 \tag{A.26}$$

$$= -l_1 a_1 + 2|q_{bit}(t) - \tilde{\xi}_1|(\tilde{\theta}_1 - \theta_1) \tag{A.27}$$

$$\frac{\partial f_1}{\partial \tilde{\theta}_1} = -(q_{bit}(t) - \tilde{\xi}_1)|q_{bit}(t) - \tilde{\xi}_1| \tag{A.28}$$

$$\frac{\partial f_1}{\partial \tilde{\theta}_2} = v_3(t) \tag{A.29}$$

$$\frac{\partial f_2}{\partial \tilde{\xi}_1} = -2\gamma_1 |q_{bit}(t) - \tilde{\xi}_1|\tilde{\xi}_1 + \gamma_1 (q_{bit}(t) - \tilde{\xi}_1)|q_{bit}(t) - \tilde{\xi}_1| \tag{A.30}$$

$$\frac{\partial f_3}{\partial \tilde{\xi}_1} = -\gamma_2 v_3 \tag{A.31}$$

The Jacobian is continuous as both $q_{bit}(t)$ and $v_3(t)$ is continuous from assumptions 11 and 12. Hence f_* is locally Lipschitz in $(\tilde{\xi}_1, \tilde{\theta}_1, \tilde{\theta}_2)$. As $q_{bit}(t)$ and $v_3(t)$ are bounded from the same assumptions, the Lipschitz property holds uniformly in t.

A.4 LaSalle-Yoshizawa

The following theorem is used to establish stability and uniform boundedness in the adaptive observer design. It can be found in (Krstić, Kanellakopoulos & Kokotović 1995).

Theorem 1. *(LaSalle-Yoshizawa) Let $x = 0$ be an equilibrium point of $\dot{x} = f(x,t)$ and suppose f is locally Lipschitz in x uniformly in t. Let $V : \mathbb{R}^n \times \mathbb{R}_+ \to \mathbb{R}_+$ be a continuously differentiable function such that*

$$\gamma_1(|x|) \leq V(x,t) \leq \gamma_2(|x|) \tag{A.32}$$

$$\dot{V} = \frac{\partial V}{\partial t} + \frac{\partial V}{\partial x} f(x,t) \leq -W(x) \leq 0 \tag{A.33}$$

$\forall t \geq 0$, $\forall x \in \mathbb{R}^n$,where γ_1 and γ_2 are class $\mathcal{K}_\infty$ functions and W is a continuous function. Then, all solutions of $\dot{x} = f(x,t)$ are globally uniformly bounded and satisfy.

$$\lim_{t\to\infty} W(x(t)) = 0 \tag{A.34}$$

In addition, if $W(x)$ is positive definite, then the equilibrium $x = 0$ is globally uniformly asymptotically stable.

For a definition of class $\mathcal{K}_\infty$ functions see, (Khalil 2002).

A.5 Barbălat

The following theorem is used to establish convergence properties for parameter estimates, it can be found in (Ioannou & Sun 1996).

Lemma 2. *(Barbălat) If $\lim_{t\to\infty} \int_0^t f(\tau)dt$ exists and is finite, and $f(t)$ is a uniformly continuous function, then $\lim_{t\to\infty} f(t) = 0$.*

For a definition of uniformly continuous functions see (Ioannou & Sun 1996).